DOE/NASA/0234-1
NASA CR-182116

Cast Iron-Base Alloy for Cylinder/ Regenerator Housing

Final Report

Stewart L. Witter, Harold E. Simmons,
and Michael J. Woulds
Garrett Processing Company

August 1985

Prepared for
NATIONAL AERONAUTICS AND SPACE ADMINISTRATION
Lewis Research Center
Under Contract DEN 3-234

for
U.S. DEPARTMENT OF ENERGY
Conservation and Renewable Energy
Office of Vehicle and Engine R&D

DISCLAIMER

Printed in the United States of America

Available from
National Technical Information Service
U.S. Department of Commerce
5285 Port Royal Road
Springfield, VA 22161

NTIS price codes[1]
Printed copy: A07
Microfiche copy: A01

[1]Codes are used for pricing all publications. The code is determined by the number of pages in the publication. Information pertaining to the pricing codes can be found in the current issues of the following publications, which are generally available in most libraries: *Energy Research Abstracts (ERA); Government Reports Announcements* and Index (*GRA* and I); *Scientific and Technical Abstract Reports (STAR);* and publication, NTIS-PR-360 available from NTIS at the above address.

DOE/NASA/0234-1
NASA CR-182116

Cast Iron-Base Alloy for Cylinder/ Regenerator Housing

Final Report

Stewart L. Witter, Harold E. Simmons,
and Michael J. Woulds
Garrett Processing Company
Torrance, California 90509

August 1985

Prepared for
National Aeronautics and Space Administration
Lewis Research Center
Cleveland, Ohio 44135
Under Contract DEN 3-234

for
U.S. DEPARTMENT OF ENERGY
Conservation and Renewable Energy
Office of Vehicle and Engine R&D
Washington, D.C. 20545
Under Interagency Agreement DE-AI01-85CE50112

FOREWORD

Garrett Processing Company, Garrett Metals Casting Division (formerly AiResearch Casting Company), in support of NASA-Lewis Research Center and coordination with NASA technical project managers J. R. Stephens, J. A. Misencik, and C. M. Scheuermann, has developed an alloy, designated NASAAC-1. This is a castable iron-base, high-temperature alloy intended to replace the more costly strategic alloy Stellite 31 (X-40) used in cylinder and regenerator housings for the automotive Stirling engine.

The program at Garrett Metals Casting Division was performed by M. J. Woulds* and S. L. Witter.** Editorial review is by H. E. Simmons.***

The authors wish to acknowledge the significant contributions to this program by Michele Mitchell, Research and Development Contract Administrator at Garrett Metals Casting Division, and Coulson M. Scheuermann, Technical Project Manager, NASA-Lewis Research Center.

*Deceased
**No longer at Garrett Metals Casting Division
***Garrett Metals Casting Division, retired. Presently consultant to the company.

TABLE OF CONTENTS

SUMMARY

The objective of this program is to develop an Fe-base alloy that can meet the requirements of the automotive Stirling engine cylinders and regenerator housings. The scope of work was to test various alloys and select the one best demonstrating the following characteristics:

- It must be a cast alloy, using nonstrategic metals.
- It must withstand stress for a 2500-hr rupture life at 200 MPa/775°C.
- Oxidation/corrosion resistance must be comparable to that of N-155.
- It must be compatible with hydrogen.
- Fatigue properties must be superior to alloy XF 818.
- Cost must be less than or equal to that of 19-9DL.

To meet the program objective, a thorough literature search was conducted to determine those alloy systems most likely to meet the projected goals. Supplemental information was obtained by direct contact with people who have had extensive experience with iron-base superalloys.

Based on findings from these preliminary investigations, the decision was made to concentrate effort on three specific alloys systems. These were designated as (a) Group 1 - Nickel manganese (NiMn), (b) Group 2 - Nickel (Ni), and (c) Group 3 - Manganese (Mn).

Both NASA and Garrett Metals Casting Division personnel realized the extreme importance of establishing casting parameters to optimize alloy properties. The overall program must necessarily include both proper alloy selection and controlled casting procedures.

Therefore, to meet program requirements, major tasks were designed to include the following:

- Selection, processing, and evaluation of candidate alloys within each alloy group system.
- Determination of casting parameters.
- Selection of a candidate alloy and establishment of a data base for this alloy.

In the initial phase of the program designated as Round 1, a series of alloys representing each alloy system was cast and tested. In all there were 5 alloys of the nickel-manganese Group 1, 13 alloys of the nickel Group 2, and 3 alloys of the manganese Group 3. The aim was to maintain the chemistry of the major element(s) shown and vary the percentage of other elements to study their influence.

Results strongly favored the nickel Group 2 system, particularly with tungsten additions. Group 1 alloys exhibited limited possibility, while Group 3 alloys showed no candidacy and were eliminated from further evaluation.

In the secondary phase of the program, designated as Round 2, emphasis was placed on the nickel Group 2 system (15 alloys processed and tested). To ensure that some potential was not overlooked from the nickel-manganese Group 1 system, five heats with further chemistry adjustments from those of Round 1 were also processed and tested.

Results confirmed those of Round 1. Certain of the nickel Group 2 alloys showed strong potential as candidate materials. The nickel-manganese Group 1 alloys were eliminated at this stage from the program.

The direction of the program was now defined. Group 2 alloys exhibiting the best performance to date would be used. Concurrently, Garrett would pay close attention to casting parameters and the resultant effects on microstructure and stress-rupture life. Further, heat treat potential as a means of improving alloy capability would be investigated.

The candidate alloys were narrowed down to eight and processed under controlled casting conditions, with special attention to pouring temperature. Heat treat cycles were attempted to improve alloy stability and properties.

Results were very favorable, especially for certain of the eight alloys being compared. Because of the excellent fluidity of this nickel Group 1 alloy system pouring temperatures could be kept relatively low. This reduces metal shrinkage and thereby improves alloy properties. Further, using a heat treat cycle of 1177°C for 2 hr provides consistency of properties, a highly desirable characteristic of any alloy.

We now were readily able to establish a recommended composition range for our candidate alloy. To more closely define and narrow this composition range three alloys based on the nickel Group 2 system having chemistries within the range were selected for final processing and testing. Processing was done under controlled casting conditions, and subsequently all castings and test bars were heat treated at the aforementioned 1177°C for 2 hr.

All work in the program was performed using investment shell molds. A trial was made at this point to reduce cost by utilizing Airset sand molds as well as investment shell molds. There was no change in melting and pouring procedures. The quality of the sand castings and test bars excised from these castings was definitely inferior to the quality of the investment shell castings and test bars, and after discussion with NASA personnel, the investment shell approach was chosen as the preferred method.

Evaluation of results obtained from this series of tests enabled us to closely define the chemistry range for our candidate alloy, designated NASACC-1. A master heat was made to this composition. The heat was melted and poured under controlled casting conditions previously established and poured into investment shell molds. All castings and test bars were heat treated before actual testing.

From a practical standpoint, NASACC-1 proved to be an excellent alloy for casting because it could be melted in air and had good fluidity and fill characteristics.

The alloy met or exceeded all program goals.

- Stress rupture and low cycle fatigue life was equivalent to that of X-40.
- Oxidation/corrosion resistance surpassed that of N-155.
- Alloy was compatible with hydrogen.
- As an added dimension -- welding and brazing characteristics are excellent.

Finally, the cost of NASACC-1 is significantly lower than X-40 but slightly higher than 19-9DL.

INTRODUCTION

As part of the DOE-funded, NASA Lewis Research Center-managed effort to transfer Stirling engine technology from USAB in Sweden to the United States and to develop a competitive automotive Stirling engine, Garrett Metals Casting Division was awarded a contract to develop a Stirling engine cylinder/ regenerator housing iron-base alloy. This alloy had to have the following characteristics:

- It must be a cast alloy.
- It must be made of nonstrategic metals.
- It must withstand a stress of 200 MPa with a minimum rupture life of 2500 hr at 775°C.
- It must have oxidation/corrosion resistance at least comparable to alloy N-155.
- It must be compatible with hydrogen.
- Its cost must not exceed that of alloy 19-9 DL.
- It must have fatigue properties superior to alloy XF 818.

This report describes the effort at Garrett Metals Casting Division to develop such an alloy. A preliminary mechanical property data base is presented for the alloy considered to have the best combination of properties for this application. This alloy is designated NASACC-1 and has the following nominal composition in weight percent: 18.5 Cr, 18.5 Ni, 5.25 Mo, 2.45 W, 1.9 Cb, 1.2 B, 0.55 Si, 0.3 Mn, 0.5 C, balance Fe.

ALLOY DEVELOPMENT

Literature Review

A literature search was performed. The primary aim was to search for effects of alloying elements on high-temperature strength of Fe-base materials. Secondary emphasis related to the effect of these elements on environmental resistance; i.e., oxidation/hot corrosion, and hydrogen embrittlement. These computer searches were conducted by Defense Technical Information Center (DTIC), NASA, and Savage Information Services in Rancho Palos Verdes, California (Covering Metadex, Chemical Abstracts, Scisearch, Weldasearch, Compendex, and NTIS). A total of 1035 citations was generated, many with abstracts, from which approximately 40 citations were selected for complete review. In addition, personal discussions were conducted with Dr. David Sponseller of Climax Molybdenum Company, Dr. George Aggen of Allegheny Ludlum Steel Company, and Mr. Fred Hagen of Chrysler Corporation.

Because the primary goal was increased rupture strength--2500 hr life at 775°C under a 200-MPa stress being the actual target--the search concentrated on alloying for strength with minor emphasis on environmental resistance. In particular the search concentrated on those factors necessary to develop a sound basis for selecting the starting chemistries of alloys for the preliminary stress-rupture screening study.

Alloy Design Philosophy

Extensive literature exists on the philosophy and techniques of designing metal alloys for high-temperature service. However, this literature can be reduced readily to a few basic concepts: solid-solution strengthening, precipitation strengthening, composites (dispersion-strengthened, fiber-reinforced, etc.), and combinations of any of these techniques. For a low-cost application requiring casting, composites are virtually ruled out as being either not technically feasible or too complex to fit within cost guidelines. This requirement points to solid solution and precipitation strengthening as the only viable approach.

Historically, the development of solid-solution-strengthened alloys for elevated temperature service under high stresses has progressed from relatively simple materials containing chromium, nickel, and iron, such as Type 310 stainless steel, through the more complex materials such as Vitallium, N-155, S-816, etc., to the current relatively simple systems exemplified by materials such as Hastelloy X, Inconel Alloys 617 and 625, and Haynes 188. Many of the more complex intermediate alloys contain substantial carbon for additional strengthening by carbide precipitation. Included in this group is the 19Cr-9Ni series (DL, DX, etc.) based on Type 304 stainless, and many of the casting alloys. High carbon in high-temperature casting alloys is still practiced extensively today, as evidenced by materials such as HK (cast Type 310 stainless) and X-40 (HS-31).

As temperature and strength requirements increased, the development of precipitation-hardenable alloys based on gamma-prime $Ni_3(Al, Ti)$ evolved from the simple upgraded stainless steel (A-286) to the complex cast alloys like IN 738 and IN 792. To drive the precipitation reaction effectively, a considerable amount of nickel in the alloy is necessary--generally at least 25 percent.* Further, this level must be increased as the Ti + Al content is raised above approximately 2 percent. Thus, the stronger alloys are predominantly Ni-based, with little iron; as such, they are high in alloy cost compared to the 19-9 DL target set for this program.

One of the more interesting features of the Ni-based, high-temperature alloys is the generally negative effect of chromium on high-temperature creep strength (ref. 1). For years, researchers worked on the tradeoffs of strength and oxidation/hot corrosion resistance by lowering chromium and adjusting the Al/Ti ratio. For gas turbine service, especially turbine blades, some form of coating invariably has been found necessary for the high-strength alloys. A similar phenomenon exists in stainless steels, e.g., creep strength in the Type 400 ferritic grades decreases as one progresses from an 11 percent Cr alloy (Type 409), to a 17 percent Cr alloy (Type 430), to a 26 percent Cr alloy, Type 446 (ref. 2). Although a similar parallel is difficult to draw in the austenitic Type 300 grades because of the need to increase nickel level simultaneously, creep properties of materials like Types 309 and 310 stainless steels, RA330, and Incoloy Alloy 800 are not markedly different from those of Types 316 and 457 stainless steels, despite the higher alloy content of the former.

Effects of Alloying Elements

Discussion of the function of alloying elements in high-temperature alloys is pertinent. Because of the cost restraints (cost similar to or less than that of 19-9DL), the emphasis is necessarily tailored to base materials of relatively low alloy content, i.e., upgraded stainless steel or downgraded lower-cost superalloys.

Table 1 shows a generalized rating of individual elements in the types of base compositions of interest to this Stirling engine program. Apparently, cost can be controlled only by using a minimum content of elements from the group nickel, molybdenum, columbium, and tungsten; use of any quantity of either tantalum or hafnium is costly. (The effect of boron on cost is not completely clear because of the sole-source nature of Fe-B and Ni-B additions; this could require a separate study should a high boron alloy prove promising.) The use of manganese as a substitute for nickel has shown considerable promise with the Series 200 stainless steels (ref. 3), and with more highly alloyed materials such as 21-6-9 and 22-13-5 (now called Nitronic 40 and 50, respectively) (ref. 4). When combined with sufficient carbon/nitrogen, these materials have shown very good properties in stable austenite structures.

*Alloy compositions are given in weight percent.

TABLE 1

EFFECTS OF ALLOYING ELEMENTS IN HIGH-TEMPERATURE, Fe-BASED MATERIALS

Elements	Comments
Chromium	Strong ferrite stabilizer--provides oxidation/corrosion resistance
Nickel	Strong austenite stabilizer--improves strength and corrosion resistance
Molybdenum Tungsten	Strong ferrite stabilizers--provide solid solution strengthening and carbide precipitates; Mo promotes pitting resistance
Aluminum	Ferrite stabilizer--provides oxidation resistance
Tantalum Columbium Vanadium Hafnium	Ferrite stabilizers--carbide and nitride forming elements
Manganese	Austenite stabilizer--can substitute for nickel on a basis of two Mn for one Ni
Silicon	Ferrite stabilizer--normally present as a tramp from deoxidation; reduces oxide scaling tendency; improves fluidity
Boron	Promotes fluidity, improves creep strength, forms borides
Carbon Nitrogen	Austenite stabilizers; interstitial; reacts to form precipitates--carbides, nitrides, and carbonitrides
Iron	Base (select scrap)

The structure of the base alloy is worthy of discussion. The nature of the slip systems is such that the face-centered cubic (FCC) (austenitic) structure is favored over the body-centered cubic (BCC) (ferritic) structure for high-temperature service. Although certain systems exhibiting a microduplex structure of ferrite finely dispersed in austenite have shown very good strength characteristics, the presence of ferrite is generally undesirable for phase stability and hydrogen compatibility, as discussed below. Thus, the alloy composition must be balanced to produce an essentially FCC structure that is solid solution strengthened and carbide precipitation hardened. If nickel is used minimally, then manganese, carbon, and nitrogen must be used liberally.

Relative to castability, certain elements have been known to increase metal fluidity, including carbon, silicon, and manganese. Boron is a known melting-point depressant, which also may increase castability. Loading of an alloy with any of these elements will change the casting parameters, and adjustments undoubtedly will be necessary.

Phase stability, particularly at 775°C, is a major concern. The necessarily low nickel alloys, probably strengthened with molybdenum, will be susceptible to both sigma and chi phase formation (ref. 5). This may not be of direct concern because these phases often can lead to strengthening at high temperatures. The greater concern is in low-temperature ductility (e.g., during winter in the northern states), where mechanical or thermal shock could cause problems should a phase change occur. In particular, the austenitic FCC structure must remain stable to about -50°C to prevent martensite formation, which would be embrittling.

Carbide precipitation also can be embrittling, as is apparently the case with Hastelloy X in the 650° to 870°C range. Within a few thousand hours at 760°C, nearly continuous grain boundary networks are found, with tensile ductility at ambient temperature dropping to only a few percent. Any system using carbide strengthening may need to be balanced so that the carbides precipitate predominantly within the grains, preferably as a result of heat treatment so the strength is available for initial service.

Review of Candidate Alloy Systems

Development of alloy candidate systems was conducted extensively in the post-World War II years up to the mid-1950's, when alloys such as A-286 began to pave the way for the gamma-prime-strengthened, nickel-based superalloys. During this period, AF-71 was developed by Allegheny Ludlum (ref. 6). It is an austenitic nickel-free Cr-Mn-C-Fe alloy, further stabilized with nitrogen and boron, and strengthened with molybdenum and vanadium. Babcock and Wilcox studied 45 percent Fe-based alloys for replacement of Vitallium (refs. 7 and 8). These materials were nominally 20Cr-28Ni strengthened with triple additions selected from the group Ta, Cb, Ti, Zr, Mo, W, and N with Ta-Mo-W and Cb-Mo-W producing the highest strengths. Cornell Aeronautical Laboratory studied additions of Ti, B, V, Zr, N, and C to the 18Cr-8Ni austenitic stainless steel matrix and concluded that titanium/boron were the most effective elements for increasing hot strength (ref. 9).

In the mid to late 1950's considerable work was conducted at the University of Michigan, with hundreds of experimental compositions being cast (ref. 10). A promising series of 18Cr-18Ni iron-based materials based on strengthening by formation of an Mo-B eutectic from an austenitic matrix was developed (ref. 11); Sponseller has since carried on this work at Climax Molybdenum's Research Laboratory, culminating in Alloys XF-818 (18Cr-18Ni-8Mo-0.4Cb-0.8B) and XF-527 (27Cr-30Ni-5Mo-0.9B) (refs. 12 through 15). Reference 11 is of particular importance to this current study in showing the general effects and interactions of carbon, boron, molybdenum, and tungsten in the 18Cr-18Ni-Fe austenitic matrix.

Work in the 1960's at Chrysler Corporation during development of the automotive gas turbine led to a series of four Fe-base casting alloys that contained 18-24Cr, 5Ni, 5Mn, 1W, and 1Mo, plus 1-2Cb and substantial additions of carbon and nitrogen (ref. 16). These were designated CRM-6D, -15D, -17D, and 18D. These materials are characterized by low ductility, apparently due to the high carbon level (ref. 8), which leads to a different microstructural form of the eutectic than that found in the lower carbon (<0.3 percent) molybdenum-boron XF-818 and XF-527 (ref. 10).

Oxidation and Hot Corrosion Resistance

Extensive literature is available on the oxidation and hot corrosion resistance of metals, primarily generated by the gas turbine industry (see ref. 1, for example). Alloys designed for high-temperature oxidation resistance invariably have high chromium (20 percent and greater), often in combination with a lesser amount of aluminum. Hastelloy X is one aluminum-free alloy; some manganese is needed in this alloy to assist in $CrMnO_4$ spinel formation on the surface, as opposed to pure Cr_2O_3. Of the alloys containing aluminum, Inconel Alloy 601 and Inconel Alloy 617 (both containing nominally 1 percent Al) are examples of recent trends in alloy design.

The addition of rare earth metals has proven to be a powerful tool in enhancing environmental resistance, probably by improving resistance of the oxide film to spalling. This is demonstrated in Hastelloy S and Haynes 188, where a few hundredths of a percent of lanthanum are effective. Work on systems involving the use of yttrium has led to the development of a series of MCrAlY coatings, where M can be iron, nickel, or cobalt, each in combination with fairly high chromium, moderate aluminum, and a small addition of yttrium. The MCrAlY alloys by themselves are not particularly strong; hence, they have application only as coatings (except for oxide-dispersion-strengthened materials, e.g., MA-956, which are expensive).

Various studies have been done on silicon additions in combination with aluminum/rare earth metals. High silicon levels (generally over 1 percent) have long been recognized for reducing the tendency for oxide scaling in austenitic alloys, e.g., Type 302B stainless steel and RA330. Some recent work in Japan on nominally 300-type stainless steels (19 percent Cr, 13 percent Ni) with 3 percent Si showed promise of improved resistance to oxide spalling when rare earth metals/calcium were added to the base metal (ref. 17).

A combination of internal oxides and a defect structure is now generally recognized as being created beneath the normal protective oxide when the rare earth metals are added, markedly influencing the behavior of the external scale.

Relative to hot corrosion resistance, the 775°C temperature is within the range of formation of molten salts (primarily Na_2SO_4-NaCl mixtures), which will flux the normally protective oxide from the metal surface. Accordingly, the full understanding of fuel composition is important. For example, in the presence of sulfur, nickel alloys are particularly susceptible to sulfidation damage, as the nickel-sulfide eutectic can form, causing liquid damage below 650°C (ref. 18). Austenitic stainless steels such as 304 and 347 are susceptible to grain boundary attack in the presence of sodium chloride, even as a vapor, above about 575°C (ref. 19).

For resistance to grain boundary attack, the general alloy philosophy has been to increase chromium as high as possible, although, as noted earlier, higher chromium tends to reduce creep-rupture strength, especially in nickel-based alloys. Alternatively, coatings have been used, such as diffused aluminides and the MCrAlY types. More recently, combinations of alumide coatings with thin noble metal barriers have been used. Gaseous aluminizing/chromizing also may offer a way to provide protection to otherwise poor oxidation/hot corrosion-resistant alloys. Gaseous treatment can be applied to the finished assembly (or subassembly) and will reach all surfaces readily. An inexpensive coating may be necessary to meet the cost restraints imposed on the material.

No problems are foreseen with ambient temperature or cold corrosion. Materials that have been engineered for adequate oxidation/hot corrosion resistance would not be expected to corrode under mild aqueous conditions, with two notable exceptions: sulfuric acid condensation and chloride salt deposits. Short of burning high-sulfur fuel, sulfuric acid condensation would not be expected at 200°C and above (ref. 20), and the small amount formed at shutdown should be no worse than in similar equipment now in operation (e.g., diesel engines and exhaust systems). Protection against hot sulfuric acid is so difficult that designers generally keep operating temperatures above the condensation point.

Salt deposits containing chloride ions can lead to pitting if condensed moisture creates an electrolyte. Again, most high-temperature alloys would contain sufficient chromium and molybdenum to retard pitting during down periods, but conditions conducive to pitting should be avoided as much as possible. As noted above, the presence of chlorides in the engine is also undesirable relative to hot corrosion problems.

Hydrogen Embrittlement

Hydrogen damage can take two forms: hydrogen can either enter the metal lattice (charging), or react instantaneously with an advancing crack tip (creating notch sensitivity). In carbon steels, for example, an internal reaction between carbon and hydrogen is believed to form methane, which collects to form blisters or pores with resulting cracks in the material. By adding sufficient chromium, vanadium, or other elements to form stable carbides, methane formation can be minimized or eliminated (ref. 21).

In the austenitic alloys, a good correlation exists between stability (freedom from deformation martensite) and resistance to high-pressure hydrogen. Similarly, the high-strength martensitic (and PH) steels are highly susceptible to hydrogen embrittlement. The effect of the presence of soft ferrite is not completely clear because tests on duplex (austenite-ferrite) steels have been limited, but results to date have not shown a deleterious effect because of the presence of a small amount of ferrite in austenite (ref. 22).

Literature on hydrogen embrittlement is also abundant. Most of it is directed toward discussions of mechanisms, however, as opposed to alloying effects on resistance. It is generally known that nickel-based alloys are fairly susceptible, whereas austenitic iron-based alloys are the least susceptible to hydrogen damage. Several papers have been written on the effects of alloying elements on hydrogen embrittlement of A-286 (refs. 23 and 24).

Smugeresky (ref. 23) showed that a high Ti + Al content enhances resistance to hydrogen damage. Conversely, Thompson and Brooks (ref. 24) showed that removal of manganese was beneficial, especially in the presence of increased (5 percent) nickel, with adverse effects from titanium and aluminum additions. At this point, the alloying effects are not clear; testing will be necessary.

SELECTION OF ALLOY GROUPS, CANDIDATE ALLOYS, AND ALLOY DESIGNATIONS

As described in the literature review, work on Fe-base alloy systems for high-temperature service has been limited in recent years, with primary emphasis on oxidation-resistant ferritic alloys that simply lack the required strength to meet the targets of this program. The review has identified several candidate austenitic systems for further exploration. These include CRM-6D, XF-818, and AF-71 as the most promising; 19-9DL appears to have little potential and already has been heavily investigated (DX, WMo, WX). Initially, the two items of concern are stress rupture strength and cost, which are covered in fig. 1 and table 2, respectively.

Data in fig. 1 are from a DMIC compilation (ref. 25) and a NASA publication (ref. 28); costs were calculated from the virgin air-melt alloy element costs as of January 1985 and are shown in table 2.

The basic approach of this study is to work with an Fe-base austenitic matrix, i.e., Cr-Ni, Cr-Ni-Mn, or Cr-Mn, and strengthen it by one or more of the following techniques: (1) M_3B_2 eutectic with molybdenum or tungsten; (2) carbides of columbium, vanadium, chromium, molybdenum, and tungsten; and (3) solid solution with molybdenum or tungsten. In Cases (1) and (2), applicable heat treatments include high-temperature solutioning to spheroidize, plus aging to form precipitates, especially carbides. Starting compositions for the first half of the screening study are given in table 3, and are referenced to the starting alloys.

Group 1 - Nickel Manganese (NiMn)

Group 1 of table 3 is based on CRM-6D. Since the predominant austenite stabilizers in Group 1 are nickel (Ni) and manganese (Mn) the alloy group prefix designation is NiMn. As indicated in fig. 1, creep strength is near the target level. Projected cost was below that of 19-9DL, giving room for alloy additions from elements such as Mo, W, Cb, and V. Such additions would provide both solid solution and carbide strengthening. Solution treating and aging to enhance strength should be possible through precipitation of carbides. Chromium level also has been reduced to enhance creep strength.

Group 2 - Nickel (Ni)

The basis for Group 2 is XF-818. The alloy group prefix designation is nickel (Ni) because the alloy matrix is stabilized by nickel. Varying levels of molybdenum, columbium, and vanadium are used for strengthening. Some alloy variations will also contain tungsten. Because it has a cost above the target level, the alloying approach is to reduce the molybdenum level while adding boron, nitrogen--in the form of high nitrogen ferrochrome, and carbon to increase strength. In some cases manganese has been substituted for nickel to reduce cost.

Group 3 - Manganese (Mn)

The Group 3 base is AF-71, which, by virtue of being nickel-free, has the lowest base cost, as shown in Table 2. Manganese (Mn) is the prefix designation for this alloy group. Because it was developed as a wrought alloy, a substantial increase in alloy content is possible, particularly boron, which has been reported to lead to significantly improved strength (ref. 26). Vanadium is reported to be effective in promoting precipitates when aged at 704°C (refs. 6 and 26). A molybdenum increase also may prove beneficial, e.g., to form the M_3B_2 type eutectic in a nickel-free base.

To allow the early test results to influence the choice of compositions to be investigated, the initial alloy composition matrix was limited to 26 alloys, as agreed by ACC and NASA-Lewis Research Center during a review meeting held September 26, 1980, at NASA-Lewis.

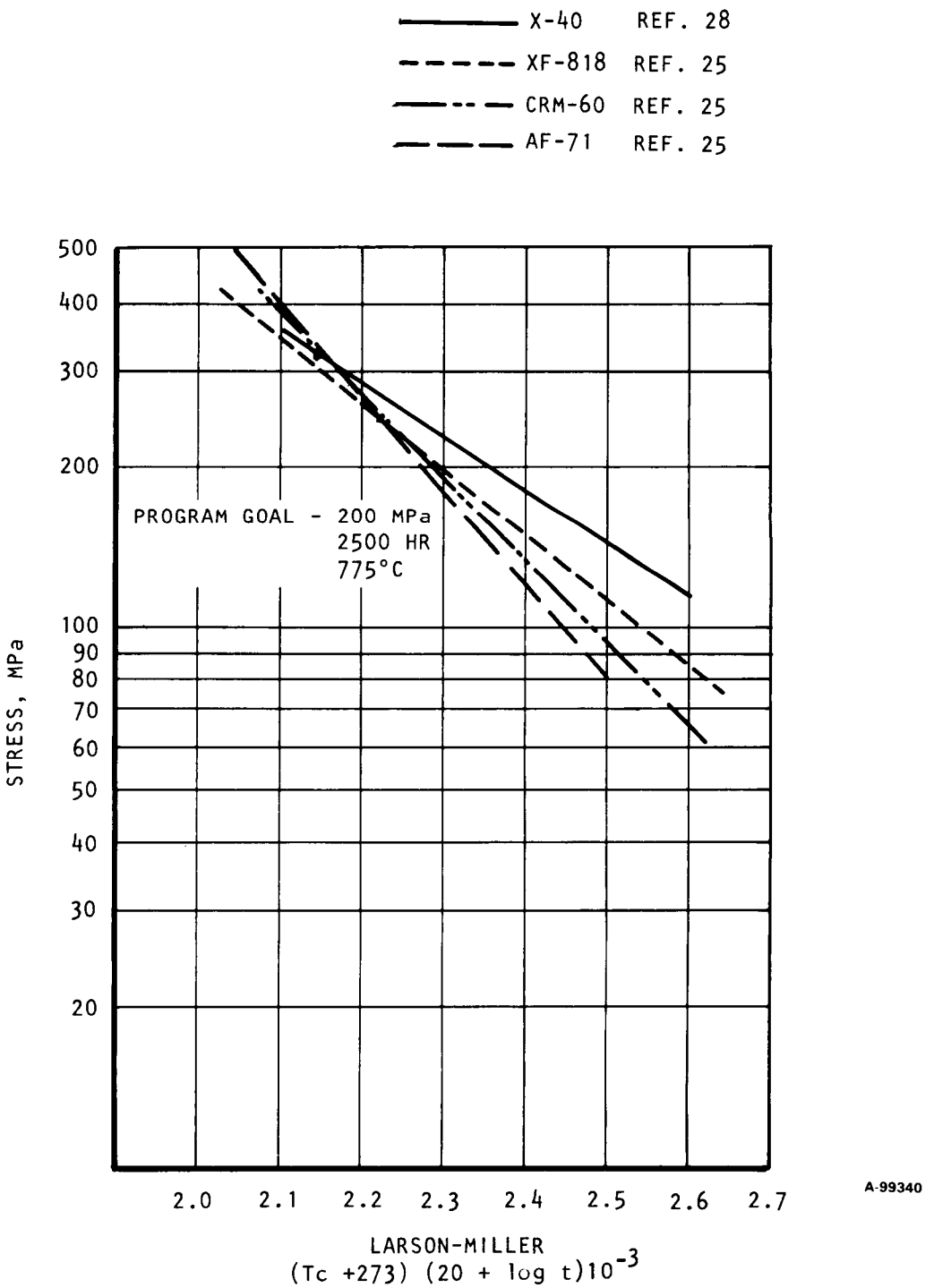

Figure 1.--Stress-Rupture Properties of Candidate Starting Alloys, and Target Alloy (X-40).

TABLE 2

COMPOSITIONS (WEIGHT PERCENT) OF CANDIDATE STARTING ALLOYS AND REFERENCE MATERIALS

Designation	C	N	Mn	Si	Cr	Ni	Co	Mo	W	Cb	Fe	Ti	B	V	Approximate raw material cost, $/kg*
AF-71	0.3	0.2	18.0	0.3	12.0	-	-	3.0	-	-	Bal.	-	0.2	0.90	0.60
CRM-6D	1.05	-	5.0	0.5	22.0	5.0	-	1.0	1.0	1.0	Bal.	-	0.003	-	0.59
XF-818	0.2	-	0.1	0.3	18.0	18.0	-	7.5	-	0.4	Bal.	-	0.6	-	0.93
19-9DL	0.3	-	1.1	0.6	19.0	9.0	-	1.25	1.2	0.4	Bal.	0.3	-	-	0.64
N-155	0.15	0.15	1.5	0.5	21.0	20.0	20	3.0	2.5	1.0	Bal.	-	-	-	2.28
X-40 (HS-31)	0.5	-	1.0	0.5	22.5	10.5	Bal.	-	7.5	-	2.0	-	0.01	-	4.71

*Based on virgin air-melt material prices on 1/15/85.

TABLE 3

ALLOY APPROACH

Alloy no.	Composition - Wt. percent (bal. Fe)										
	C	Mn	Si	Cr	Ni	Mo	B	N	W	Cb	V
Group 1 - Base, CRM-6D											
NiMn-1	1.0	5	0.3	22	5	1.0	-	-	1.0	1.0	-
NiMn-2	1.0	5	0.3	17	5	3.0	-	-	1.0	1.0	-
NiMn-3	1.0	5	0.3	17	5	2.0	-	-	2.0	1.0	-
NiMn-4	1.0	5	0.3	17	5	1.0	-	-	1.0	1.5	0.5
NiMn-5	1.0	5	0.3	17	5	1.0	-	-	1.0	1.0	1.0
Group 2 - Base, XF-818											
Ni-1	0.2	0.2	0.3	18	18	7.5	0.7	0.1	-	0.4	-
Ni-2	0.35	0.2	0.3	18	18	5.0	1.0	0.1	-	0.4	-
Ni-3	0.5	0.2	0.3	18	18	5.0	1.25	0.1	-	0.4	-
Ni-4	0.5	0.2	0.3	18	18	7.6	1.25	0.1	-	0.4	-
Ni-5	0.08	0.2	0.3	18	18	6.0	1.5	0.1	-	-	-
Ni-6	0.5	0.2	0.3	18	18	5.0	1.25	0.2	-	0.4	-
Ni-7	0.25	0.2	0.3	18	18	5.0	1.25	-	2.0	-	-
Ni-8	0.5	0.2	0.3	18	18	5.0	1.25	-	2.0	-	-
Ni-9	0.5	0.2	0.3	18	18	4.0	1.25	-	2.0	2.0	-
Ni-10	0.5	0.2	0.3	18	18	4.0	1.25	-	2.0	1.0	1.0
Ni-11	0.25	3.0	0.3	18	10	5.0	1.25	-	2.0	-	-
Ni-12	0.5	3.0	0.3	18	10	4.0	1.25	-	2.0	1.0	1.0
Ni-13	0.65	0.2	0.3	18	18	5.0	2.0	-	-	-	-
Group 3 - Base, AF-71											
Mn-1	0.3	18	0.3	12	-	3.0	0.2	0.2	-	-	0.9
Mn-2	0.3	18	0.3	12	-	3.0	0.75	0.2	-	-	0.9
Mn-3	0.3	18	0.3	12	-	5.0	1.25	0.2	-	-	0.9

PRELIMINARY STRESS-RUPTURE SCREENING -- ROUND 1

Procedure

Casting.--Wax injection tools for the stress-rupture specimen shown in fig. 2 and the castability test specimen shown in fig. 3 were procured. Tooling for the round tensile test specimen shown in fig. 4 was already available at Garrett AiResearch. Wax patterns were assembled as shown in fig. 5, with each assembly consisting of four stress-rupture specimen patterns, three tensile test specimen patterns, and one castability test specimen pattern. Wax patterns were dipped in refactory slurries and stuccos to build up shell molds, following standard precision casting foundry practice. A mold system with a zircon face coat bonded with colloidal silica was used. After steam autoclave dewaxing, molds were loaded into a preheat furnace and held at least 3 hr for firing.

Raw materials used for casting the experimental alloys listed in table 3 are shown in table 4.

Melting procedures for the three groups of alloys are given in table 5. Alloys were induction-melted in air as 4.5-kg heats using an MgO crucible. Heats N10001, N10002, and N10003 were melted in a silica crucible. An argon cover was used in melting the alloys of Groups 1 and 3 because of their higher manganese content. Pouring temperatures were 1538°C for the alloys of Group 1 and 1482°C for the remainder of the alloys. Melts were poured into molds that had been heated to 1038°C and allowed to cool for 3 to 3-1/2 min before pouring (shown by thermocouple measurement to result in a mold temperature of 816° to 871°C). An exothermic hot-topping compound was used to improve metal feeding.

Testing.--A typical casting is shown in fig. 6 after mold removal and after sandblasting. Specimens were cut off from the cast assembly, inspected by X-ray radiography, and ranked according to radiographic quality. The best two specimens were selected for stress-rupture testing.

Specimens for chemical analysis and preliminary metallographic examination were cut from the bottom ring gate of each casting. Chemical analysis was determined by spark emission spectrography, except for two groups of elements: (1) chrominum, nickel, and molybdenum, which were analyzed by X-ray fluorescence, and (2) carbon, oxygen, and nitrogen, which were analyzed by Leco combustion-methods.

Group 1 specimens were heat treated for 100 hr at 649°C, as recommended for CRM-6D (ref. 25). No heat treatment was performed on specimens from Group 2. Solution treatment experiments on the Group 3 modifications of AF-71 indicated that partial melting occurred, even at 1066°C, though solution treatment at temperatures as high as 1121°C is recommended for AF-71 (ref. 6). Therefore, Alloys Mn-2 and Mn-3 were given aging treatments only, and Alloy Mn-1 (AF-71) was solution treated and aged. A protective foil pouch was used for solution treatment.

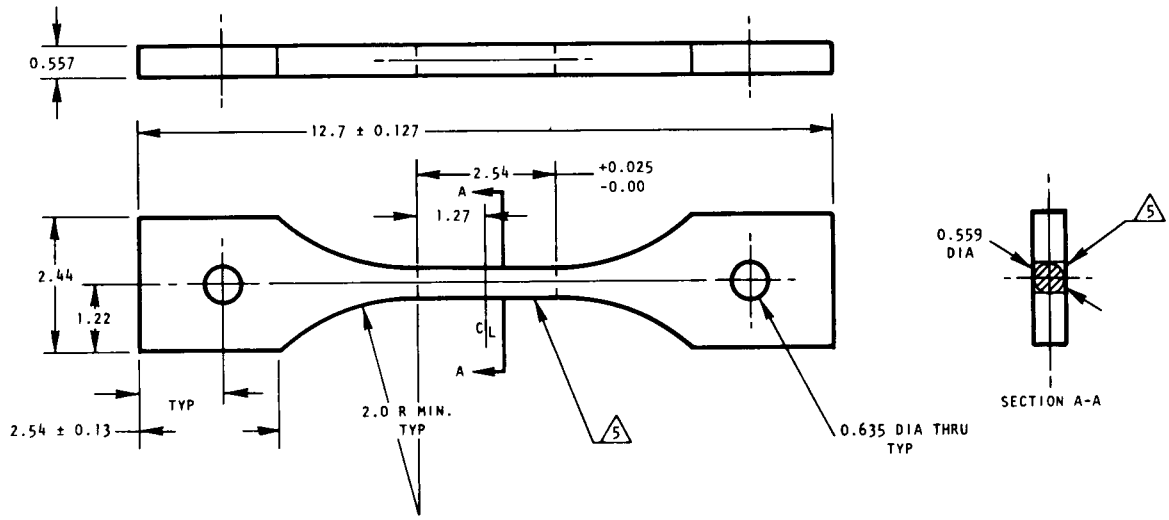

NOTE:

1. DIMENSIONS ARE IN CENTIMETERS.
2. DIMENSIONS DO NOT INCLUDE SHRINK. SHRINK IS TO BE 1.023 CM/CM.
3. DIMENSIONS ±0.064 EXCEPT AS NOTED.
4. TRANSITION FROM SQUARE TO ROUND MUST BE SMOOTH.

A-83245-A

Figure 2.--Stress-Rupture Specimen.

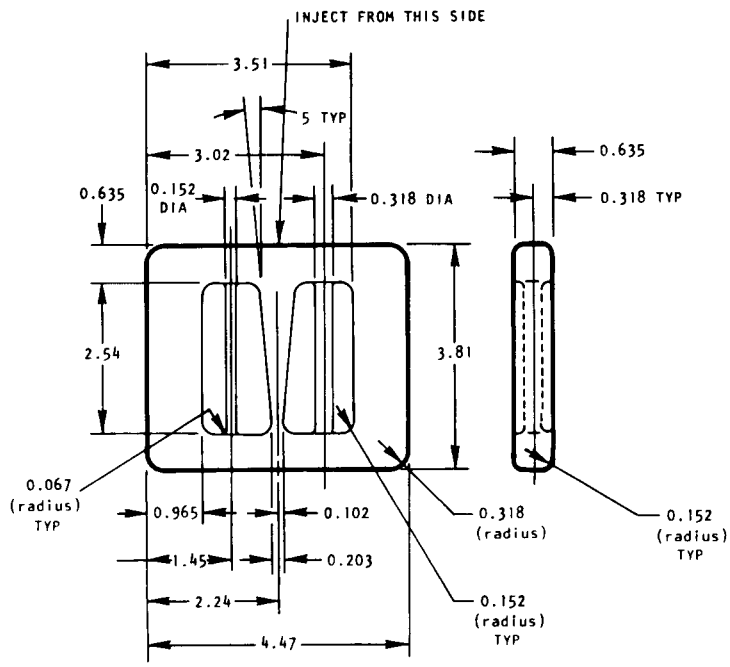

NOTE:

1. STAMP TOOLING WITH THE FOLLOWING USING 0.229 HIGH LETTERING:
   NASA LEWIS
   CONTRACT NO. DEN 3-234
   TOOL NO. T-63254
2. DIMENSIONS ARE IN CENTIMETERS.

A-75793-A

Figure 3.--Castability Test Specimen.

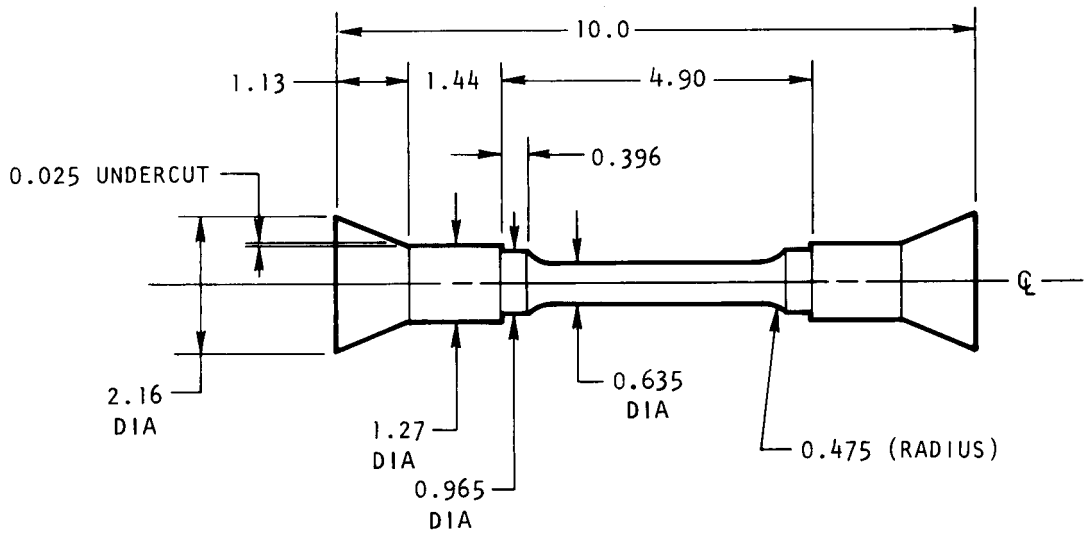

A-75794

NOTE:
DIMENSIONS IN CENTIMETERS.

Figure 4.--Tensile Test Specimen.

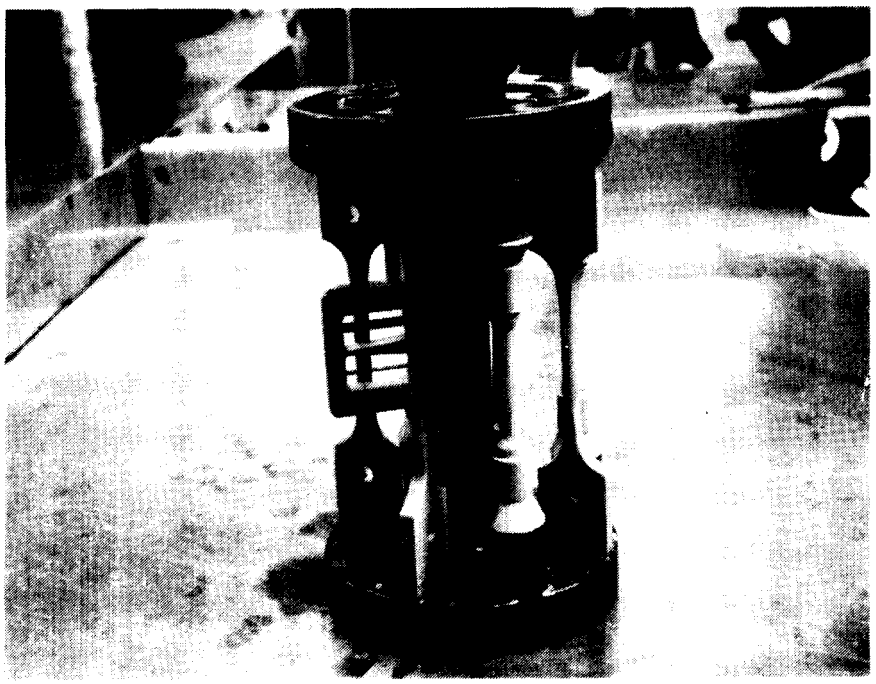

F-33235

Figure 5.--Wax Pattern Assembly.

TABLE 4

RAW MATERIALS FOR MELTING

Electrolytic iron
Carbonyl nickel
Vacuum grade chromium
Pure molybdenum, melting grade
Pure tungsten
Electrolytic manganese
Ferroboron (17.5 percent B)
Ferrovandium (78 percent V)
Ferrocolumbium (60 percent Cb)
Ferrosilicon (75 percent Si)
Asbury 607 carbon
High nitrogen ferrochromium (5.5 percent N, 65 percent Cr)

TABLE 5

HEAT PROCEDURES

Group 1 Alloys (Argon blanket)

Charge Fe, Ni, W, C, 1/3 Cr, 1/3 FeSi
Melt down
Add Mo
Heat to 1593°C
Add balance of FeSi, balance of Cr
Adjust to 1593°C
Add FeCb, FeV, Mn
Adjust to 1538°C
Slag
Pour

Group 2

Charge Fe, Ni, High N FeCr, C, 1/3 Cr, 1/3 FeSi
Melt down
Add Mo
Heat to 1593°C
Add balance of FeSi, Mn, balance of Cr
Reheat to 1593°C
Cool to 1538°C, slag
Add FeCb, FeB
Adjust to 1482°C
Pour

Group 3 Alloys (Argon Blanket)

Charge Fe, Ni, High N FeCr, C, 1/3 Cr, 1/3 FeSi
Melt down
Heat to 1538°C
Add balance of FeSi, balance of Cr
Adjust to 1538°C
Cool to 1482°C slag
Add FeV, FeB
Adjust to 1482°C
Pour

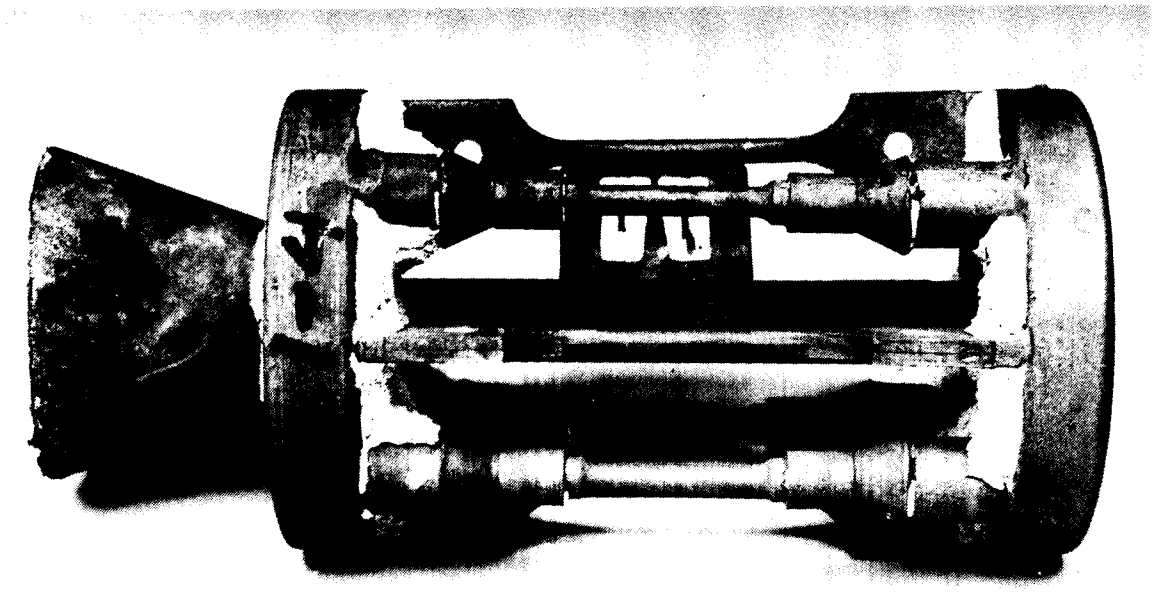

83913-4

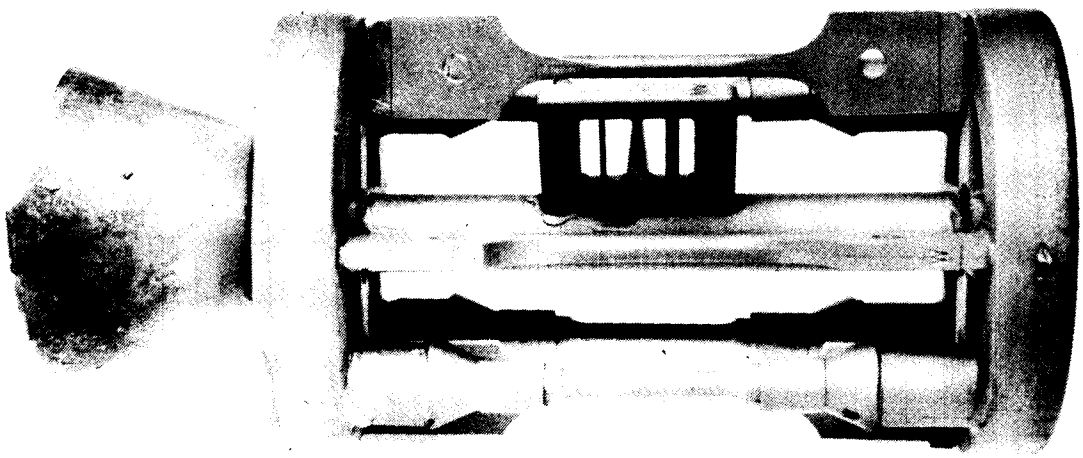

N 10004

ALLOY NiMn-4

83913-3

F-33237-A

Figure 6.--Alloy NiMn-4 Casting (Heat N10004). Top, As Cast; Bottom, Sandblasted.

Stress-rupture testing was conducted at 830°C and 200 MPa using calibrated test facilities at Garrett AiResearch. Stress-rupture life of approximately 330 hr at this temperature is equivalent to the target life of 5000 hr at 775°C.

Results

Visual inspection.--No major difficulties were encountered in melting and pouring any of the experimental alloys. The high manganese Group 3 alloys showed evidence of oxide evolution during melting, even with use of an argon blanket. Surface quality of all castings, typified by the example of fig. 6, was good to excellent. Group 3 parts, although fully acceptable, exhibited poorer surface quality than the other groups. Examination of castability test tabs revealed no problems with hot tearing or lack of fluidity.

Radiography.--X-ray radiography revealed internal porosity in some of the specimens. Only those specimens with no observable porosity were used for stress-rupture testing.

Chemical analysis.--Compositions of experimental castings are shown in table 6. Except for apparent inadvertent omission of tungsten in five alloys of Group 2 and lower nitrogen than expected in several alloys (most notably the three alloys of Group 3), compositions were judged acceptable for purposes of this screening study.

Metallography.--Metallographic structures of all 26 heats are shown in figs. 7 through 9.

Group 1 (base CRM-6D) alloys all have structures containing the expected austenite matrix with interdendritic carbides. Two distinct types of carbides can be seen. The first is a massive carbide that is semicontinuous in alloys NiMn-1 (CRM-6D) and NiMn-2. The second is a lamellar form found as an eutectic with austenite. More than one lamellar form may exist. The alloy with lowest total content of the carbide formers Cr, Mo, W, Cb, and V (alloy NiMn-4) appears to have the smallest amount of total carbide (alloy NiMn-4).

Group 2 (base XF-818) alloys have the expected austenite matrix with carbide/boride interdendritic phases that are either continuous or semicontinuous. The addition of columbium and vanadium yields continuous grain boundary carbides--see alloy Ni-12 (fig. 8). Conversely, alloy Ni-13 (fig. 8) without these additions exhibits short semicontinuous eutectic borides. Alloy Ni-10 with tungsten shows considerable chinese script structure.

Group 3 (base AF-71) alloys contain a combination of dendritic matrix and continuous or semicontinuous interdendritic eutectic. A substantial difference exists among the three alloys in this series in both the quantity and nature of the interdendritic eutectic. Alloy Mn-1 with the lowest amount of boron shows the least interdendritic phase. Alloy Mn-3 with the highest boron content has the greatest quantity of interdendritic phase. The structure of alloy Mn-2 lies between Mn-1 and Mn-3.

TABLE 6

ANALYSES OF EXPERIMENTAL ALLOYS

Alloy No.	Heat No.	Weight percent (bal. Fe)											
		C	Mn	Si	Cr	Ni	Mo	B	N	W	Cb	V	O
Group 1---base CRM-6D													
NiMn-1	N10001	0.84	4.09	0.57	21.64	4.83	1.01	<0.001	0.040	1.04	1.12	<0.01	0.061
	Aim	1.0	5.0	0.3	22.0	5.0	1.0	-	-	1.0	1.0	-	-
NiMn-2	N10002	0.90	4.19	0.51	16.41	4.82	2.86	<0.001	0.050	1.10	1.10	<0.01	0.025
	Aim	1.0	5.0	0.3	17.0	5.0	3.0	-	-	1.0	1.0	-	-
NiMn-3	N10003	0.97	4.65	0.46	17.51	4.96	1.96	<0.001	0.039	<0.05	1.13	<0.01	0.019
	Aim	1.0	5.0	0.3	17.0	5.0	2.0	-		2.0	1.0	-	-
NiMn-4	N10004	0.89	5.05	0.33	16.89	4.75	1.16	0.028	0.072	1.04	1.57	0.28	0.015
	Aim	1.0	5.0	0.3	17.0	5.0	1.0	-	-	1.0	1.5	0.5	-
NiMn-5	N10005	0.93	4.80	0.32	17.17	4.72	1.17	0.009	0.071	1.10	1.13	1.16	0.014
	Aim	1.0	5.0	0.3	17.0	5.0	1.0	-	-	1.0	1.0	1.0	-
NiMn-6	N10022	1.02	4.86	0.36	16.60	5.35	2.35	0.021	0.045	2.07	1.44	<0.01	0.01
	Aim	1.0	5.0	0.3	17.0	5.0	2.0	-	-	2.0	1.0	-	-
Group 2---base XF-818													
Ni-1	N10006	0.18	0.20	0.29	18.49	18.12	7.98	0.72	0.038	<0.05	0.51	<0.01	0.005
	Aim	0.2	0.2	0.3	18.0	18.0	7.5	0.7	0.1		0.4	-	-
Ni-2	N10007	0.32	0.25	0.35	20.18	17.72	5.61	1.15	0.041	<0.05	0.54	<0.01	0.007
	Aim	0.35	0.2	0.3	18.0	18.0	5.0	1.0	0.1	-	0.4	-	-
Ni-3	N10008	0.46	0.26	0.36	20.59	17.36	5.57	1.27	0.038	<0.05	0.50	<0.01	0.009
	Aim	0.5	0.2	0.3	18.0	18.0	5.0	1.25	0.1	-	0.4	-	-
Ni-4	N10009	0.48	0.27	0.39	19.07	18.37	8.11	1.26	0.052	<0.05	0.52	<0.01	0.012
	Aim	0.5	0.2	0.3	18.0	18.0	7.5	1.25	0.1	-	0.4	-	-
Ni-5	N10010	0.11	0.26	0.36	19.74	17.91	6.54	1.44	0.072	<0.05	0.034	<0.01	0.004
	Aim	0.08	0.2	0.3	18.0	18.0	6.0	1.5	0.1	-	-	-	-
Ni-6	N10011	0.45	0.28	0.42	20.35	17.53	5.61	1.35	0.050	<0.05	0.52	<0.01	0.005
	Aim	0.5	0.2	0.3	18.0	18.0	5.0	1.25	0.2	-	0.4	-	-
Ni-7	N10015	0.25	0.39	0.37	19.57	17.73	5.37	1.35	0.047	<0.01	0.031	<0.01	0.008
	Aim	0.25	0.2	0.3	18.0	18.0	5.0	1.25	-	2.0	-	-	-
Ni-8	N10016	0.46	0.28	0.37	19.60	17.90	5.38	1.44	0.049	<0.01	0.031	<0.01	<0.008
	Aim	0.5	0.2	0.3	18.0	18.0	5.0	1.25	-	2.0	-	-	-
Ni-9	N10017	0.44	0.27	0.37	19.26	17.93	4.40	1.25	0.064	<0.01	2.01	<0.01	<0.011
	Aim	0.5	0.2	0.3	18.0	18.0	4.0	1.25	-	2.0	2.0	-	-
Ni-10	N10018	0.49	0.25	0.37	19.26	18.01	4.35	1.32	0.054	2.31	1.07	0.98	0.009
	Aim	0.5	0.2	0.3	18.0	18.0	4.0	1.25	-	2.0	1.0	1.0	-
Ni-11	N10019	0.28	2.53	0.33	20.49	7.90	5.58	1.31	0.075	<0.01	0.032	<0.01	0.009
	Aim	0.25	3.0	0.3	18.0	10.0	5.0	1.25	-	2.0	-	-	-
Ni-12	N10020	0.46	2.39	0.36	19.80	10.13	4.57	1.10	0.069	2.37	0.97	1.12	0.007
	Aim	0.5	3.0	0.3	18.0	10.0	4.0	1.25	-	2.0	1.0	1.0	-
Ni-13	N10021	0.52	0.31	0.38	20.74	17.63	5.46	1.81	0.044	<0.01	0.032	<0.01	0.004
	Aim	0.65	0.2	0.3	18.0	18.0	5.0	2.0	-	-	-	-	-
Ni-14	N10026	0.24	0.29	0.38	18.60	18.03	5.03	1.37	0.029	2.06	0.036	<0.01	0.006
	Aim	0.25	0.2	0.3	18.0	18.0	5.0	1.25	-	2.0	-	-	-
Ni-15	N10027	0.52	0.25	0.33	18.92	17.63	5.19	1.22	0.040	2.05	0.032	<0.01	0.010
	Aim	0.5	0.2	0.3	18.0	18.0	5.0	1.25	-	2.0	-	-	-
Ni-16	N10028	0.51	0.28	0.42	18.82	18.04	4.12	1.33	0.047	2.13	2.38	<0.01	0.009
	Aim	0.5	0.2	0.3	18.0	18.0	4.0	1.25	-	2.0	2.0	-	-
Ni-17	N10029	0.28	2.83	0.35	18.97	10.25	5.24	1.31	0.037	2.06	0.038	<0.01	0.005
	Aim	0.25	3.0	0.3	18.0	10.0	5.0	1.25	-	2.0	-	-	-
Group 3---base AF-71													
Mn-1	N10012	0.38	11.58	0.34	12.70	<0.10	4.00	0.25	0.043	<0.05	0.041	1.21	0.008
	Aim	0.2	18.0	0.3	12.0	-	3.0	0.2	0.2	-	-	0.9	-
Mn-2	N10013	0.34	17.80	0.31	11.82	<0.10	3.44	0.42	0.067	<0.05	0.025	0.76	0.006
	Aim	0.3	18.0	0.3	12.0	-	3.0	0.75	0.2	-	-	0.9	-
Mn-3	N10014	0.34	17.36	0.37	11.47	<0.10	5.87	0.88	0.097	<0.05	0.034	1.07	0.003
	Aim	0.3	18.0	0.3	12.0	-	5.0	1.25	0.2	-	-	0.9	-

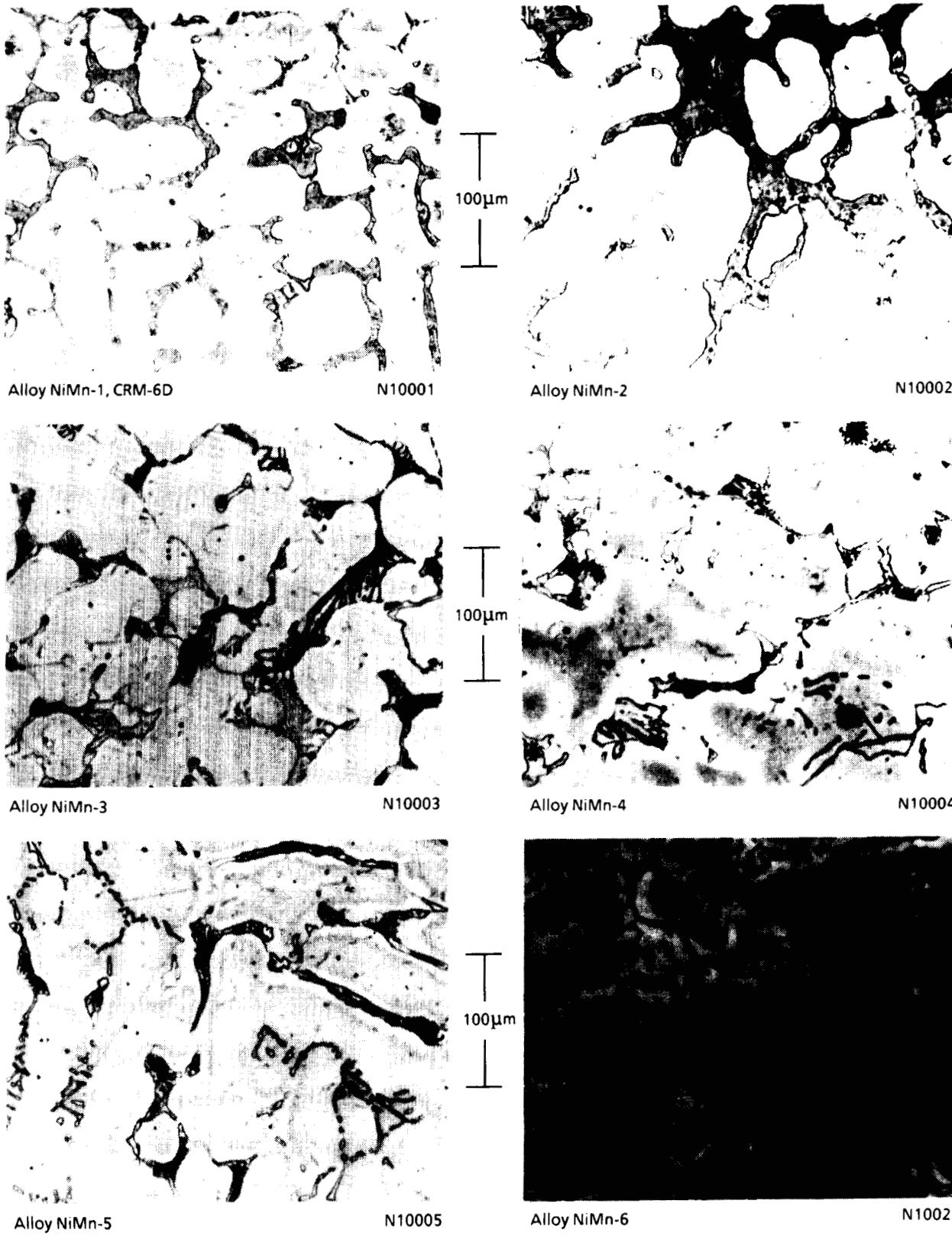

Figure /.--Optical Micrographs of Group 1 Alloys - Round 1
Etchant: Fry's Reagent.

F-33230 -A

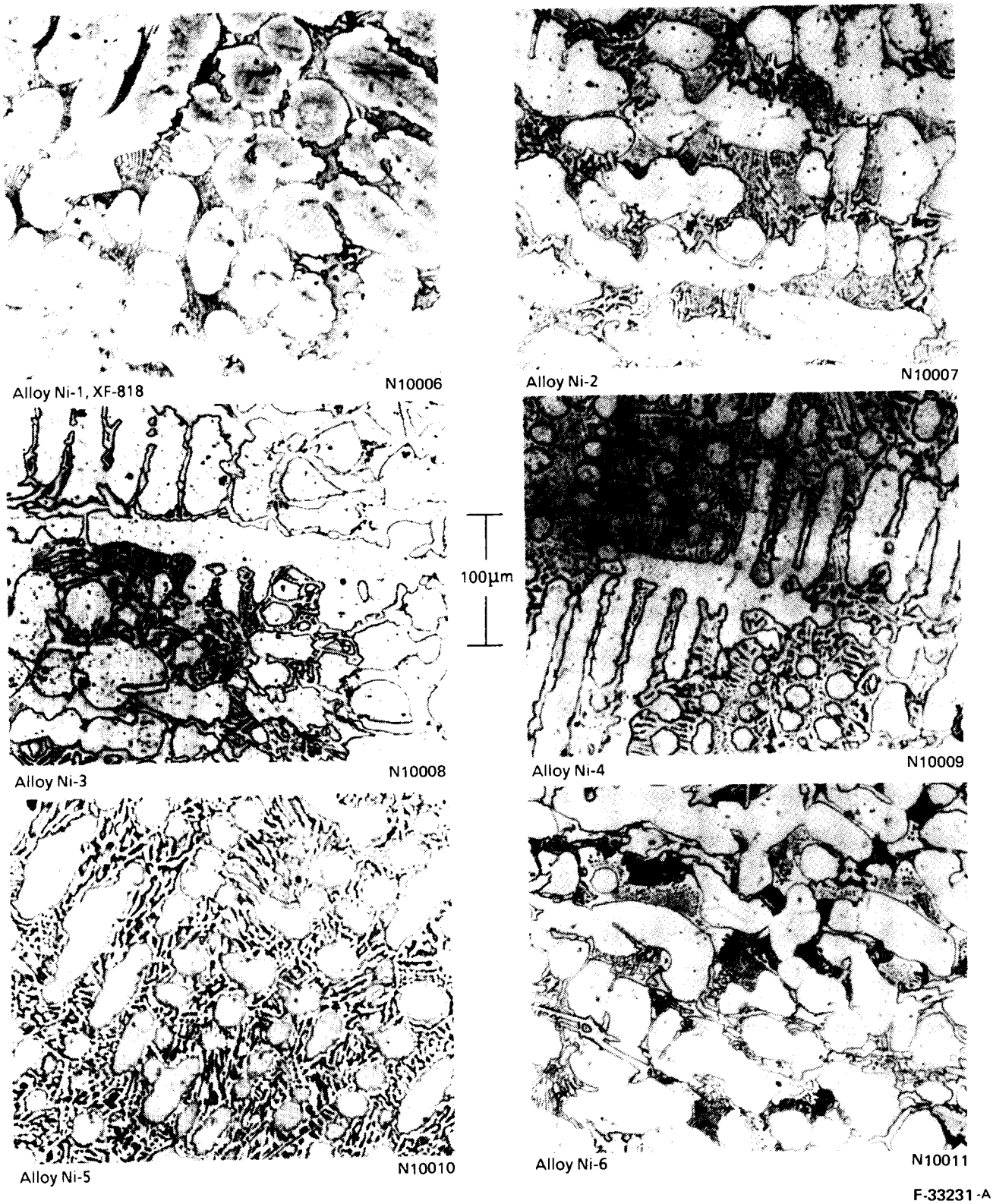

Figure 8.--Optical Micrographs of Group 2 Alloys - Round 1
Etchant: Fry's Reagent.

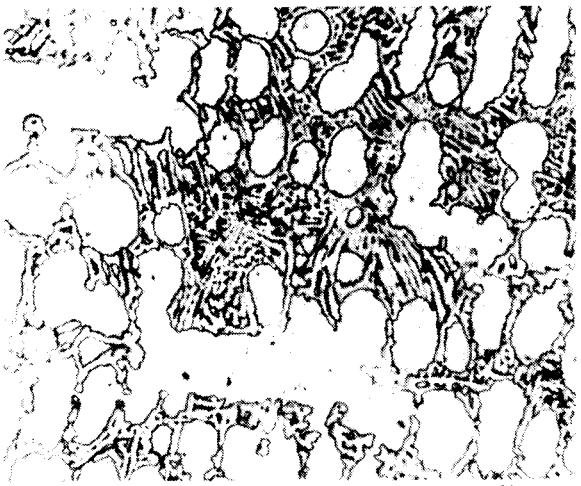

Figure 8.--Continued.

Alloy Ni-10 N10018

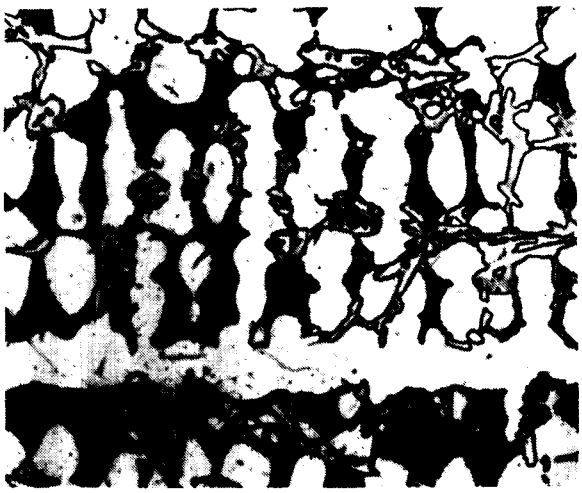

Alloy Ni-11 N10019

100µm

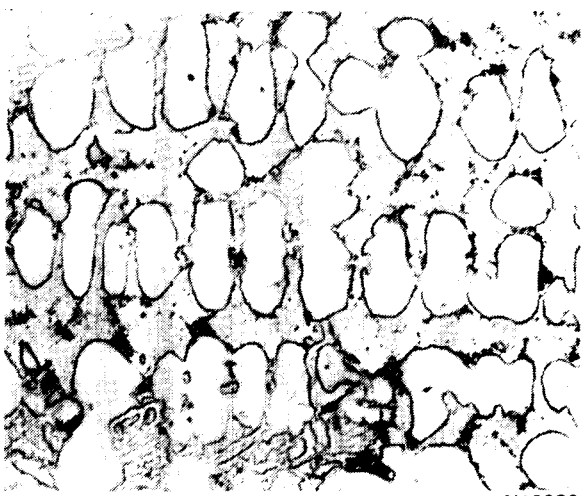

Alloy Ni-12 N10020

Alloy Ni-13 N10021

F-33232-A

Figure 8.--Continued.

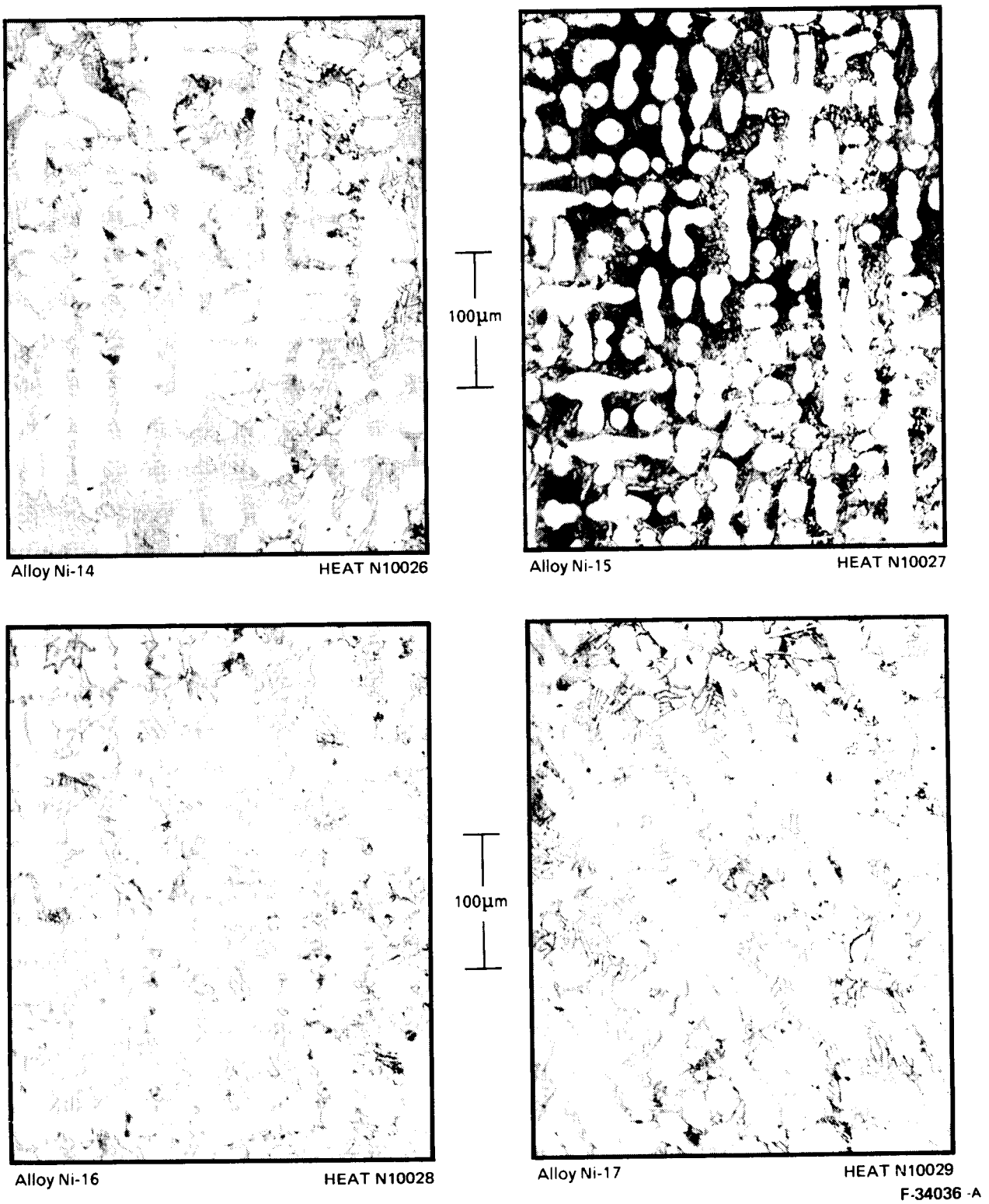

Figure 8.--Concluded.

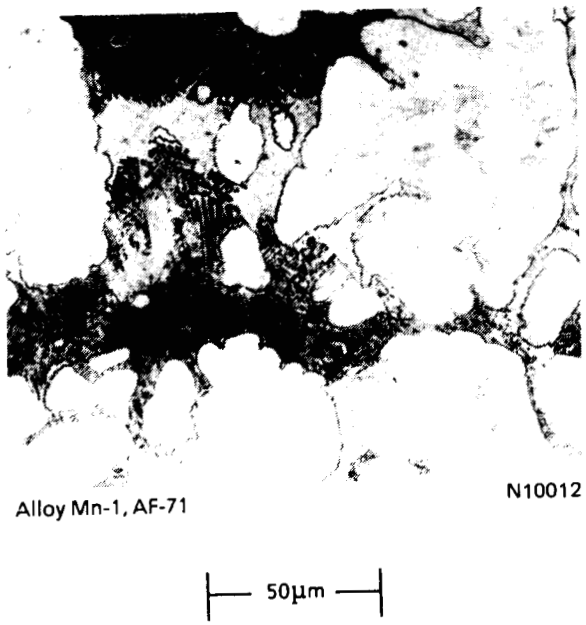

Figure 9.--Optical Micrographs of Group 3 Alloys - Round 1
Etchant: Fry's Reagent.

Stress rupture.--The results of stress rupture testing for the 26 alloys processed in the first round of screening are shown in table 7. Tests were conducted at 830°C and 200 MPa. Rupture ductility is given in percent elongation and in percent reduction in area. Also shown are applicable aging treatments.

Discussion

Table 7 shows that the stress rupture goal of 329 hr at a stress of 200 MPa and a temperature 775°C is achievable with alloys from the Group 2 base. Alloy Ni-9 surpasses the target, and alloys Ni-8, Ni-15, and Ni-16 show promise. An analysis of the results follows.

Group 1 (base CRM-6D).--Alloy NiMn-1, the Group 1 CRM-6D base composition, shows a stress-rupture result that agrees with the literature values for the alloy (fig. 1). No substantial improvement is afforded by increasing molybdenum and reducing chromium (alloy NiMn-2). However, intermediate levels of molybdenum and chromium, without tungsten, result in slight improvement (alloy NiMn-3). Vanadium additions do not result in a corresponding increase in stress-rupture life (alloys NiMn-4 and NiMn-5). None of the variations in Group 1 investigated approaches the target stress-rupture properties.

Group 2 (base XF-818).--Alloy Ni-1, the Group 2 XF-818 base composition, has stress-rupture life somewhat lower than the reported level for the alloy. However, all of the modifications have substantially better stress-rupture life. Alloy Ni-3 (containing more carbon, chromium, and boron, but less nickel and molybdenum than the base alloy) has over 20 times the rupture life of Ni-1. The higher molybdenum level appears to be detrimental (compare alloys Ni-3 and Ni-4). Increasing boron to 1.44 percent does not compensate for a reduction in carbon to 0.11 percent.

The alloys based on modified XF-818 have the best stress-rupture properties of all those investigated. In particular, alloy Ni-9 exceeds the target life, and as noted previously, Ni-8, Ni-15, and Ni-16 exhibit definite promise. In Ni-15 solution treatment resulted in improved rupture ductility, but at the expense of rupture life. Alloys with vanadium (Ni-10 and Ni-13) had very loose scale after stress-rupture testing, indicating that oxidation resistance is poor. No effect of vanadium on stress-rupture life was seen. These observations eliminated vanadium additions from further consideration.

Group 3 (base AF-71).--Alloy Mn-1, the base alloy has a stress rupture life close to that expected, even without nitrogen. Although some improvement was realized by increasing boron, solution treating the modified alloys is not possible; therefore, their potential appears to be limited. Additions, particularly of boron, result in incipient melting at solution-treatment temperatures. Oxidation during solution treatment also is severe. Aging without solution treatment did not result in promising stress-rupture life for the boron-modified alloys.

The overall analysis of this series of melts in Round 1 indicates a favorable prognosis, especially for Group 2 with tungsten additions. Group 1 has very limited possibility, yet will be kept in the program to measure the effect of slightly increased molybdenum and tungsten. Group 3 was eliminated from further study. Vanadium additions were eliminated in all groups because of the adverse effects of oxidation resistance.

TABLE 7

STRESS-RUPTURE DATA, ROUND 1

Alloy No.	Heat No.	Condition	Stress-rupture life, hr at 830°C, 200 MPa (E) (percent elongation/percent reduction of area)	Oxide characteristics
NiMn-1	N10001	As-cast 100/hr/649°C	X 31.3(4/3.7), 9.7(2/6.4)	Grey-black, tight
NiMn-2	N10002	As-cast 100 hr/649°C	X 16.0(3/14.1), 4.1(2/12.2)	Black, tight
NiMn-3	N10003	As-cast 100 hr/649°C	X 24.5(2/9.9), 84.5*	Black, tight
NiMn-4	N10004	As-cast 100 hr/649°C	X 12.9(4/7.1), 9.7(4/21.6)	Black, tight
NiMn-5	N10005	As-cast 100 hr/649°C	X 58.5(4/15.6), 9.0(4/10.7)	Black, tight
NiMn-6	N-10022	As-cast 100 hr/649°C	X 19.3(9/12.5), 11.9(10/47.5)	Grey-black, tight
Ni-1	N10006	As-cast	3.9(12/29.4), 3.6(9/20.0)	Green-black, tight
Ni-2	N10007	As-cast	22.5,* 38.4(7/15.9), 40.7(3/13.3)	Green-black, tight
Ni-3	N10008	As-cast	49.4,* 110.9(6/11.4), 89.6(5/10.7)	Black, tight
Ni-4	N10009	As-cast	55.3(2/6.5), 45.3(2/5.4)	Gray, tight
Ni-5	N10010	As-cast	12.4(7/14.6), 48.0(5/11.3)	Green-black, tight
Ni-6	N10011	As-cast	42.9(6/9.7)	Green-black, tight
Ni-7	N10015	As-cast	136(11/9.7), 57.5(6/11.4)	Green-black, tight
Ni-8	N10016	As-cast	151(3/3.6), 199.2,* 185.4(3/5.4)	Black, tight
Ni-9	N10017	As-cast	413.9(3/11.4), 318(7/15.1)	Black, tight
Ni-10	N10018	As-cast	62.8(11/13.2), 92.9(4/7.3)	Black, very loose
Ni-11	N10019	As-cast	63.1(11/20.7), 14.0(12/5.2)	Brown-green, tight
Ni-12	N10020	As-cast	67.3(4/14.1), 68.0(4/13.3)	Black, very loose
Ni-13	N10021	As-cast	15.3(10/18.1), 23.9(14/15.9)	Brown, tight
Ni-14	N10026	As-cast	128,* 107.2(6/12.1)	Green-black, tight
Ni-15	N10027	As-cast 1 hr/1177°C	177.2(2/6.2), 163.1(4/7.2), 68(12/19.5)	Green-black, tight
Ni-16	N10028	As-cast	215.4(9/14.1), 228.2(4/5.5)	Black, tight
Ni-17	N10029	As-cast	76.1(4/4.7), 112.6(8/8.3)	Brown-green, tight
Mn-1	N10012	As-cast 1 hr/1066°C/WG 16 hr/704°C	X 11.1(7/27.6), 2.0(12/32.3) 2.0(26/36.8)	Black, heavy
Mn-2	N10013	As-cast 16 hr/704°C	X X	---
Mn-3	N10014	As-cast 16 hr/704°C	X 14.4(2/8.9), 74.5(4/14.0)	Black, tight

LEGEND:

E 329 hr at 830°C and 200 MPa is equivalent in Larson-Miller parameter to 5000 hr at 775°C and 200 MPa.

X No test conducted in this condition.

* Test terminated because of equipment malfunction. Specimen not broken.

PRELIMINARY STRESS-RUPTURE SCREENING -- ROUND 2

Procedure

Casting.--As a result of the first round screening, the second series of compositions, corresponding to heats N10030 to N10045 in table 8, was cast. Chemistry modifications were made to increase the strength of the Group 1 alloys based on CRM-6D, and to retain the strength of the Group 2 alloys while decreasing raw material cost. Initial stress-rupture tests did not yield the expected results; accordingly, three additional heats (N10046, N10047, and N10048) were made in an attempt to reproduce heats N10017 (Ni-9), N10028 (Ni-16), and N10032 (Ni-8).

Testing.--Procedures used during Round 2 for stress-rupture testing were essentially the same as previously reported in Round 1. No intentional deviations were made to the procedure.

Results

Chemical analysis.--Actual and aim chemistries for all heats processed in Round 2 are shown in table 8. Conformance between the two is very good.

Metallography.--Metallographic structures of Group 1 and Group 2 heats are shown in figs. 10 and 11. Group 1 structures (fig. 10) are similar in most respects to those seen in Round 1, even with the addition of 0.5 percent boron to all but alloy NiMn-9 (N10043). Group 1 alloys NiMn-10 (N10044) and NiMn-11 (N10045) show signs of the eutectic structures previously seen in Group 2 alloys, but not the more desirable lamellar or scriptlike form.

Group 2 structures (fig. 11) again generally follow those observed previously. Exceptionally large dendrites were seen in Ni-21 (N10036) and Ni-22 (N10037). Alloys Ni-24 (N10039) and Ni-25 (N10040) have markedly different structures, despite comparable chemistries.

Stress rupture.--The results of Round 2 accelerated stress-rupture testing at 830°C and 200 MPa are given in table 9. Rupture ductility values are shown in parentheses as percent elongation/percent reduction of area.

In the Group 1 alloy heats N10041 through N10045 results were clouded by breakage of several compositions during casting. Apparently boron additions produce very brittle materials in these alloys, even in the presence of sufficient molybdenum to form the M_3B_2 eutectic.

Stress-rupture results from this series of tests, especially for Group 2, are well below those reported for first round heats (table 7). Even the three repeat heats (N10046 through N10048) did not reproduce values comparable to those of the earlier heats.

SEM-EDX evaluation.--An attempt to clarify this problem of lower stress-rupture test results was made using the scanning electron microscope (SEM) and energy dispersive X-ray (EDX) analysis to examine the fracture surfaces of samples that exhibited greatly different rupture life (figs. 12 and 13). Metallographic cross sections of stress-rupture fracture surfaces of composition Ni-9 (heats N10017 and N10046) are shown in fig. 14. The etched surface high-lights the different dendritic direction relative to the stress axis.

Discussion

Table 8 shows that the stress-rupture properties obtained in Round 2 efforts were generally below those of Round 1.

The decision was made to discontinue further work in Group 1 alloys. Also, the extreme brittleness of alloys strengthened by M_3B_2 type eutectic was the basis to eliminate this approach from the effort that followed.

Group 2 alloys offered the strongest likelihood of success in meeting the target stress-rupture properties. Program emphasis continued in this direction.

A factor considered in these initial efforts but not given serious attention was casting parameters. For comparable chemical compositions, variations in casting conditions can have significant effect on ultimate properties. A prime example is the effect of melting conditions and pour temperature on solidification rate. This directly plays a major role in determining microstructure, including dendritic orientation and extent of porosity. To meet the goals of the program, it was mandatory that we establish and control proper casting parameters.

The direction of the remainder of the program was to use those Group 2 alloys that have yielded best test performance to data and pay close attention to casting parameters and the resultant effects on microstructure and stress-rupture life.

Heat treat potential as a means of improving alloy capability was also investigated.

TABLE 8

ANALYSES OF EXPERIMENTAL ALLOYS, ROUND 2 SCREENING

Alloy No.	Heat No.	C	Mn	Si	Mg μ	Cr	Ni	Mo	B	N	W	Cb	V	O
Ni-18	N10030	0.48	0.34	0.37	<0.001	17.57	15.89	4.87	1.21	0.058	<0.0	2.13	<0.01	0.020
	Aim	0.5	0.2	0.3	--	18	16	4.5	1.25	--	--	2	--	--
Ni-19	N10031	0.43	0.33	0.34	<0.001	18.07	18.25	4.10	1.19	0.043	<0.05	1.93	<0.01	0.013
	Aim	0.5	0.2	0.3	--	18	18	3.5	1.25	--	--	2	--	--
Ni-8	N10032	0.49	0.33	0.32	<0.001	17.89	16.37	4.96	1.17	0.053	<0.05	1.00	<0.01	0.017
	Aim	0.5	0.2	0.3	--	18	16	4.5	1.25	--	--	1	--	--
Ni-9	N10033	0.49	0.33	0.40	<0.001	18.50	18.48	3.17	1.14	0.054	<0.05	3.06	<0.01	0.010
	Aim	0.5	0.2	0.3	--	18	18	3.0	1.25	--	--	3	--	--
Ni-11	N10034	0.73	0.33	0.37	<0.001	18.00	14.22	4.87	1.11	0.053	<0.05	2.15	<0.01	0.011
	Aim	0.75	0.2	0.3	--	18	14	4.5	1.25	--	--	2	--	--
Ni-20	N10035	0.73	0.33	0.37	<0.001	18.68	13.94	3.30	1.11	0.060	<0.05	3.08	<0.01	0.013
	Aim	0.75	0.2	0.3	--	18	14	3.0	1.25	--	--	3	--	--
Ni-21	N10036	0.74	0.34	0.37	<0.001	17.91	11.95	5.24	1.10	0.073	<0.05	3.14	<0.01	0.011
	Aim	0.75	0.2	0.3	--	18	12	4.5	1.25	--	--	3	--	--
Ni-22	N10037	0.71	0.55	0.34	<0.001	17.41	11.82	5.23	1.07	0.058	<0.05	2.13	<0.01	0.011
	Aim	0.75	0.2	0.3	--	18	12	4.5	1.25	--	--	2	--	--
Ni-22B	N10037B	0.70	0.37	0.32	<0.001	18.75	11.86	5.09	1.31	0.059	<0.05	0.05	<0.01	0.009
	Aim	0.75	0.2	0.3	--	18	12	4.5	1.25	--	--	2	--	--
Ni-23	N10038	0.49	0.29	0.36	<0.001	17.34	17.91	4.75	1.02	0.062	<0.05	3.21	<0.01	0.011
	Aim	0.5	0.2	0.3	--	18	18	4.0	1.25	--	--	3	--	--
Ni-24	N10039	0.45	0.30	0.33	<0.001	18.03	17.48	4.28	1.03	0.068	<0.05	2.03	<0.01	0.009
	Aim	0.5	0.2	0.3	--	18	18	3.5	1.25	0.1	--	2	--	--
Ni-25	N10040	0.48	0.32	0.35	<0.001	18.08	17.78	4.12	1.06	0.057	<0.05	2.24	<0.01	0.018
	Aim	0.5	0.2	0.3	--	18	18	3.5	1.25	0.2	--	2	--	--
NiMn-7	N10041	0.97	4.71	0.25	<0.00	17.75	4.99	4.75	0.54	0.062	<0.05	1.13	<0.01	0.005
	Aim	1.0	5	0.3	--	17	5	4.0	0.5	--	--	1	--	--
NiMn-8	N10042	0.97	4.88	0.28	<0.001	15.38	10.26	4.73	0.52	0.082	<0.05	1.13	<0.01	0.007
	Aim	1.0	5	0.3	--	17	10	4.0	0.5	--	--	1	--	--
NiMn-9	N10043	0.81	4.94	0.23	<0.001	17.89	9.97	2.75	0.026	0.064	<0.05	1.07	<0.01	0.011
	Aim	1.0	5	0.3	--	17	10	2.0	0.5	--	--	1	--	--
NiMn-10	N10044	0.45	4.74	0.25	<0.001	18.09	9.91	2.34	0.52	0.059	<0.05	1.16	<0.01	0.012
	Aim	0.5	5	0.3	--	17	10	2.0	0.5	--	--	1	--	--
NiMn-11	N10045	0.99	4.96	0.26	<0.001	18.78	5.01	2.36	0.54	0.067	<0.05	1.14	<0.01	0.016
	Aim	1.0	5	0.3	--	17	5	2.0	0.5	--	--	1	--	--
Ni-9	N10046	0.42	0.32	0.54	<0.001	17.23	18.77	4.62	1.14	0.074	<0.05	2.20	<0.01	0.015
	Aim	0.5	0.2	0.3	--	18	18	4.0	1.25	--	2.0	2.0	--	--
Ni-16	N10047	0.45	0.24	0.42	<0.001	16.31	18.45	4.41	1.26	0.090	<2.34	2.03	<0.01	0.011
	Aim	0.5	0.2	0.3	--	18	18	4.0	1.25	--	2.0	2.0	--	--
Ni-8	N10048	0.47	0.27	0.52	<0.001	17.98	15.65	5.01	1.15	0.054	<0.05	0.87	<0.01	0.0065
	Aim	0.5	0.2	0.3	--	18	16	4.5	1.25	--	--	1.0	--	--

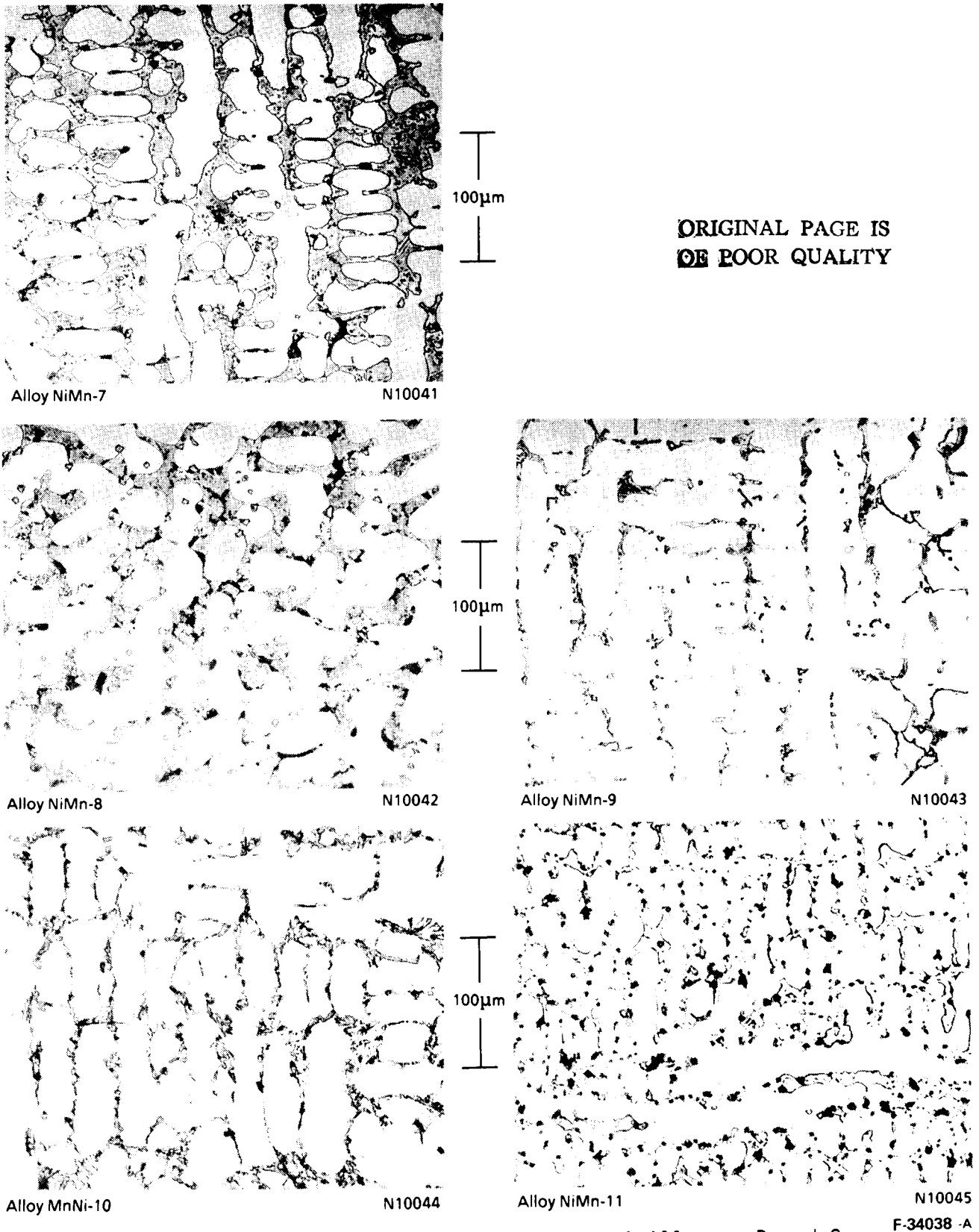

Figure 10.--Optical Micrographs of Group 1 Alloys - Round 2.
Etchant: Fry's Reagent.

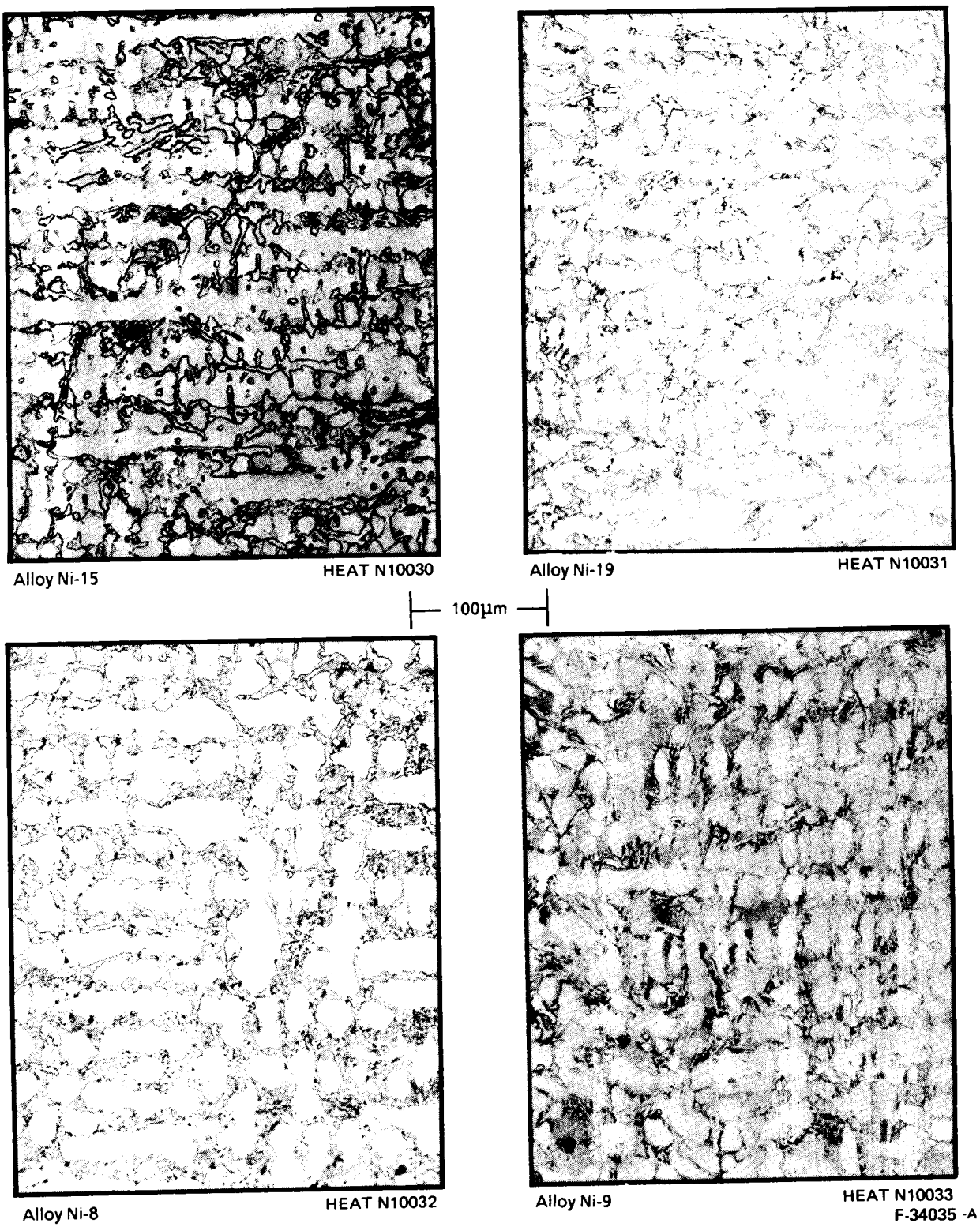

Figure 11.--Optical Micrographs of Group 2 Alloys - Round 2.
Etchant: Fry's Reagent.

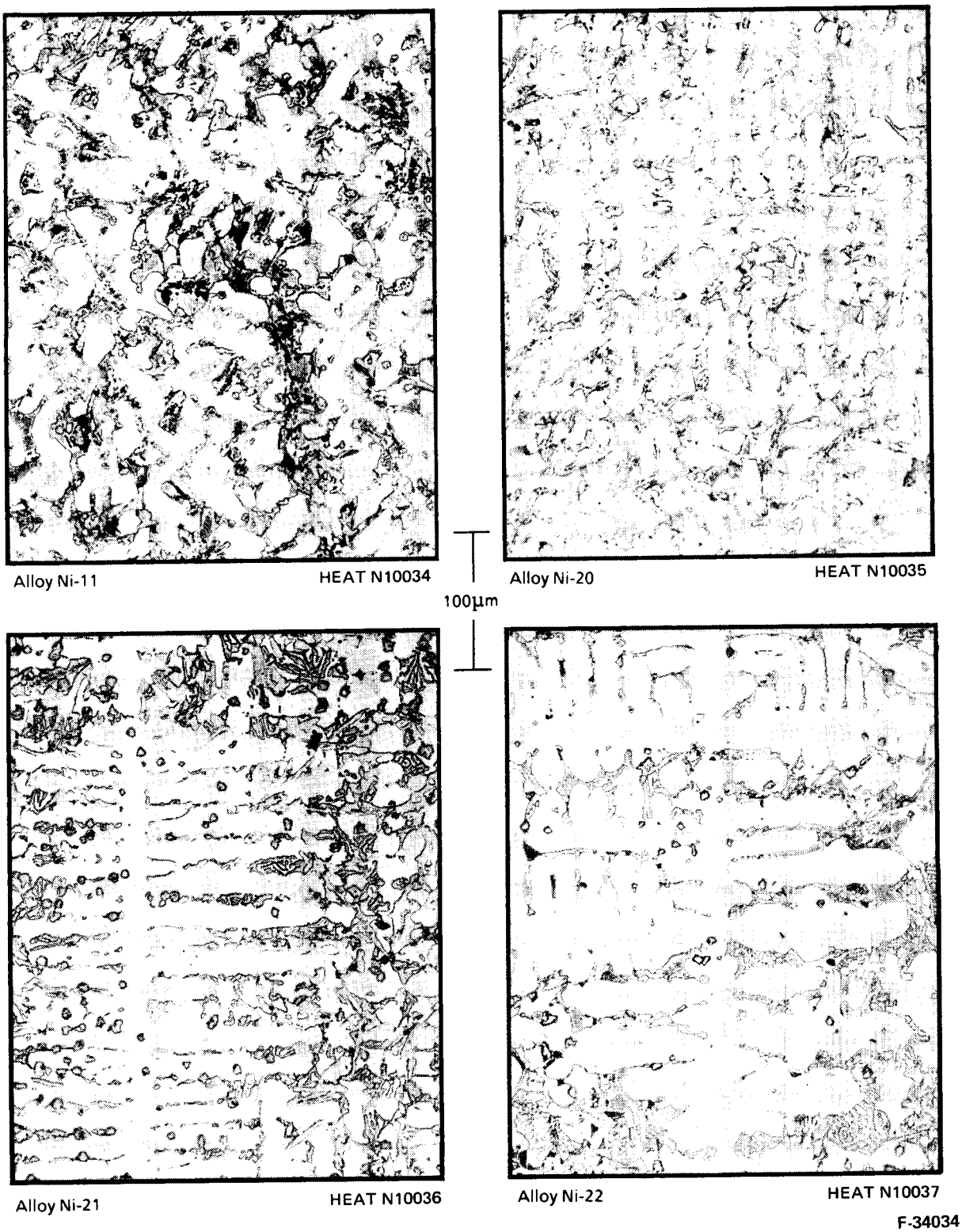

Figure 11.--Continued.

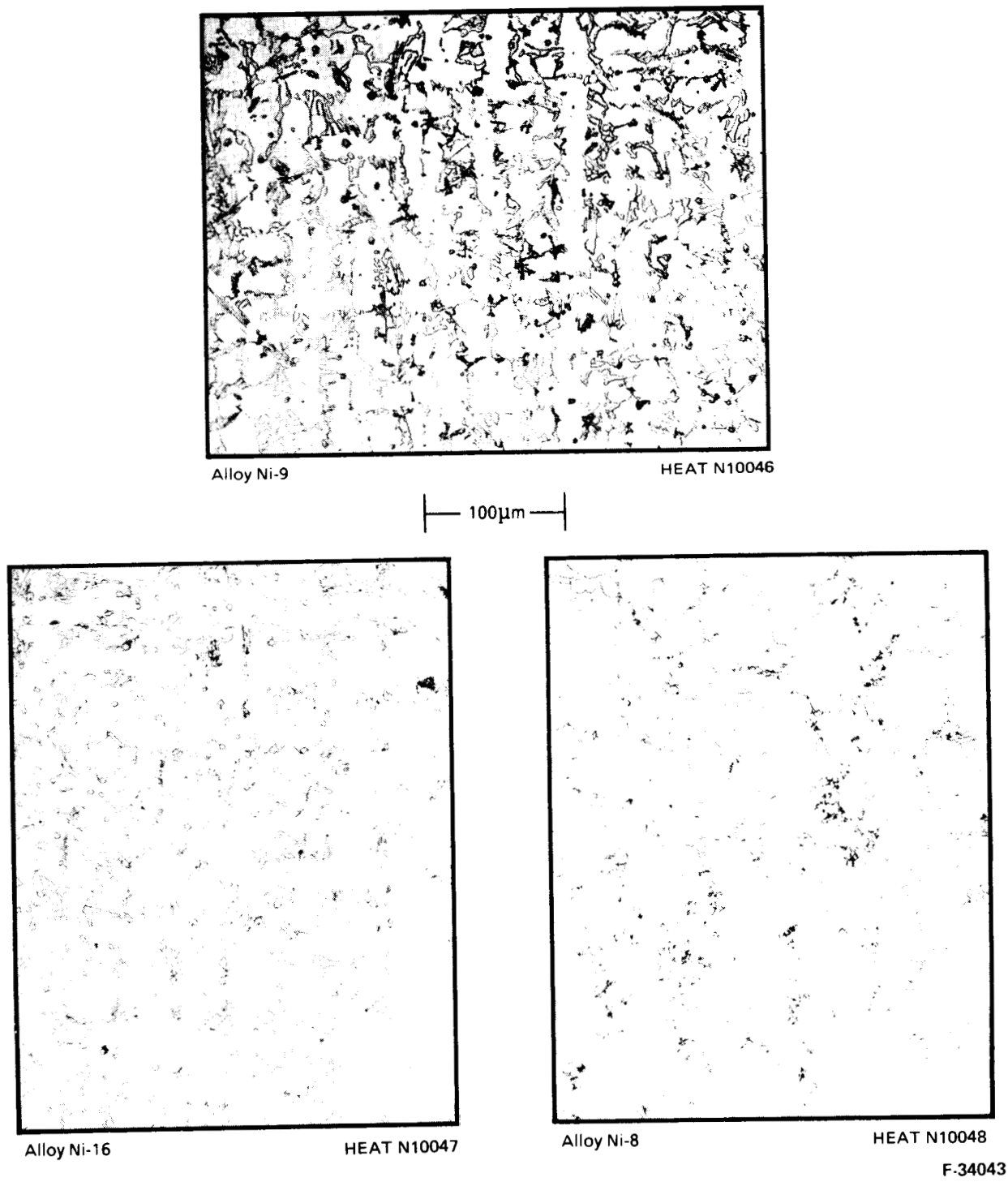

Figure 11.--Concluded.

TABLE 9

STRESS-RUPTURE DATA, ROUND 2

Alloy No.	Heat No.	Condition	Stress-rupture life, hr at 830°C, 200 MPa (E) (percent elongation/percent reduction of area)
Ni-18	N10030	As cast	137(10/15.9), 136,* 73.9(13/15.1)
Ni-19	N10031	As cast	10.8(12/13.3), 60.9(15/14.7)
Ni-8	N10032	As cast	105(9/13.8), 176(7/71), 29(10/8.9)
Ni-9	N10033	As cast	20(9/7.2), 2.6(4/1.6)
Ni-11	N10034	As cast	77,* 64(10/7.2)
Ni-20	N10035	As cast	29(5/7.9), 32(12/9.7)
Ni-21	N10036	As cast	97(9/12.4), 14(9/8.9), 39(10/11.3)
Ni-22	N10037	As cast	21(17/10.7), 36(20/14.7)
Ni-22B	N10037B	As cast	62(15/17.4), 90(20/14.7)
Ni-23	N10038	As cast	98(19/16.7), 59(10/12.5)
Ni-24	N10039	As cast	25(10/17.4), 4.5(10/12.3)
Ni-25	N10040	As cast	42(9/12.4), 35(15/12.4)
NiMn-7	N10041	As cast	50(22/4.5), 11(15/5.5)
NiMn-8	N10042	As cast	5.3(17/5.3), 6.5(8/10.7)
NiMn-9	N10043	As cast	Not tested***
NiMn-10	N10044	As cast	3.6(18/6.3), 5.8(30/13.1)
NiMn-11	N10045	As cast	Not tested***
Ni-9	N10046	As cast	54(13/15.9), 16(11/12.4)
Ni-16	N10047	As cast	66,* 159(11/8.2)
Ni-8	N10048	As cast	22(9/10.6), 19(/11.6)

*Test terminated due to equipment malfunction. Specimen not broken.
**Target is 42.0 min.
***Composition too brittle to fabricate test specimens.

LEGEND:

E 329 hr at 830°C is equivalent in Larson-Miller parameter to 5000 hr at 775°C

FRACTURE SURFACE AT 1200X

1587µm

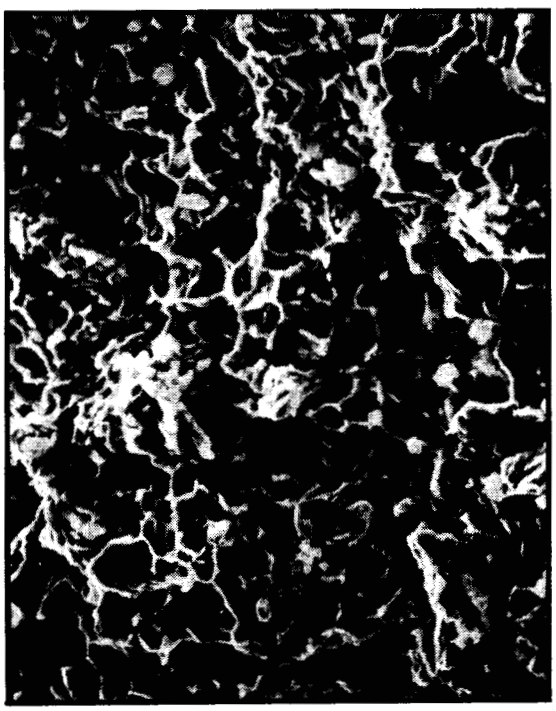

FRACTURE AREA 1 AT 800X

FRACTURE AREA 2 AT 800X

25µm

F-34041 -A

Figure 12.--Scanning Electron Microscope (SEM) Photographs of Rupture Specimen--Alloy Ni-9 Heat N10017, 414 Hr.

FRACTURE SURFACE AT 1200X

1587µm

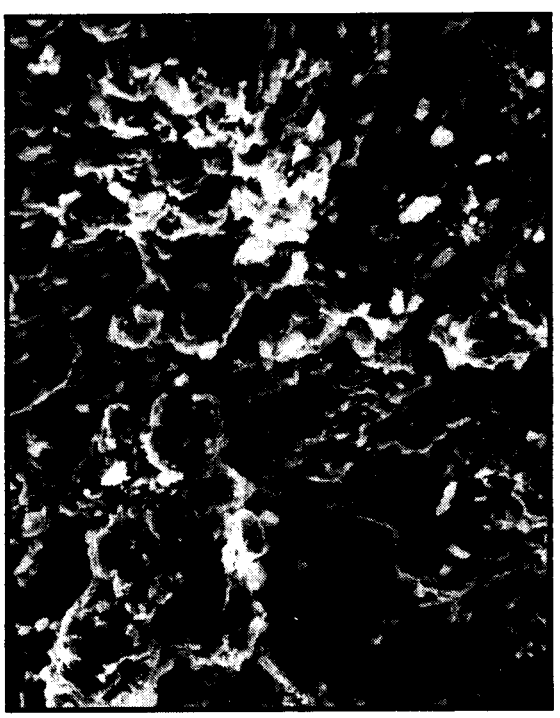

FRACTURE AREA 1 AT 800X

FRACTURE AREA 2 AT 800X

25µm

F-34042 -A

Figure 13.--SEM Photographs of Rupture Specimen--Alloy Ni-9, Heat N10046, 16 Hr.

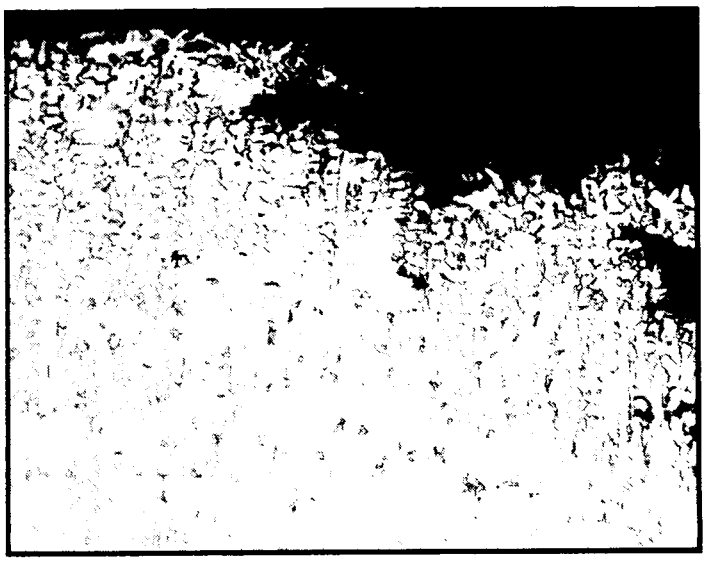

Alloy Ni-9 (FIRST MELT) HEAT N10017

(a) STRESS RUPTURE LIFE AT 830°C AND 200 MPa : 414 HR

200µm

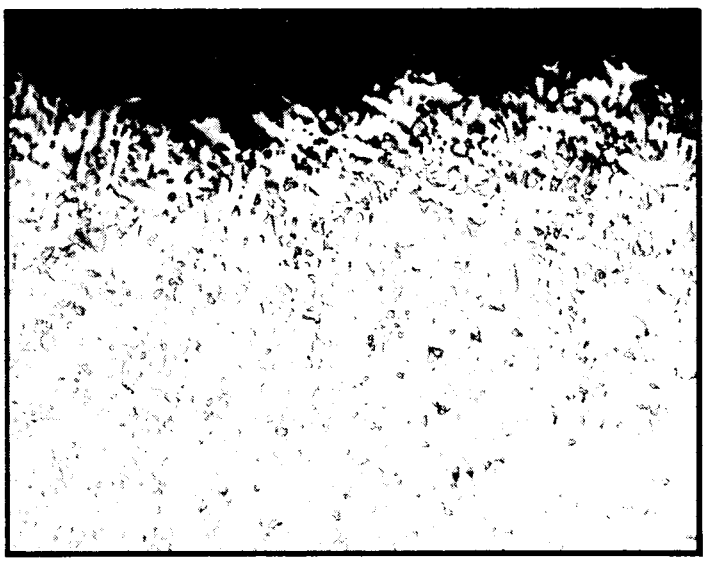

STRESS AXIS

Alloy Ni-9 (REPEAT MELT) HEAT N10046

F-34040 -A

(b) STRESS RUPTURE LIFE AT 830°C AND 200 MPa :16 HR

Figure 14.--Optical Micrographs Showing Dendrite Orientation vs Stress Rupture Life. Fracture Faces are at Top. Etchant: Fry's Reagent.

STUDY OF CASTING VARIABLES

The main objective of this study was to determine the effect of mold and metal temperature variation on stress-rupture properties.

Procedures

Casting.--Investment cast specimens were prepared using the lost wax process. Seven round stress-rupture specimens of the type shown in fig. 4 and one castability test tab, shown in fig. 3, were cast using the same gating practice as reported previously. Three of the stress-rupture specimens were cast to size (0.635-cm-dia gage section). Four others were cast using wax patterns that had been dipped in wax to increase the cross section (to about 0.69 cm), allowing for finish-machining to the 0.635-cm gage diameter, and to eliminate the effects of casting surface defects.

As discussed previously, better understanding of the effects of casting variables on these alloys was needed before attempting to fine-tune composition and perform extensive testing. Accordingly, the best three alloys, Ni-9, Ni-16 and Ni-8 (table 8), all from Group 2, were subjected to variations in casting cooling rate.

Three casting conditions were used as follows:

(1) Pour at 75°C above the liquidus into standard investment shell mold preheated to 816°C.

(2) Pour at 75°C above the liquidus into standard investment shell mold preheated to 927°C.

(3) Pour at 75°C above the liquidus into heavily Kaowool-insulated investment shell mold preheated to 927°C.

The same raw materials were used as those for previous heats, namely electrolytic Fe, carbonyl Ni, vacuum-grade Cr, melting grade Mo, electrolytic Mn, melting Grade C, elemental W, and ferroalloys of Cb, B, and Si. The melt procedure is given in table 10.

Three 4.5-kg heats of each alloy were induction-melted in air and poured into molds preheated to the temperatures shown and wrapped as noted in three casting conditions. A uniform pouring temperature of 1343°C was used. Actual liquidus and pouring temperatures are shown in table 11. The pouring temperature was 121°C lower than the pouring temperature used in the screening study.

Testing.--After mold removal, cutting, and sandblasting, specimens were radiographed to check for porosity and voids. Specimens for chemical analysis and metallographic examination were cut from the bottom gating. An additional metallographic specimen was cut from the castability test tab of each casting.

TABLE 10

MELTING PROCEDURE

Charge 1/2 Fe, Ni, C, 1/3 FeSi, 1/3 Cr, bal. Fe
Melt down
Add Mo, W
heat to 1593°C
Add balance FeSi, Mn, balance Cr
Reheat to 1593°C
Cool to 1538°C, slag
Add FeCb, FeB
Cool to liquidus (LT). (Measure LT on at least first heat of each alloy.)
Heat to LT + 75°C
Slag
Pour

TABLE 11

LIQUIDUS AND POURING TEMPERATURES

Alloy no.	Heat no.	Liquidus, °C determined from arrest	Pouring temperature, °C
Ni-9	N10049	1271	1343
	N10050	-	1343
	N10051	-	1343
Ni-16	N10052	1266	1343
	N10053	-	1343
	N10054	-	1343
Ni-8	N10055	1266	1343
	N10056	-	1343
	N10057	-	1343

Evaluation was by stress-rupture testing using duplicate standard machined test bars. The best casting procedure emerging from this series of pours would be used in further studies.

Results

Casting quality.--Quality of the casting was excellent. no misrun, non-fill, or hot tearing was observed in any casting. Note that the castability test tab includes a section that is 0.060 cm in diameter. Remarkably, this small cross section is filled consistently when an Fe-base alloy is poured at 1343°C into a mold heated to only 815°C. Radiographic quality of the test specimens was excellent, with little or no porosity. In general, quality of the round bars was better than that of the longer stress-rupture bars with flat grip sections that were cast earlier in the program.

Chemical analysis.--Results of the chemical analysis are shown in table 12. Note that within each alloy the three heats are consistent. However, systematic deviations from target levels can be noted for several elements. Tungsten, in particular, is analyzed at significantly higher levels than the 2 percent added, which suggests analytical error. The question of possible analytical error was addressed; however, the conclusions of this casting study were not substantially affected by any uncertainty regarding the exact composition.

Metallography.--Metallographic structures of specimens taken from the lower gating are shown in fig. 15. This is the same location previously used for metallographic examination, so structures could be compared with those shown previously. Fig. 16 shows structures of specimens taken from the castability test tab. These specimens were examined because the cooling rates should be comparable to those of the gage section of the test specimens since their cross sections and location within the casting are similar.

As expected, the microstructure shows that dendrite arm spacing varies with casting condition and with section size. Specimens from the 0.635-cm section of the castability test tab show much finer structures than those from the 1.90-cm section gating of the same casting.

Stress-rupture.--Results of stress-rupture testing are shown in table 13. Two tests results are shown for each condition. In general, all specimens except those from the insulated molds gave stress-rupture lives that were in the range of interest; i.e., they equalled or exceeded the 65-hr life of X-40 at the same test conditions. The best properties were obtained from Alloy Ni-8 in the most rapidly cooled condition (816°C mold). Stress-rupture lives essentially equal to the 329-hr target were obtained. As-cast surfaces might have led to some of the inconsistencies noted previously; however, as-cast specimens consistently gave longer stress-rupture lives in this study than did those from which the surface was removed by machining.

TABLE 12

ANALYSES OF EXPERIMENTAL ALLOYS

Alloy No.	Heat No.	Weight percent (bal. Fe)											
		C	Mn	Si	Mg	Cr	Ni	Mo	B	N	W	Cb	O
Ni-9	N10049	0.53	0.24	0.43	<0.001	17.95	17.81	4.43	1.27	0.061	<0.05	2.08	0.011
	N10050	0.50	0.20	0.38	<0.001	17.83	17.71	4.51	1.20	0.053	<0.05	2.07	0.011
	N10051	0.50	0.23	0.39	<0.001	18.20	17.67	4.50	1.22	0.048	<0.05	2.10	0.0073
	Target	0.50	0.20	0.30	--	18.00	18.00	4.00	1.25	--	--	2.00	--
Ni-16	N10052	0.51	0.26	0.43	<0.001	17.00	17.85	4.28	1.23	0.046	2.67	1.99	0.0079
	N10053	0.48	0.24	0.43	<0.001	16.71	17.47	4.24	1.27	0.051	2.49	2.00	0.0092
	N10054	0.50	0.26	0.45	<0.001	17.06	17.23	4.32	1.28	0.057	2.75	2.09	0.011
	Target	0.50	0.20	0.30	--	18.00	18.00	4.00	1.25	--	2.00	2.00	--
Ni-8	N10055	0.53	0.25	0.40	<0.001	17.25	17.16	5.30	1.24	0.048	2.52	0.076	0.0067
	N10056	0.49	0.22	0.35	<0.001	17.20	17.45	5.19	1.26	0.042	2.49	0.11	0.0064
	N10057	0.47	0.23	0.36	<0.001	17.29	17.07	5.14	1.27	0.050	2.65	<0.05	0.0080
	Target	0.50	0.20	0.30	--	18.00	18.00	5.00	1.25	--	2.00	--	--

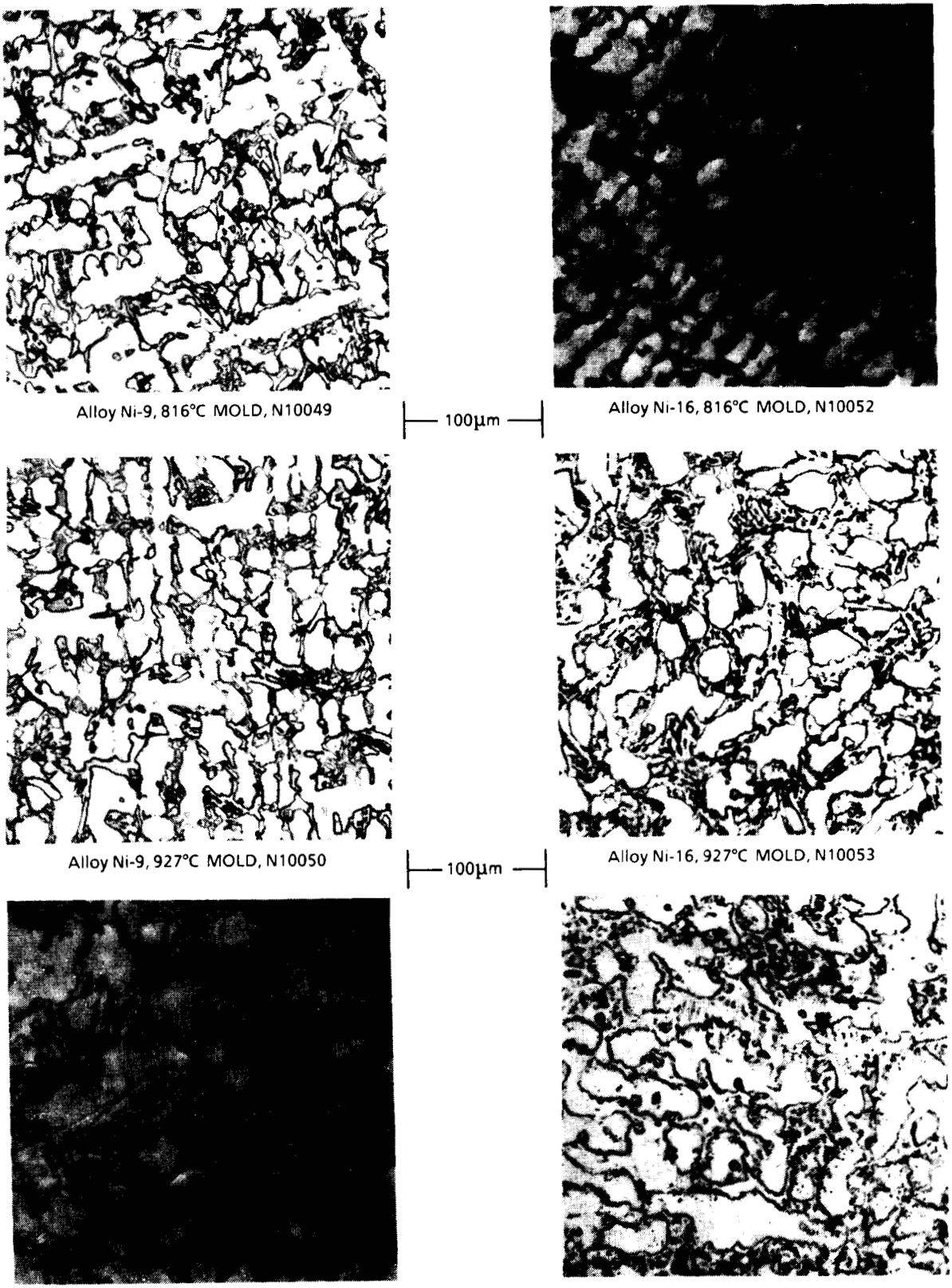

Figure 15.--Optical Micrographs from Lower Gates of Molds; Etchant, Fry's Reagent. F-34667-A

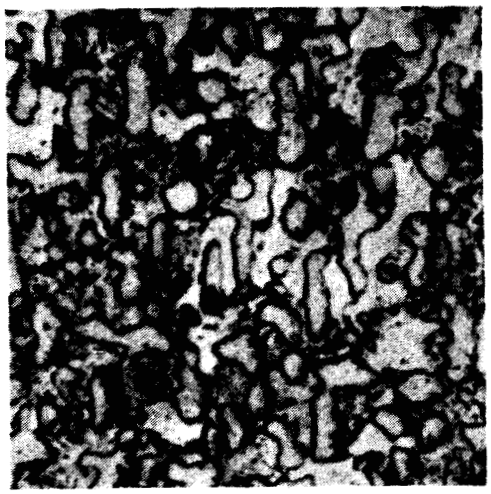

Alloy Ni-8, 816°C MOLD, N10055

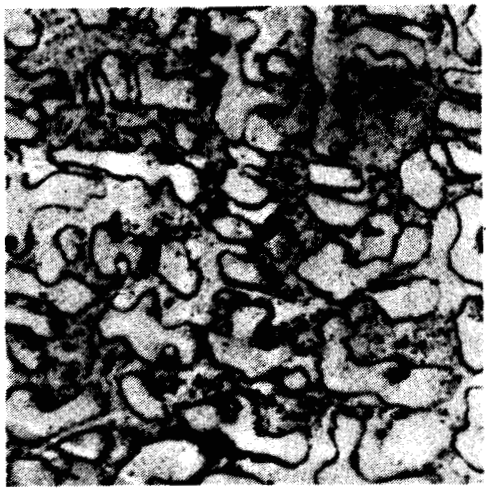

Alloy Ni-8, 927°C MOLD, N10056

Alloy Ni-8, INSULATED 927°C MOLD, N10057

F-34666 -A

100µm

Figure 15.--Concluded.

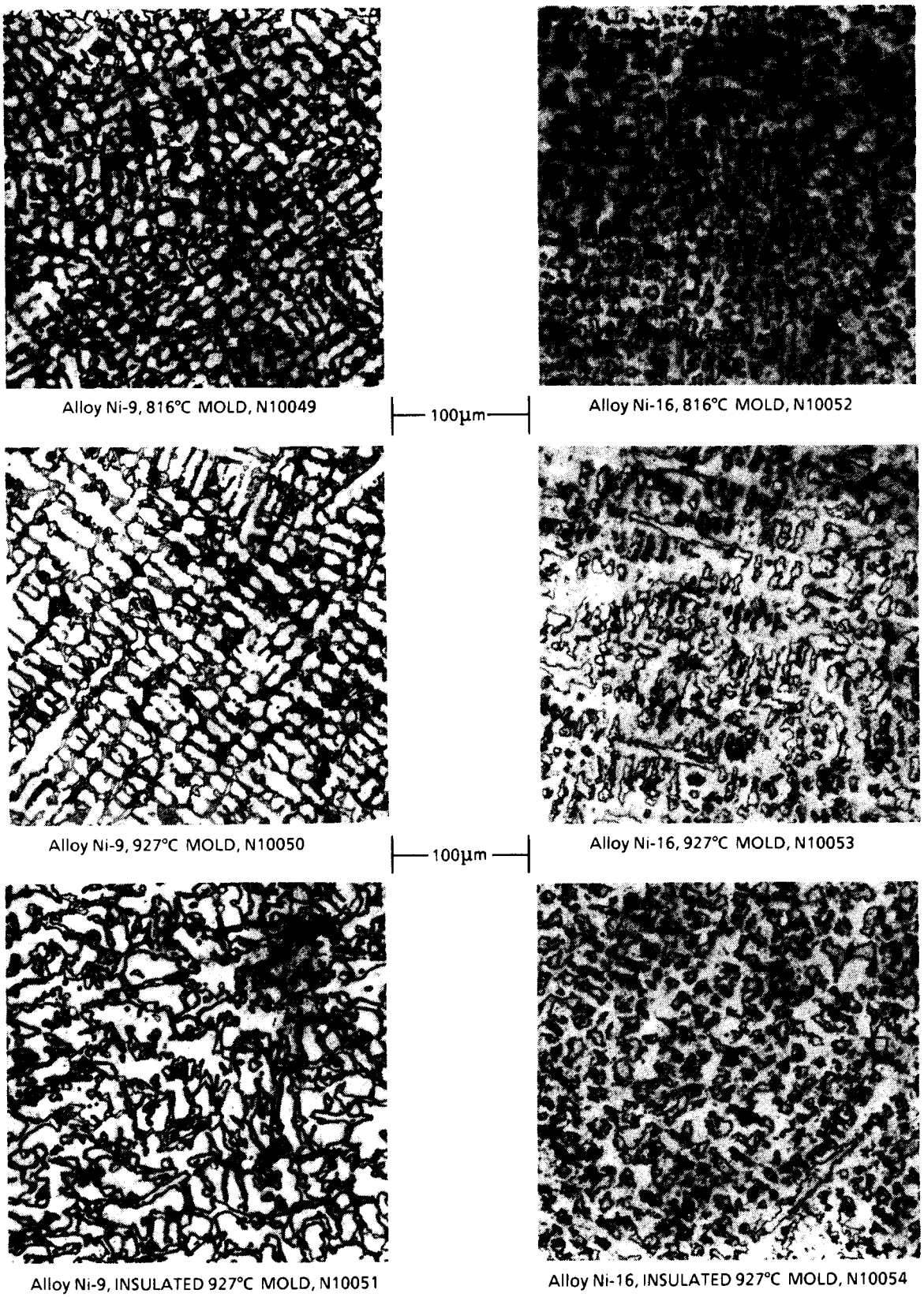

F-34665 -A

Figure 16.--Optical Micrographs from Castability Tabs; Etchant, Fry's Reagent.

TABLE 13

STRESS-RUPTURE RESULTS

Alloy No.	Heat No.	Casting condition[1]	Estimated average dendrite arm spacing,[2] microns	Stress-rupture life, hours at 830°C and 200 MPa (elongation, %/red. of area, %)			
				As-cast		Machined	
Ni-9	N10049	A	450	N/A[3]	N/A	92.6 (10.2/12.5)	93.7 (10.5/13.0)
	N10050	B	500	105.0 (9.0/13.9)	96.4 (8.9/12.3)	62.8 (10.5/13.3)	63.9 (9.3/13.5)
	N10051	C	625	31.8 (7.0/10.0)	30.0 (6.5/13.0)	20.9 (8.0/11.0)	21.7 (9.3/10.8)
Ni-16	N10052	A	350	163.3 (11.0/14.7)	183.2(11.0/14.3)	119.9 (9.9/13.0)	102.5 (11.6/15.8)
	N10053	B	450	196.4 (6.8/9.2)	175.4 (4.6/7.2)	110.3 (8.2/9.0)	104.4 (7.2/10.1)
	N10054	C	475	32.2 (12.4/16.0)	39.5 (11.8/13.9)	29.7 (7.5/9.8)	34.5 (9.7/12.2)
Ni-8	N10055	A	415	326.4 (8.0/11.3)	320.5 (5.3/7.7)	232.7 (8.5/16.0)	336.7 (8.7, 10.1)
	N10056	B	700	175.0 (4.0/6.5)	201.9 (4.8/8.0)	153.2 (5.6/6.7)	125.0 (5.2/6.7)
	N10057	C	800	47.2 (5.6/11.6)	46.8 (5.3/17.0)	39.8 (7.3/11.6)	46.0 (7.6/13.2)

[1]Casting conditions: A = cast into 816°C mold; B = cast into 927°C mold; C = cast into 927°C mold insulated with two layers of 1-cm Kaowool.

[2]From cross sections of castability test tabs.

[3]N/A = Specimen not available because of breakage during mold removal and cutoff.

Discussion

The result of the study of casting variables showed that pour temperature and mold preheat temperature must be kept to a minimum while maintaining casting quality. The compositions of these alloys will allow pouring temperatures as low as 1343°C, and possibly lower. The mold temperatures should be no higher than 816°C. The benefit of rapid cooling on stress-rupture properties, combined with the low freezing temperature of the alloys, suggests that techniques such as permanent-mold casting, die casting, or sand or investment casting using mold materials selected for maximum chill effect may improve properties greatly. In the case of the first two methods, productivity also could be maximized.

SELECTION OF EIGHT ALLOYS

The decision was made on completion of the second round of preliminary processing and testing to continue the program with Group 2 alloys only. The need for 18 percent nickel for stabilizing the ductile austenitic matrix and 18 percent chromium for corrosion resistance is recognized. Also, molybdenum is required for solution strengthening as well as for the precipitation of molybdenum borides. Since molybdenum contents above 5 percent did not increase rupture life, 5 percent is sufficient for maximum strengthening. The variables not sufficiently understood are the effects of precipitation strengtheners such as boron, tungsten, and columbium; therefore, by varying the amounts of these three elements over eight compositions, the effects on rupture life and elongation can be measured. Table 14 represents the attempted and actual chemistries for the eight selected alloys in the first iteration evaluation.

TABLE 14

ANALYSES OF EXPERIMENTAL ALLOYS, ALLOY EVALUATION

Alloy No.	Heat No.	Weight Percent (Balance Fe)														
		C	Mn	Si	Cr	Ni	Mo	W	Cb	B	Co	Cu	N	O	S	P
Ni-26	N10058	0.52	0.24	0.42	17.10	18.06	5.45	0.062	1.64	1.04	N.A.	N.A.	0.047	0.017	0.006	0.007
	target	0.5	0.2	0.3	18.0	18.0	5.0	0	2.0	0.9	-	-	-	-	-	-
Ni-27	N10059	0.50	0.21	0.34	17.03	17.88	5.09	2.19	<0.05	1.09	N.A.	N.A.	0.040	0.012	0.005	0.007
	target	0.5	0.2	0.3	18.0	18.0	5.0	2.0	0	0.9	-	-	-	-	-	-
Ni-28	N10060	0.51	0.24	0.40	16.86	18.39	5.19	2.26	1.20	1.07	N.A.	N.A.	0.040	0.0087	0.004	0.007
	N10071	0.53	0.21	0.38	16.70	18.28	5.34	2.33	1.94	0.92	N.A.	N.A.	0.058	0.0088	0.005	0.009
	target	0.5	0.2	0.3	18.0	18.0	5.0	2.0	2.0	0.9	-	-	-	-	-	-
Ni-29	N10061	0.52	0.22	0.33	17.81	17.74	5.52	<0.05	<0.05	1.07	0.05	0.05	0.064	0.012	0.005	0.006
	target	0.5	0.2	0.3	18.0	18.0	5.0	0	0	0.9	-	-	-	-	-	-
Ni-30	N10062*	0.48	0.24	0.43	16.70	18.14	5.34	<0.05	1.96	0.52	N.A.	N.A.	0.022	0.013	0.005	0.007
Ni-30B	N10067	0.47	0.21	0.40	16.69	18.30	5.39	<0.05	1.95	1.26	N.A.	N.A.	0.047	0.0071	0.005	0.009
	target	0.5	0.2	0.3	18.0	18.0	5.0	0	2.0	1.50	-	-	-	-	-	-
Ni-31	N10063*	0.49	0.19	0.29	16.52	17.82	5.17	2.18	<0.05	0.52	N.A.	N.A.	0.084	0.016	0.004	0.006
Ni-31B	N10068	0.53	0.21	0.30	16.53	18.25	5.18	2.28	<0.05	1.31	N.A.	N.A.	0.033	0.0086	0.005	0.007
	target	0.5	0.2	0.3	18.0	18.0	5.0	2.0	0	1.50	-	-	-	-	-	-
Ni-32	N10064	0.50	0.21	0.43	15.96	18.27	5.26	2.23	2.03	0.48	N.A.	N.A.	0.048	0.017	0.005	0.008
Ni-32B	N10069	0.49	0.24	0.48	16.58	18.63	5.37	2.31	2.41	1.19	N.A.	N.A.	0.046	0.0078	0.004	0.010
	target	0.5	0.2	0.3	18.0	18.0	5.0	2.0	2.0	1.50	-	-	-	-	-	-
Ni-34	N10065*	0.41	0.31	0.25	17.58	18.15	4.99	0.14	<0.05	0.33	1.27	<0.05	0.045	0.015	0.005	0.005
Ni-34B	N10070	0.53	0.24	0.33	18.31	18.05	5.54	<0.05	0.47	1.21	N.A.	N.A.	0.051	0.0114	0.007	0.007
	target	0.5	0.2	0.3	18.0	18.0	5.0	0	0	1.50	-	-	-	-	-	-
N-155	N10066**	0.078	0.92	0.54	23.86	19.60	3.24	2.48	1.13	<0.001	19.46	0.18	0.13	0.035	0.006	0.006
	target	0.1	1.5	0.5	21.0	20.0	3.0	2.5	1.0	-	20.0	0.3	0.15	-	-	-

* = No mechanical testing or oxidation testing performed due to low B
** = Oxidation testing only

LEGEND:

N.A. = Not analyzed

EVALUATION OF EIGHT ALLOYS -- FIRST ITERATION

Procedure

Casting.--Investment cast specimens were prepared using the lost wax process. For each mold, 16 round tensile/creep-rupture specimen wax patterns (fig. 20) were dipped in wax to provide oversized cast specimens of 0.712 cm diameter. Four additional wax patterns were used for oxidation test specimens. One castability test tab pattern (fig. 3) was included. A partial wax pattern assembly is shown in fig. 17, which also shows the numbering system for the individual specimens. An inserted ceramic pouring cup was used for each mold to add sufficient strength to allow pouring on the rollover furnace. An assembled mold is shown in fig. 18.

Melts of the eight target compositions shown in table 14 were prepared from the raw materials shown in table 4 with the deletion of high nitrogen ferrochromium and ferrovanadium. A heat of alloy N-155 was prepared for use in comparative oxidation testing.

Melt charge weight was 11 kg. Molds were preheated to 816°C and metal pouring temperature was 55°C above the liquidus temperature for each heat. Alloys were melted according to the melt procedure shown in table 15 using a 90-kw air induction rollover furnace with a magnesia crucible. After mold removal, cutting, and sandblasting, samples were radiographed to check for porosity and voids. Chemical analysis revealed (and melt records confirmed) an error in the boron addition to Heats N10062 through N10065. Remelts were prepared and, except for metallographic examination, no further testing was conducted on Heats N10062, N10063, and N10065. Heat N10064 was carried through the test program to further evaluate the effects of lower boron content in the highest columbium and tungsten ranges. Compositions of all heats melted are shown in table 14.

Inclusions with high X-ray density were detected in radiographs of several heats; however, sufficient specimens without inclusions were available for testing. SEM-EDX examination showed the inclusions to contain columbium and iron. Apparently, insufficient time had been allowed for complete dissolution of ferrocolumbium in the melt. Heats subsequently melted were subjected to a longer hold at temperature after the ferrocolumbium addition.

Testing.--Duplicate tensile tests were conducted at 26° and 775°C. Specimen gage sections were machined to 0.635-cm dia. The loading rate was 0.005 cm/cm/min until yield and 0.05 cm/cm/min thereafter. Data were recorded for 0.2 percent offset yield stress, ultimate tensile stress, percent of elongation, and percent reduction in area.

Duplicate creep tests were conducted at 775°C and at a stress level of 200 MPa, in accordance with ASTM Standard E139. Specimens were step-loaded to the test load, and strain on loading was measured. Continuous strain-vs-time records were made, and data were plotted. Testing was terminated by step loading to rupture after a 1 percent strain was reached, or after 500 hr, whichever came first. Time to 1 percent creep or creep deformation before loading to

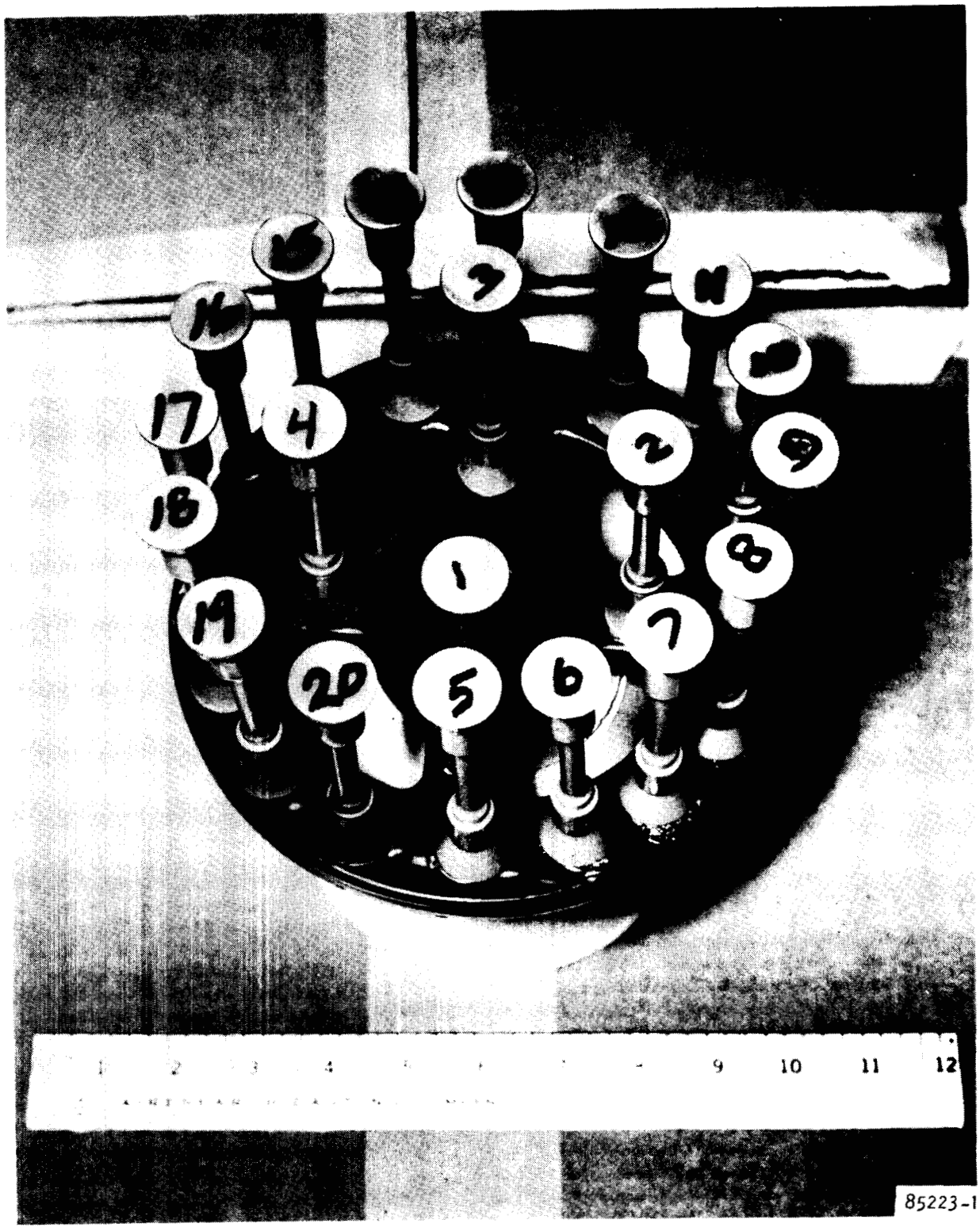

Figure 17.--Partial Wax Pattern Assembly Showing Sequence of Identification Numbers.

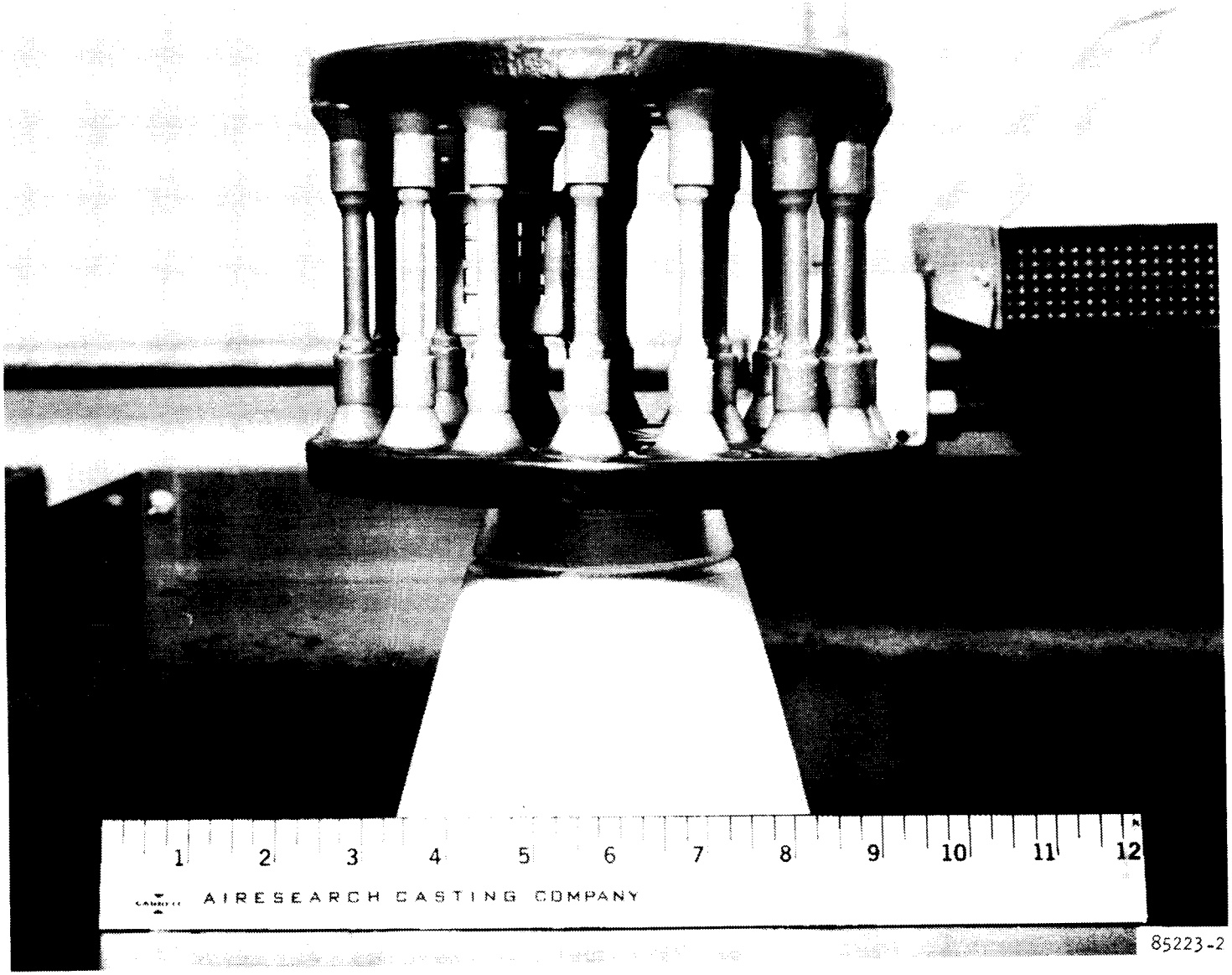

Figure 18.--Wax Pattern Assembly Before Dipping to Form Mold.
(Note Ceramic Pouring Cup at Bottom).

TABLE 15

MELTING PROCEDURE

Charge 1/2 Fe, Ni, C, 1/3 FeSi, 1/3 Cr, bal. Fe
Melt down
Add Mo, W
Heat to 1593°C
Add balance FeSi, Mn, balance Cr
Reheat to 1593°C
Cool to 1538°C slag
Add FeCb, FeB
Reheat to 1538°C, hold 1 min*
Cool to liquidus (LT)
Heat to LT + 55°C
Slag
Pour

*Used on Heats N10067 through N10071 only

failure, time to rupture (same as time at final creep reading), total elongation to rupture, and reduction in area were recorded. Minimum creep rate was determined from the plot of creep deformation vs time.

For oxidation test specimens, gage sections of 0.635-cm dia as-cast tensile test bars were ground to 0.610 cm dia (fig. 19). Specimens were cleaned with alcohol, weighed, and placed in quartz crucibles at 17 mm I.D. by 30 mm height. Crucibles with samples were weighed. Duplicate specimens were exposed in a resistance-heated muffle furnace. Each cycle included 60 min at temperature. Cooling was accomplished by manually removing the specimen tray from the furnace and waiting at least 5 min. Specific weight change ($\Delta W/A$) was determined after 1, 7, 14, 20, 40, 60, 80, and 100 hr of cumulative exposure. Samples were reweighed without crucibles after the test was completed.

Four as-cast tensile specimens from each of the heats to be evaluated for hydrogen embrittlement were placed in a tubular retort fabricated from Type 316 stainless steel. The system was flushed at ambient temperature overnight with cryogenic argon; then the argon was flushed out with ultrapure hydrogen to achieve approximately 50 volume changes. Specified oxygen content of the hydrogen was 1.0 ppm maximum. Analysis of the hydrogen for water showed 0.1 ppm. The retort was heated in about 3-1/2 hr to 775°C, with hydrogen flowing at 3.15 cu cm/sec (10 volume change per hour). A muffle furnace was used. After the

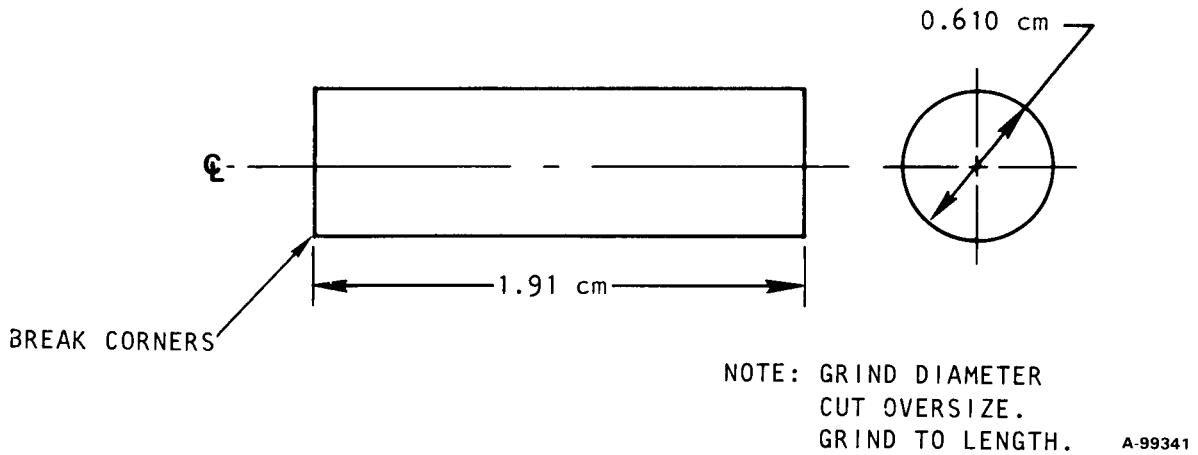

Figure 19.--Oxidation Test Specimen.

temperature had stabilized, the pressure regulator was set for 0.136 MPa (absolute) and the exit valve from the retort was closed, creating the desired test condition. After being held for 100 hr, hydrogen pressure was relieved by opening the exit valve, argon was used to flush the hydrogen, and the retort was quickly removed from the furnace and allowed to cool while argon flow continued. The retort was cut open to remove the specimens.

Duplicate tensile tests were conducted at 26° and at 775°C. Four specimens of Heat N10059 (Ni-27) also were exposed in argon at 775°C for 100 hr and tensile-tested at 26° and 775°C to distinguish the effect of hydrogen exposure from that of elevated temperature alone.

Candidate alloy Ni-32 was selected for the weldability test. The object of this test was to check for cracking in the weld-affected zone. Two 3.81-cm by 7.62-cm samples of alloy Ni-32 were sectioned to produce four 3.81-cm by 3.81-cm squares. The first two squares were butt welded together using a heliarc welder. The second samples had weld beads implanted on their surfaces.

Braze wetting tests were conducted by grinding the cross section of the slice cut from the bottom gating of each casting to a -240 mesh finish, then degreasing and acid-pickling (HNO_3-HF-H_2O). A spot of braze alloy powder, ASW designation BNi-2 (Ni, 4Si, 3B, 7Cr, 3Fe) in a resin binder, was placed on the surface of each sample and allowed to dry. Samples were placed in a vacuum brazing furnace, heated to 1025°C, under 10^{-7} Pa vacuum, held for 30 min, and cooled under vacuum. Specimens were photographed and selected specimens sectioned and examined by optical metallography.

Results

Metallography.--Examination of microstructures in figs. 20 and 21 shows several striking effects of composition variations. As expected, the total amount of interdendritic phase increases with increasing boron content. (Compare N10063 with N10068, and N10065 with N10061.) Comparison of Heats N10061 and N10059 shows that addition of tungsten changes the structure of the interdendritic phase, but does not have a pronounced effect on the relative distribution of the primary phase and the interdendritic phases. Separate addition of columbium causes striking changes in the morphology of the interdendritic phases, as shown by comparison of N10061 (no Cb) with N10058 (1.64 Cb) and N10067 (1.95 Cb). A similar effect of columbium on interdendritic phase morphology is seen in the presence of tungsten, as shown by comparison of N10059 (2.19 W, 0 Cb) with N10069 (2.31 W, 2.41 Cb). However, as shown in the following paragraphs, the striking differences in morphology of the interdendritic phases do not result in major differences in creep behavior. Total amount of these phases, or total boron content, does have an important effect on creep behavior.

Tensile.--Examination of the tensile test data in table 16 shows that changes in composition within the ranges investigated have relatively minor effects. Room-temperature yield strength is essentially the same for all heats. The standard deviation of the entire group is only 29.7 MPa, with a mean value of 492 MPa. Ultimate tensile strength at room temperature shows somewhat more variation (standard deviation = 62.1 MPa), mean UTS = 614 MPa. The only pattern that emerges is that the highest combined contents of boron and columbium give the highest strengths (N10067 and N10069), while the combination of tungsten and high boron is not as effective. However, the highest weight percentages of tungsten represent a substantially lower atomic percentage than do the highest weight percentages of columbium because atomic weight of the former is approximately twice that of the latter.

No such differences between the effects of tungsten and columbium are seen when tensile properties are examined at elevated temperature (775°C). The only effect observed is the reduction in yield strength and UTS and the increase in ductility with low boron, shown by N10064 with 0.48 B, 2.23 W, and 2.03 Cb.

Creep Rupture.--Table 17 gives tensile properties of X-40 and creep-rupture properties of X-40 and Mar-M-509. A direct comparison can be made between these properties and those of the iron-base alloys being evaluated. The effects of compositional variations on creep-rupture properties can be seen by comparing creep-rupture test data of table 18 with the compositions of table 14. All heats evaluated by creep-rupture testing contain essentially the same levels of carbon, molybdenum, and all other elements except boron, tungsten, and columbium. Levels of the latter elements are shown in table 18 for reference.

When creep-rupture data from table 18 are compared with data on cobalt-base alloys X-40 and Mar-M-509 shown in table 17, the alloys of this study compare favorably. The best alloys from this study are essentially equivalent to Mar-M-509 with regard to the 500-hr, 1 percent creep stress at 775°C. No direct comparison is available for X-40.

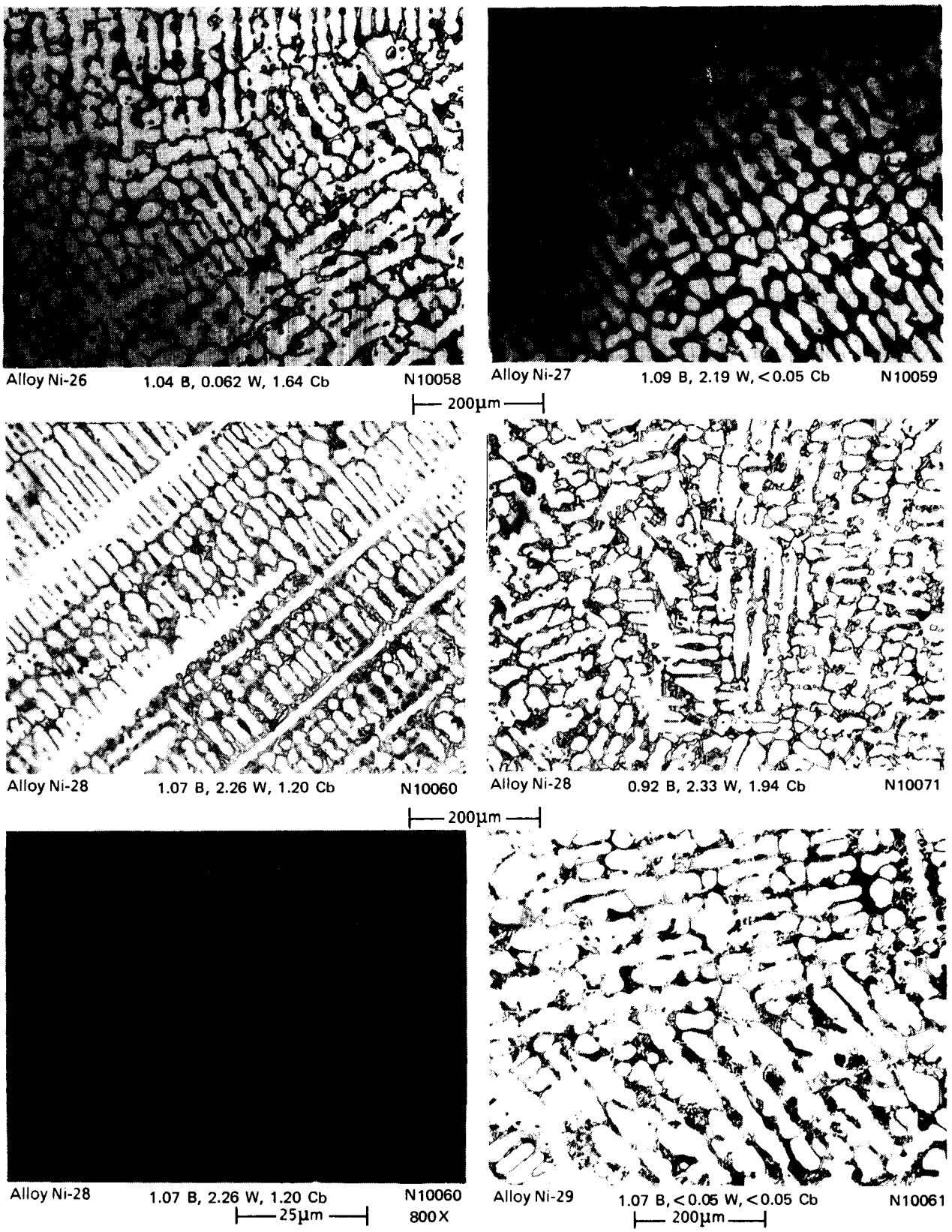

F-35369 -A

Figure 20.--Optical Micrographs of Sections Cut from Castability Test Tabs (0.635-cm Cross Section). Etchant: Fry's Reagent.

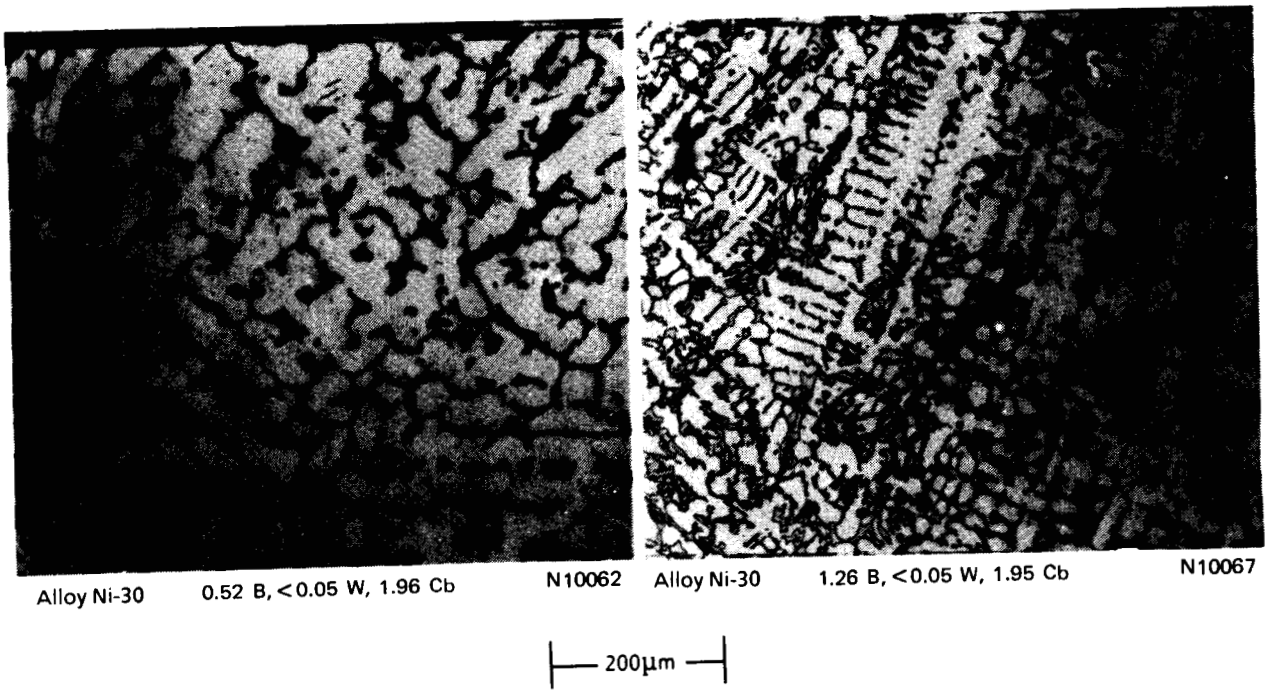

Figure 20.--Continued.

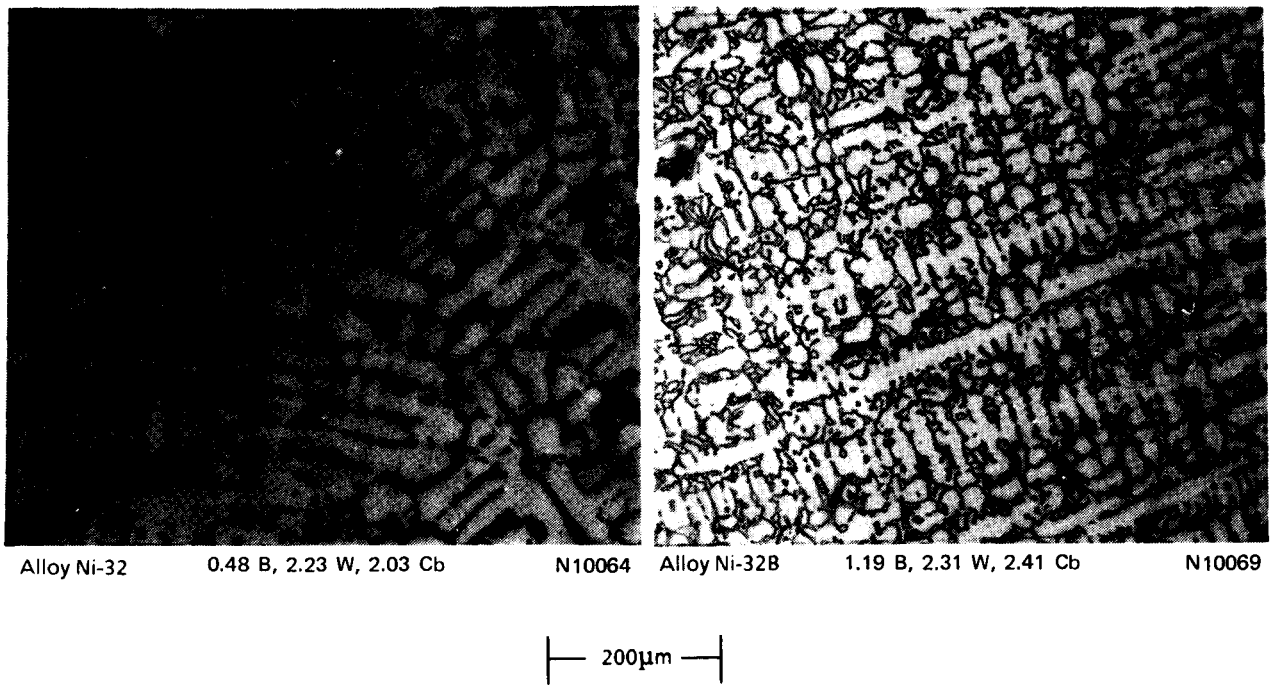

Figure 20.--Concluded.

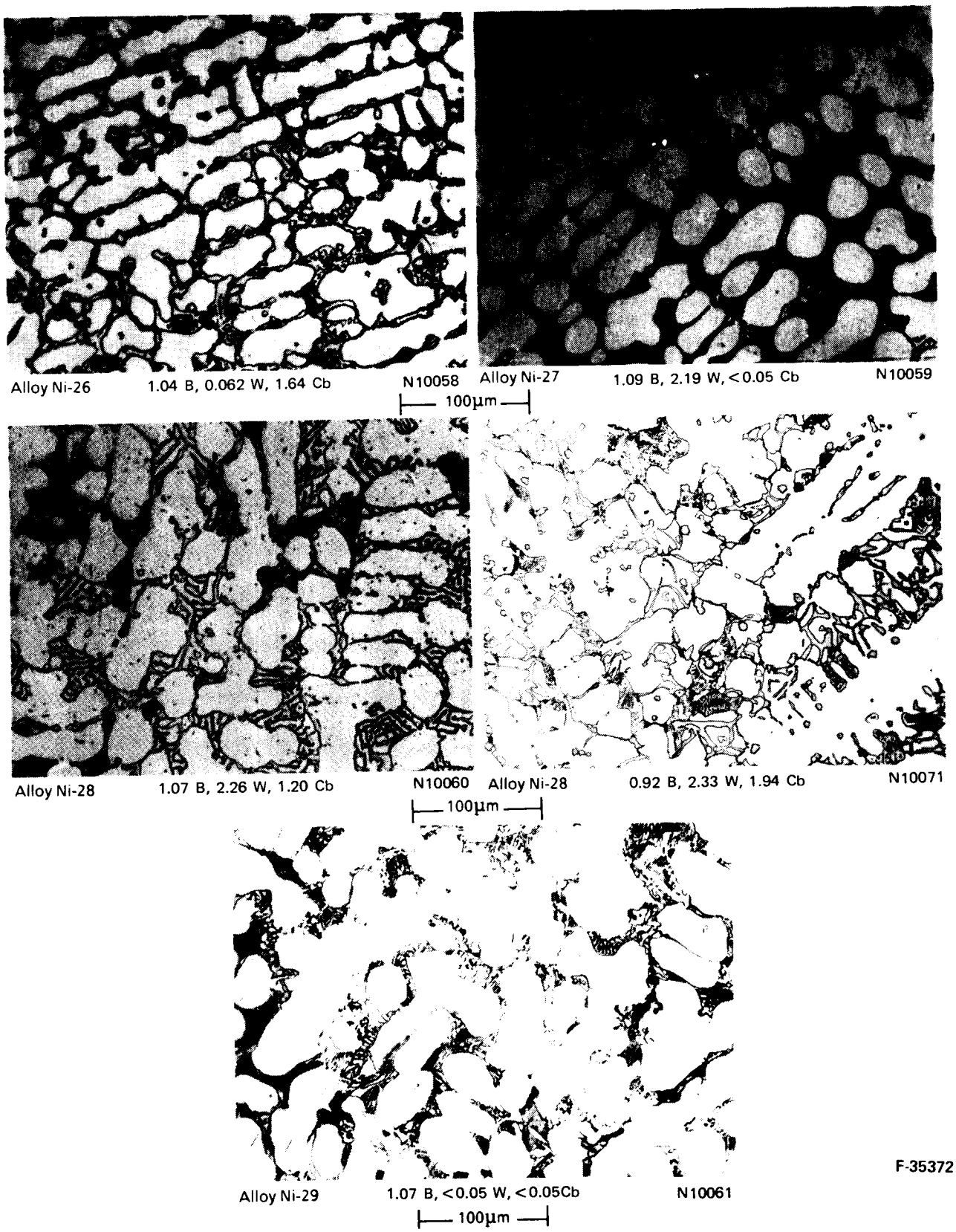

Figure 21.--Optical Micrographs of Sections Cut from Bottom Gating (1.59 by 2.54 cm Cross Section). Etchant: Fry's Reagent.

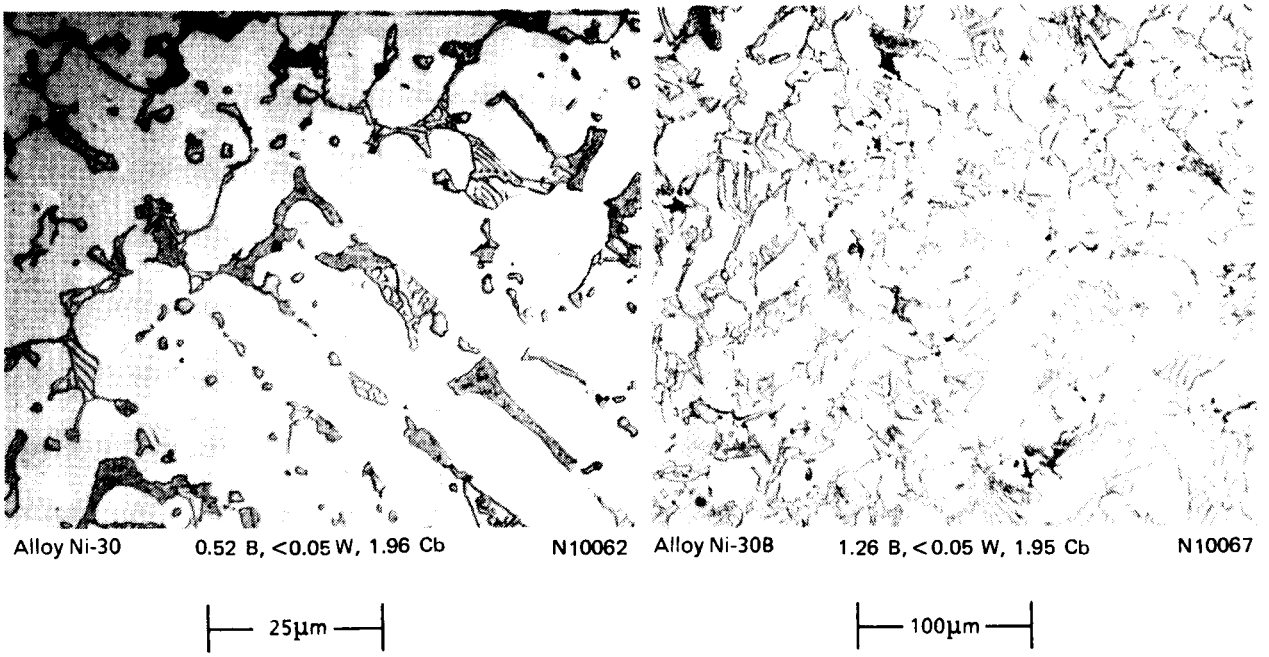

Figure 21.--Continued.

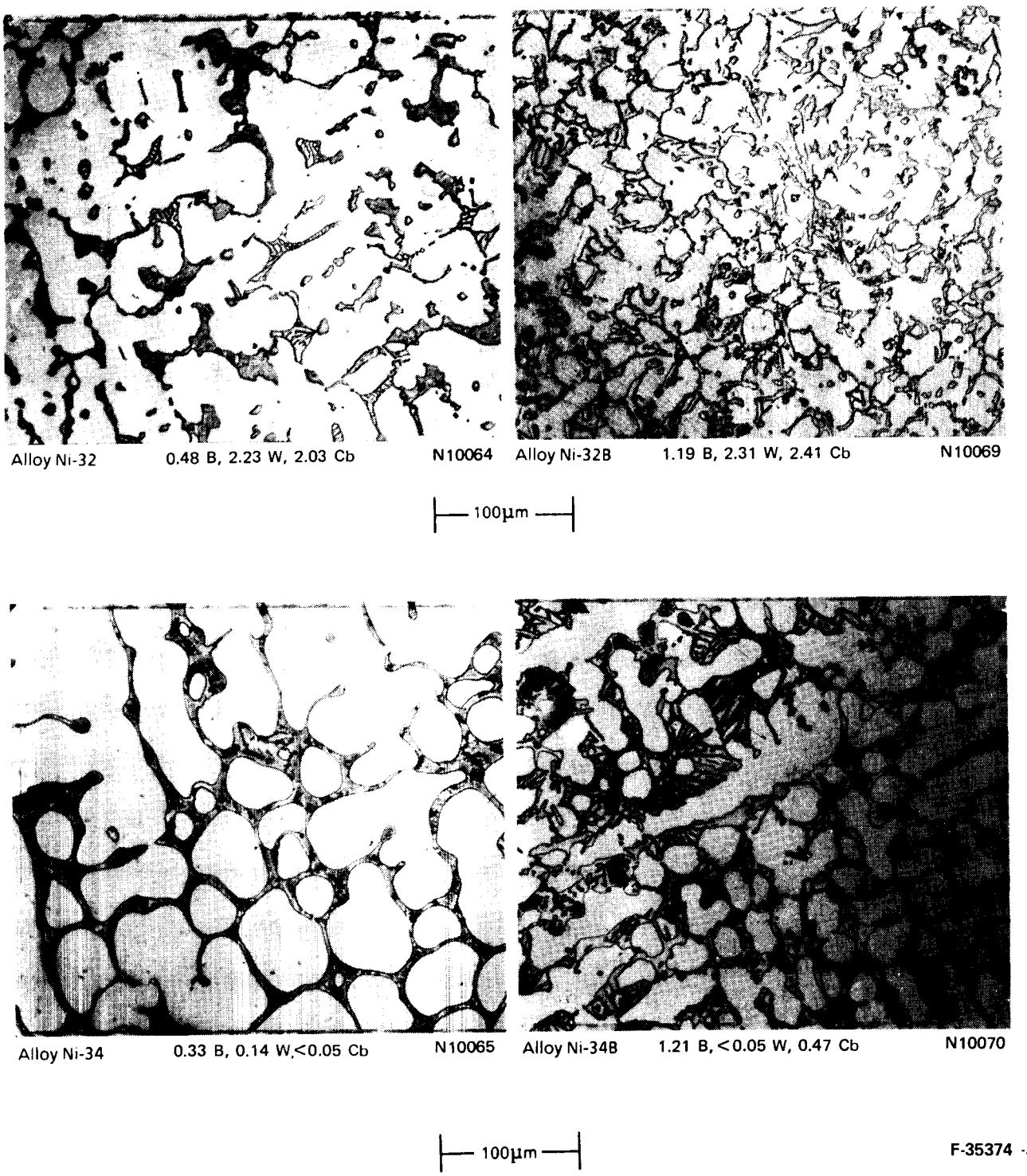

Figure 21.--Concluded.

TABLE 16

AS-CAST TENSILE TEST DATA

26°C Test						775°C Test					
Alloy No.	Heat No.	Specimen No.	0.2% offset YS,* MPa	UTS, MPa	Elong. in 4D, %	Alloy No.	Heat No.	Specimen No.	0.2% offset YS,* MPa	UTS, MPa	Elong. in 4D, %
Ni-26	N10058	10	483	635	1.1	Ni-26	N10058	11	352	515	4.4
		15	481	629	1.2			13	346	522	2.7
Ni-27	N10059	10	327	610	0.7	Ni-27	N10059	13	370	555	1.3
		17	519	566	0.8			18	375	588	2.2
Ni-28	N10060	12	467	548	0.8	Ni-28	N10060	13	377	545	2.2
		15	417	612	1.7			18	386	545	1.7
Ni-28B	N10071	9	454	659	0.7		N10071	4	396	555	1.6
		16	467	545	0.8			10	319	527	2.1
Ni-29	N10061	10	514	655	0.7	Ni-29	N10061	11	367	543	1.6
		15	501	589	0.7			14	336	539	2.0
Ni-30B	N10067	14	492	732	0.6	Ni-30B	N10067	15	375	551	1.7
		18	500	734	0.8			20	374	560	1.9
Ni-31B	N10068	1	477	521	0.6	Ni-31B	N10068	4	344	546	1.1
		13	558	558	0.5			10	369	561	1.4
Ni-32	N10064	4	482	572	2.2	Ni-32	N10064	13	303	546	6.2
		19	506	560	0.7			18	308	548	6.5
Ni-32B	N10069	13	478	689	1.0	Ni-32B	N10069	12	375	536	1.6
		17	487	667	0.8			19	381	545	3.4
Ni-34	N10070	17	513	551	0.6	Ni-34	N10070	13	399	552	1.4
		18	527	554	0.6			19**			

*YS = yield strength
**Specimen not tested due to porosity

TABLE 17

PROPERTIES OF COBALT-BASE ALLOYS

a. X-40 Alloy Tensile Test (ref. 28)

Temp., °C	0.2% Offset YS, MPa	UTS, MPa	Elong., %
RT	305	373	2
425	218	376	6
760	152	276	20

b. X-40 Alloy Creep Tests

Creep Strain, %	Time, hr	Temp., °C	Stress, MPa	References
1.0	500	815	110	(ref. 27)
1.0	150	760	200	(ref. 28)
Rupture	167	775	200	(ref. 28)

Minimum creep rate = 7.45×10^{-8} sec^{-1} (0.028%/hr) at 775°C, 200 MPa

c. Mar-M-509 Creep Test (ref. 29)

Creep strain, %	Time, hr	Temp., °C	Stress, MPa
1.0	500	775	200

TABLE 18

CREEP-RUPTURE TEST DATA AT 775°C, 220 MPa

Alloy No.	Heat No.	Analysis, wt. %			Final creep reading ductility after rupture						
		B	W	Cb	Specimen No.	Strain on loading, %	Time, hr	Deformation, %	Elongation in 4D, %	Reduction of area, %	Minimum creep rate, % per hour
Ni-26	N10058	1.04	0.06	1.64	9	0.168	358.4	1.001	4.2	4.8	0.00150
					12	0.172	371.9	1.000	3.7	3.9	0.00160
Ni-27	N10059	1.09	2.19	<0.05	9	0.155	500.0	0.912	3.6	4.0	0.00143
					11	0.154	475.5	1.002	2.7	2.7	0.00158
Ni-28	N10060	1.07	2.26	1.20	11	0.133	500.0	0.863	3.8	3.8	0.00103
					16	0.137	384.9	1.002	4.9	6.9	0.00205
Ni-28B	N10071	0.92	2.33	1.94	13	0.147	328.2	1.005	2.5	2.2	0.00215
					18	0.131	277.5	1.009	3.6	5.0	0.00237
Ni-29	N10061	1.07	<0.05	<0.05	9	0.176	56.6	1.008	2.7	3.6	0.0115
					12	0.160	67.0	1.003	4.7	5.0	0.0110
Ni-30	N10067	1.26	<0.05	1.95	9	0.136	314.6	1.003	2.4	2.2	0.00175
					19	0.132	230.5	1.002	3.6	3.5	0.00217
Ni-31	N10068	1.31	2.28	<0.05	9	0.134	332.2	1.015	2.4	2.0	0.00125
					16	0.147	256.7	1.003	1.7	1.7	0.00138
Ni-32	N10064	0.48	2.23	2.03	3	0.207	17.0	1.015	4.8	5.1	0.0385
					9	0.216	32.6	1.002	4.5	5.0	0.0210
Ni-33	N10069	1.19	2.31	2.41	14	0.159	470.2	1.003	3.0	3.4	0.00125
					20	0.135	500.0	0.849	3.4	2.9	0.00097
Ni-34	N10070	1.21	<0.05	0.47	16	0.166	116.0	1.003	2.7	3.3	0.00234
					20	0.160	114.3	1.006	2.2	2.3	0.00253

Oxidation testing.--The raw data from cycle oxidation testing was inconclusive. The specimens were not weighed separated from the crucibles, and sufficient crucible oxidation occurred to influence the weight gain. Accurate oxidation tests are performed in the second iteration.

Hydrogen compatability.--Review of tables 19 and 20 shows that room temperature ultimate tensile strength is not reduced by exposure to hydrogen after 100 hr at 236 MPa. However, at 775°C most specimens showed a reduction in strength under the same test conditions in either hydrogen or argon. Scanning electron micrographs showing room temperature tensile fracture surfaces of unexposed and hydrogen-exposed specimens are included as fig. 22.

Weldability.--No cracks were found in welded specimens. In addition welding did not cause any cracking along the weld interface in either of the two (2) geometries (figs. 23 and 24). View 4 (fig. 23) is the transition zone. Fig. 24 shows the weld surface for the implanted weld bead. Again no cracking is observed in Views 1 through 3, and View 4 is the transition zone.

Braze wetting.--The braze wetting test showed that the braze alloy wetted and flowed acceptably on all samples. Photomicrographs of a representative specimen cross section, including the braze alloy-specimen interface, is shown in fig. 25. No deleterious phases or excessive penetration were found.

Discussion

Tensile properties.--The alloy compositional variation did not cause significant change in the elevated or room temperature tensile properties. The only measurable effect is the reduction in yield strength and ultimate tensile strength and the increase in ductility with the low boron, shown by alloy Ni-32 (N10064), table 16. Borides (M_3B_2) and carbide precipitates caused the lower elongation values below 1 percent, but these precipitates proved stable for high-temperature strength.

Creep Rupture.--Increasing boron from 0.48 to 0.92 percent in the presence of tungsten and columbium caused the time to 1-percent creep to increase more than 10 fold. However, even a 1.07 percent boron level was not sufficient for good creep-rupture strength without tungsten or columbium (N10061).

Some ambiguity exists in assessing the effect of tungsten in combination with boron. The combination of 1.09 B and 2.19 W (alloy Ni-27) results in creep-rupture properties of 500 and 475.5 hr with 0.912 and 1.002 percent creep, respectively. Furthermore, when tungsten is eliminated, the time to 1-percent creep is decreased to 56.6 and 67.0 hr. The ambiguity occurs when the boron level (in the presence of 2.28 W) is increased to 1.31 as in alloy Ni-31. Alloy Ni-31 has a minimum creep rate 50 percent lower than Ni-27; however, Ni-31 has a time to 1-percent creep 25 percent less than Ni-27.

The alloying effect of columbium without tungsten is seen by comparing the alloys Ni-26 (N10058), Ni-29 (N10061), and Ni30 (N10067), table 18. Ni-26

TABLE 19

TENSILE TEST DATA AT 26°C

Alloy No.	Heat No.	As-cast specimens					Specimens exposed to H_2 for 100 hr at 200 MPa and 775°C (except as noted)				
		Specimen No.	0.2% offset YS, MPa	UTS, MPa	Elong. in 4D, %	Reduction of area %	Specimen No.	0.2% offset YS, MPa	UTS, MPa	Elong. in 4D, %	Reduction of area, %
Ni-26	N10058	10	483	635	1.1	0.7	16	421	668	1.1	1.7
		15	482	629	1.2	1.2	19	445	665	0.8	1.6
Ni-27	N10059	10	513	610	0.7	1.3	1	440	660	1.1	1.7
		17	519	566	0.8	1.2	20	467	619	0.6	1.0
							2*	463	687	1.0	0
							4*	456	683	1.0	0
Ni-28	N10060	12	467	648	0.8	1.2	14	473	676	1.1	1.6
		15	417	612	1.7	2.7	17	470	677	1.0	1.4
Ni-28B	N10071	9	454	659	0.7	1.6	11	411	659	1.0	1.5
		16	467	546	0.8	1.2	1	410	607	0.7	1.6
Ni-29	N10061	10	514	655	0.7	0.9	13	421	623	0.7	0.9
		15	501	589	0.7	1.0	19	459	676	1.1	1.3
Ni-30B	N10067	14	492	731	0.6	0.7	16	466	697	0.7	1.1
		18	500	734	0.8	0.6	17	437	720	1.0	1.3
Ni-31B	N10068	1	477	521	0.6	0.9	17	429	602	0.4	0.8
		13	558	578	0.5	0.6	20	456	590	0.7	0.9
Ni-32	N10064	4	482	572	2.2	3.6	1	395	529	1.1	2.5
		19	505	560	0.7	1.0	12	332	586	2.1	3.2
Ni-32B	N10069	13	478	689	1.0	1.7	10	472	657	0.8	1.0
		17	487	667	0.8	1.1	15	444	556	0.5	0.9
Ni-34	N10070	17	513	551	0.6	0.9	14	443	532	0.6	0.9
		18	527	554	0.6	0.4	15	457	580	0.8	1.5

*Specimens exposed to Ar for 100 hr at ambient pressure

TABLE 20

TENSILE TEST DATA AT 775°C

Alloy No.	Heat No.	As-cast specimens					Specimens exposed to H_2 for 100 hr at 200 MPa and 775°C (except as noted)				
		Specimen No.	0.2% offset YS, MPa	UTS, MPa	Elong. in 4D, %	Reduction of area %	Specimen No.	0.2% Offset YS, MPa	UTS, MPa	Elong. in 4D, %	Reduction of area, %
Ni-26	N10058	11	352	515	4.4	4.6	1	250	463	5.6	6.4
		13	346	522	2.7	2.1	18	268	474	5.6	6.3
Ni-27	N10059	13	370	555	1.3	1.3	12	272	537	2.7	3.8
		18	375	588	2.2	1.4	19	263	528	2.6	3.5
							3*	294	540	2.0	1.8
							14*	357	581	2.0	0.9
Ni-28	N10060	13	377	545	2.2	1.5	1	273	497	2.6	3.5
		18	448	545	1.7	2.1	20	294	523	5.9	6.3
Ni-28B	N10071	4	396	555	1.6	1.2	3	276	466	3.6	5.2
		10	319	527	2.1	1.5	17	311	483	3.8	5.4
Ni-29	N10061	11	367	538	1.6	3.1	16	274	502	4.3	5.3
		14	336	539	2.0	1.7	18	260	502	4.9	6.1
Ni-30B	N10067	15	375	551	1.7	1.8	11	283	501	5.2	7.6
		20	377	560	1.9	2.1	12	267	497	4.2	4.6
Ni-31B	N10068	4	344	546	1.1	1.6	2	279	526	1.4	2.0
		10	369	561	1.4	1.8	18	321	508	1.1	1.5
Ni-32	N10064	13	303	446	6.2	8.3	2	213	381	7.8	10.6
		18	308	458	6.5	9.1	14	256	392	4.6	6.5
Ni-32B	N10069	12	375	536	1.6	2.1	9	254	495	2.6	3.7
		19	381	545	3.4	4.6	16	293	497	4.2	5.1
Ni-34	N10070	13	399	552	1.4	1.4	11	281	523	1.5	1.6
		19**					12	277	519	1.6	1.7

*Specimen exposed to Ar for 100 hr at ambient pressure and 775°C
**Specimen not tested due to porosity

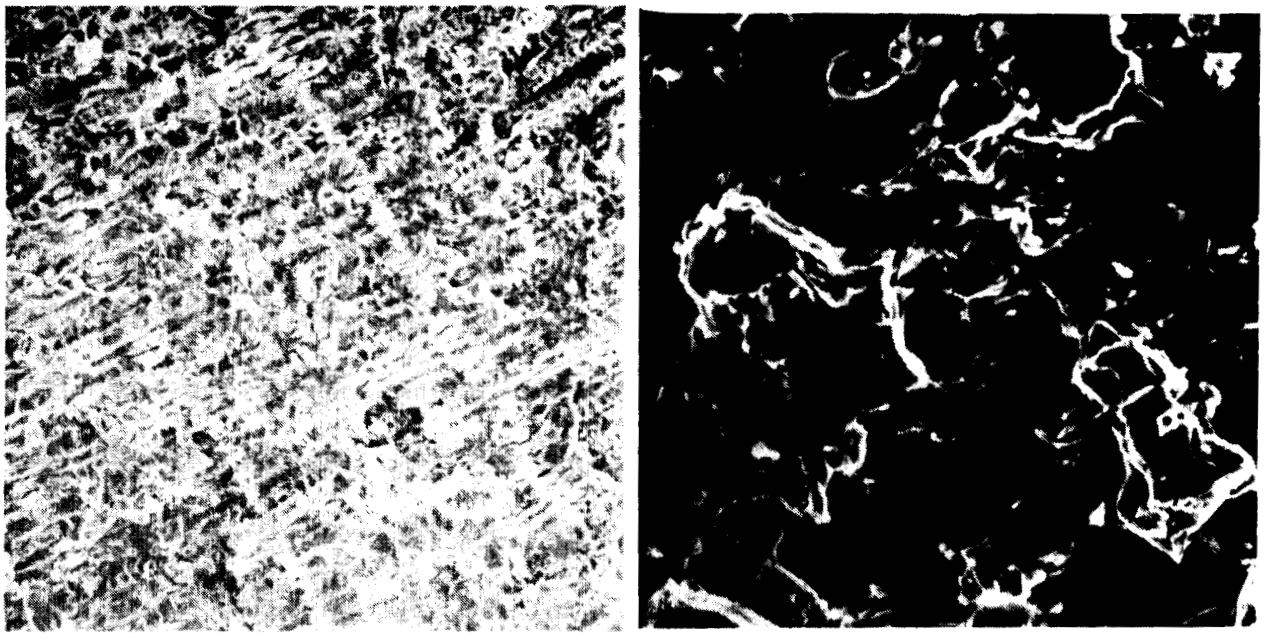

a. NOT HYDROGEN-EXPOSED (AS-CAST), SPECIMEN N10059-17

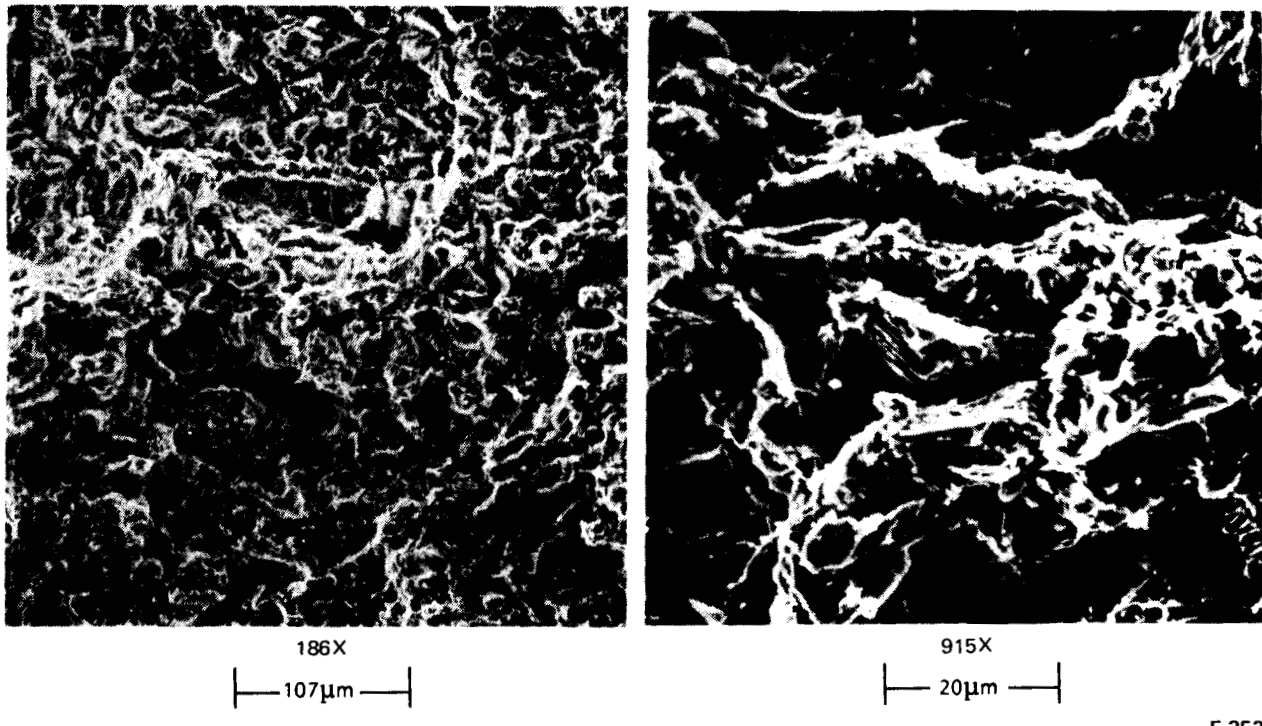

b. EXPOSED TO HYDROGEN FOR 100 HR AT 236 MPa AT 775°C, SPECIMEN N10059-1

F-35375 -A

Figure 22.--Scanning Electron Micrographs of Room-Temperature Tensile Fracture Surfaces, Unexposed and Hydrogen-Exposed Specimens, Heat N10059.

Figure 23.--Butt-Welded Samples N10069.

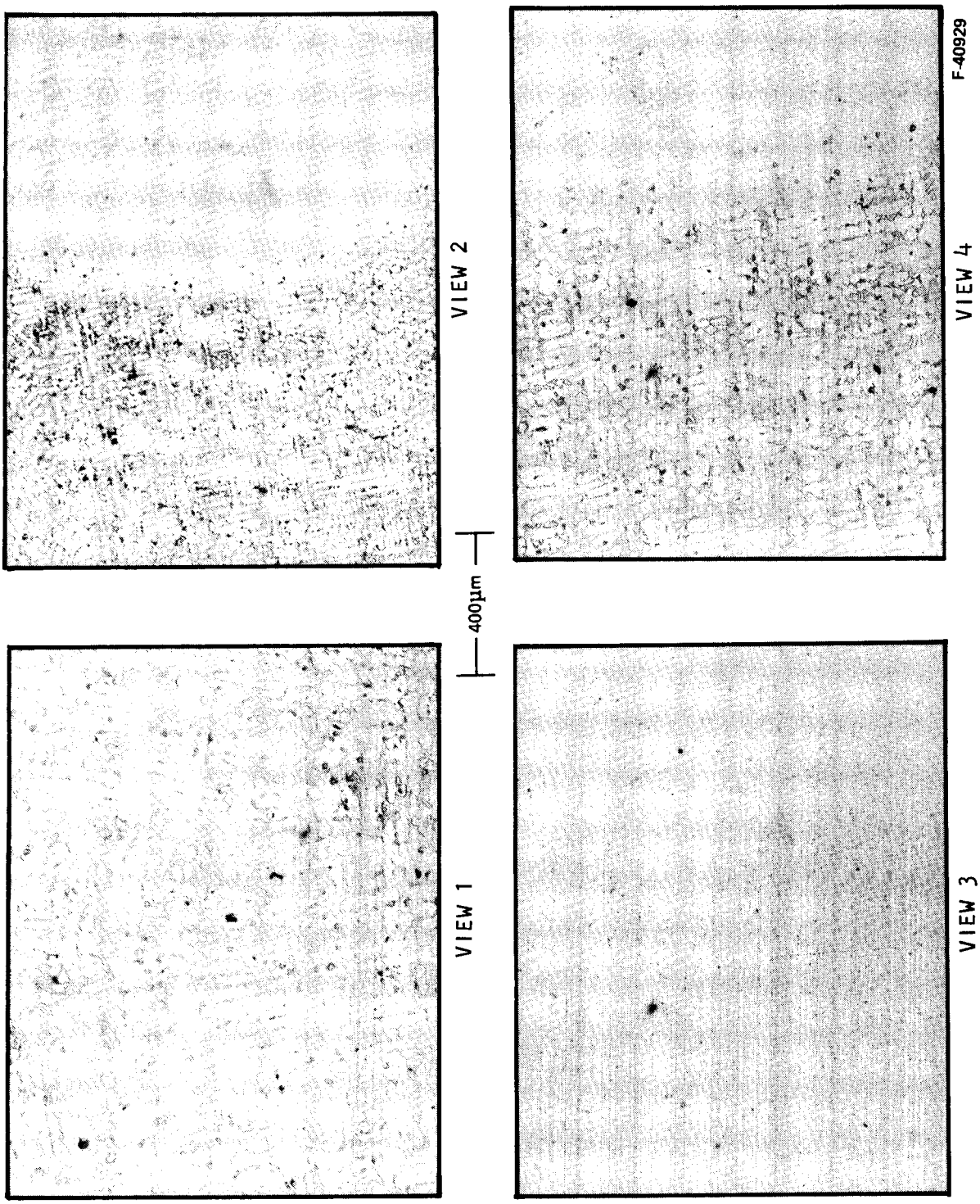

Figure 24.--Implanted Weld Bead N10069.

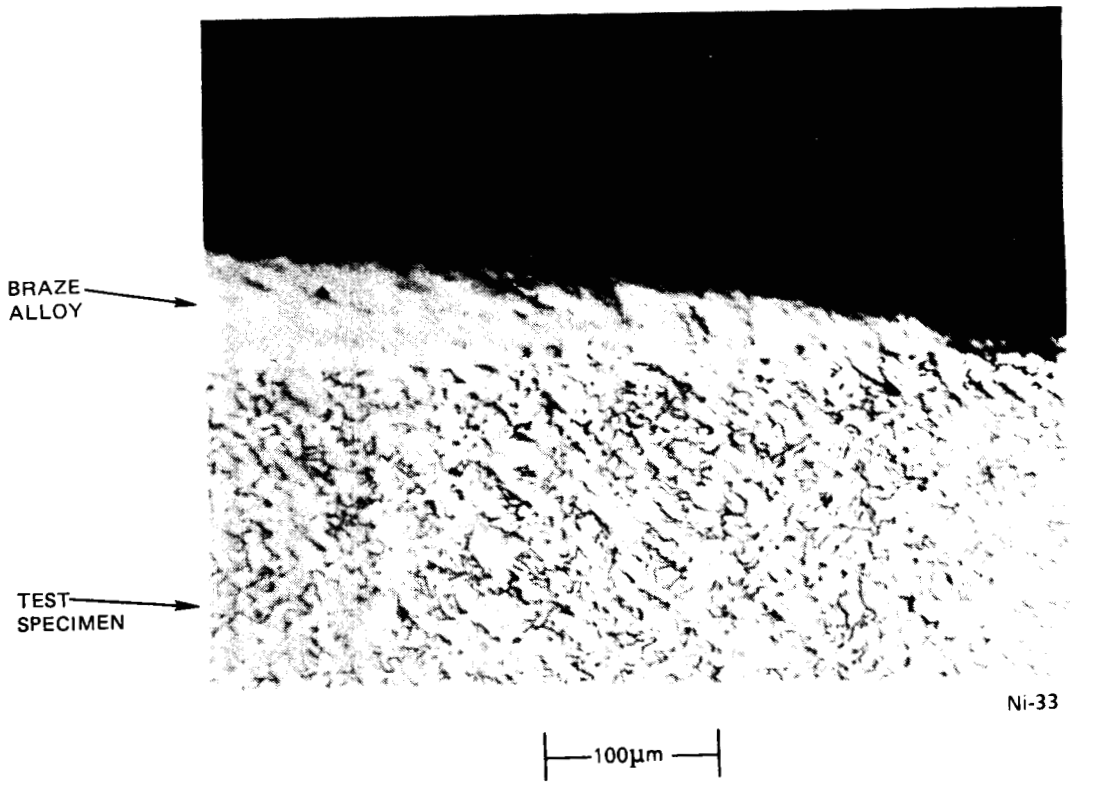

Figure 25.--Typical Cross-Section Photomicrograph of Braze Wetting Test Specimens.

(1.64 percent Cb) has an average time to 1-percent creep of 365 hr, which is 25 percent longer than Ni30 (1.95 percent Cb) and nearly six times longer than Ni-29 (0.05 percent Cb). Columbium additions above 1.64 percent apparently do not increase creep-rupture properties.

Columbium in the presence of boron and tungsten does not have a strong effect on time to 1-percent creep as seen when comparing Ni-27 and Ni-33 in table 18. The addition of columbium to these three alloys does produce the lowest minimum creep rate of the eight alloys tested in the first iteration. Also, columbium increases creep-rupture ductility but does not increase time to failure.

Oxidation testing.--No conclusions could be drawn from the oxidation tests performed in the first iterations because weight change measure included the oxidation of the crucible material. The oxidation pick-up by the crucibles was significant enough to cause error in the oxidation resistance evaluation.

Hydrogen compatibility.--The exposure to hydrogen appears to have little or no effect on alloy tensile properties or fracture surface. Tables 19 and 20 show there is a decrease when comparing the as-cast specimen to specimen exposed to hydrogen gas at 775°C for 100 hr; however, a similar decrease was seen when specimens were exposed to argon gas at 675°C for 100 hr. Also, fig. 22 shows no irregularities in the fracture surfaces that were exposed to the hydrogen atmosphere. Therefore, the decrease in tensile properties for the exposed specimens was due to aging effects and not to the hydrogen environment.

Weldability.--Welding specimens in figs. 23 and 24 show no signs of cracks along the weld interface. The conclusion is that the same results will occur with alloys of similar chemistry. No further weld tests were conducted.

Braze wetting.--Fig. 25 shows a small angle between the braze material and alloy Ni-33. The small angle between Ni-33 and the braze material proves that the alloy groups being evaluated have excellent wettability and since all the alloys being considered have very similar chemistries, the result obtained from alloy Ni-33 was considered representative of the other candidate alloys, and no further braze testing was conducted.

Conclusion

Regarding composition effects, the boron level must be at least 1 percent for adequate creep-rupture properties. Earlier work showed that the percent carbon should be a minimum of 0.4 percent. Although tungsten and columbium are beneficial for rupture life and ductility, respectively, the optimum combination has not been established.

On the basis of the evaluation of the first iteration (table 14), eight additional compositions were selected for study (table 21) in the second iteration. The purpose is to establish the optimal level of boron above the known minimum level of 1 percent. Also, greater percentages of columbium and tungsten are added to further clarify alloying effects on microstructure and properties.

TABLE 21

ANALYSES OF EXPERIMENTAL ALLOYS, SECOND ITERATION
WEIGHT PERCENT (Bal: Fe)

Alloy No.	Heat No.	Weight percent (Bal. Fe)													
		C	Mn	Si	Cr	Ni	Mo	W	Cb	B	N	O	S	P	Mg
Ni-35	N10080	0.48	0.25	0.76	16.66	18.04	5.07	4.77	<0.10	1.20	0.038	0.0091	0.0091	0.023	<0.001
	Target	0.50	0.20	0.60	18.0	18.0	5.0	4.0	-	1.1	-	-	-	-	-
Ni-36	N10084	0.43	0.23	0.88	16.95	18.39	5.25	<0.10	3.89	0.95	0.030	0.012	0.003	0.009	<0.001
	Target	0.50	0.20	0.80	18.0	18.0	5.0	-	4.0	1.1	-	-	-	-	-
Ni-37	N10095	0.47	0.22	0.87	16.92	18.16	4.96	3.58	1.04	1.19	0.045	0.0048	0.003	0.009	<0.001
	Target	0.50	0.20	0.80	18.0	18.0	5.0	3.0	1.0	1.1	-	-	-	-	-
Ni-38	N10075	0.48	0.26	0.46	18.81	18.07	5.18	3.59	0.96	1.26	0.042	0.0073	0.004	0.022	<0.001
	Target	0.50	0.20	0.30	18.0	18.0	5.0	2.0	2.0	1.1	-	-	-	-	-
Ni-39	N10076	0.39	0.24	0.40	18.64	18.15	5.08	4.74	<0.05	1.21	0.039	0.0049	0.004	0.019	<0.001
	Target	0.50	0.20	0.30	18.0	18.0	5.0	4.0	-	1.6	-	-	-	-	-
Ni-40	N10086	0.46	0.28	0.96	18.46	18.05	5.35	<0.10	3.23	1.40	0.040	0.0061	0.003	0.010	<0.001
	Target	0.50	0.20	0.80	18.0	18.0	5.0	-	4.0	1.6	-	-	-	-	-
Ni-41	N10087	0.44	0.27	0.92	17.32	18.67	4.94	3.33	0.99	1.55	0.043	0.0086	0.003	0.009	<0.001
	Target	0.50	0.20	0.80	18.0	18.0	5.0	3.0	1.0	1.6	-	-	-	-	-
Ni-42	N10079	0.40	0.28	0.52	18.65	17.86	5.30	2.49	1.97	1.21	0.043	0.0094	0.005	0.025	<0.001
	Target	0.50	0.20	0.30	18.0	18.0	5.0	2.0	2.0	1.6	-	-	-	-	-

EVALUATION OF EIGHT (8) ALLOYS -- SECOND ITERATION

Procedure

Casting.--The casting procedures used in the first iteration were duplicated for the eight alloys of the second iteration.

Testing.--Except for oxidation testing, all testing procedures were identical to those of the first iteration. The tests included metallography, tensile, creep-rupture, oxidation, and hydrogen compatibility. Weldability and braze wetting were not repeated, because these alloy systems exhibited excellent weldability and braze wetting characteristics in earlier tests. Regarding oxidation testing, specimen weight gain at specified time intervals was measured by weighing only the sample, not the crucible and sample.

Results

Microstructure.--Examination of microstructures in figs. 26 and 27 shows similarities to those of the first iteration (figs. 20 and 21). A notable exception is that the alloys with the highest boron content (Alloys No. Ni-40, boron 1.40 percent and No. Ni-41, boron 1.55 percent) lack the primary dendrites that are a distinctive part of most of the alloys. Structure is distinctly eutectic.

Tensile.--Composite plots of yield strength vs elongation for all alloys from the first and second iterations (alloys Ni-26 through Ni-42) are shown for tests at room temperature in fig. 28, and for tests at 775°C in fig. 29. Generally, alloys from the second iteration are stronger and more brittle than those from the first iteration. A preliminary examination of the fracture surfaces on broken test specimens was made; several specimens with lower elongation than the general population had inclusions or voids, which may have caused premature failure and low ductility.

Hydrogen compatibility.--Results of tensile tests at room temperature (26°F) and at 775°C are shown in tables 22 and 23, respectively, for both specimens in air, and specimens exposed to hydrogen and argon. By comparing tensile results the effect of hydrogen and the thermal cycle can be established for the eight alloys in the second iteration.

Creep-rupture results.--The results of the creep-rupture tests are shown in table 24. All tests were terminated at 500 hr or at 1 percent creep, whichever came first. Table 24 allows easy correlation between alloy chemistry changes and resistance to creep deformation by listing minimum creep rate and time to 1 percent creep or time to rupture.

Oxidation resistance.--Data from the cyclic oxidation test of the second iteration alloys are shown in table 25. No crucible contamination problem occurred during the oxidation testing of second iteration alloys. The data for specific weight change in the crucible and after removal from the crucible are considered reliable.

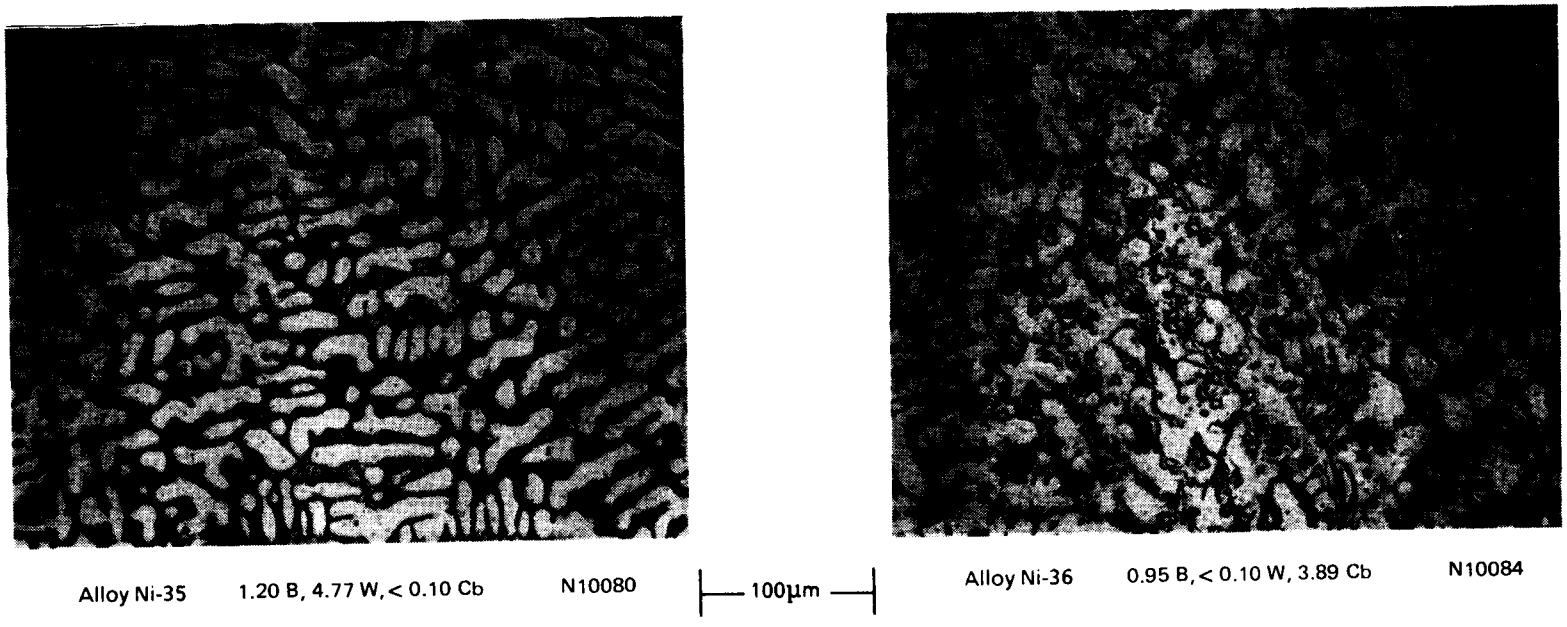

Figure 26.--Optical Micrographs of Sections Cut from Castability Test Tabs (0.635-cm Cross Section). Etchant: Fry's Reagent.

F-35988 -A

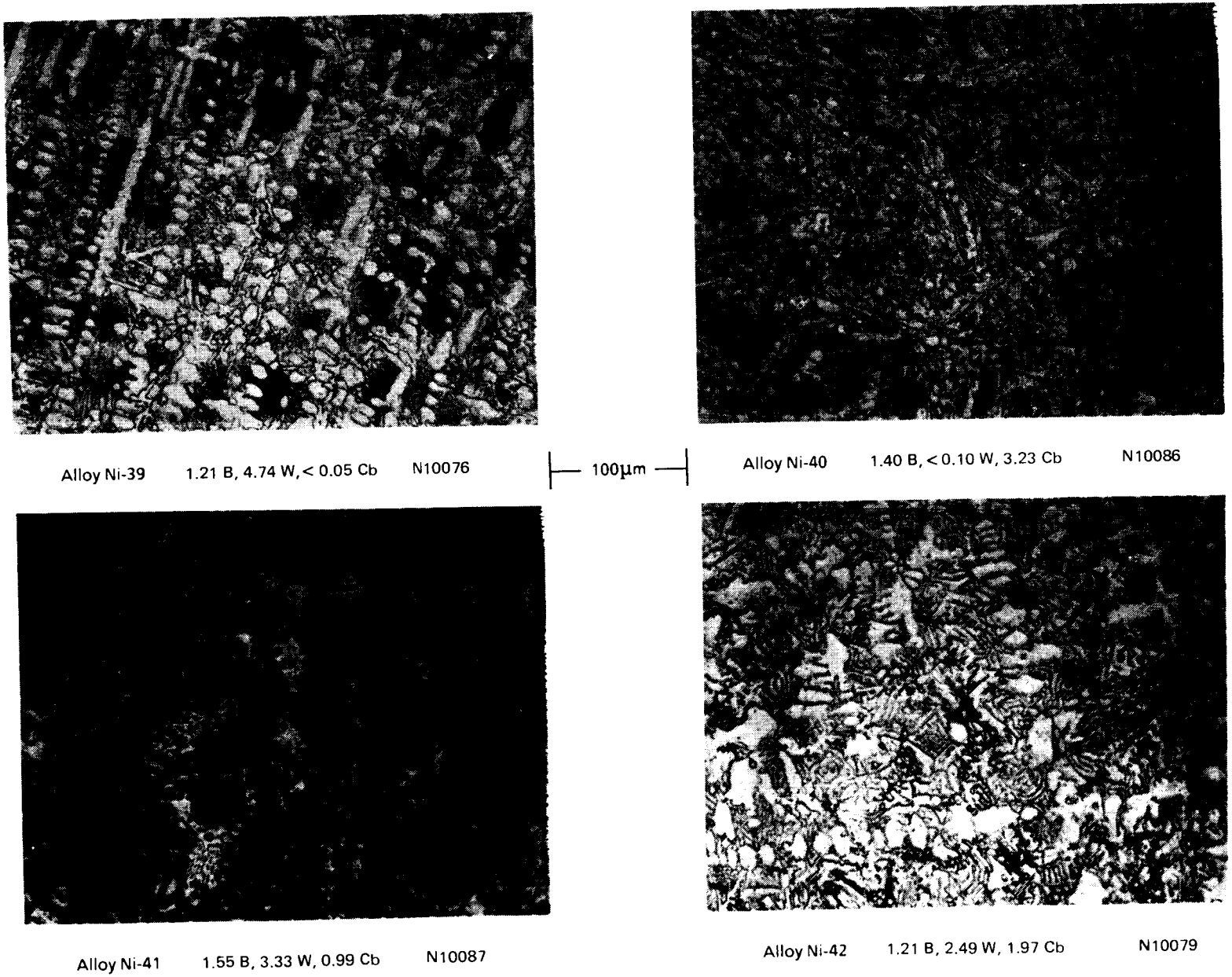

F-35989 -A

Figure 26.--Concluded.

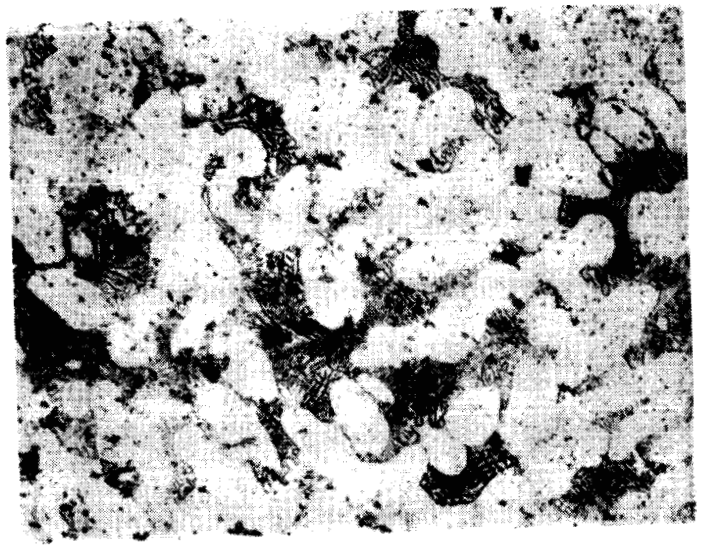

Alloy Ni-35 1.20 B, 4.77 W, < 0.10 Cb N10080

100µm

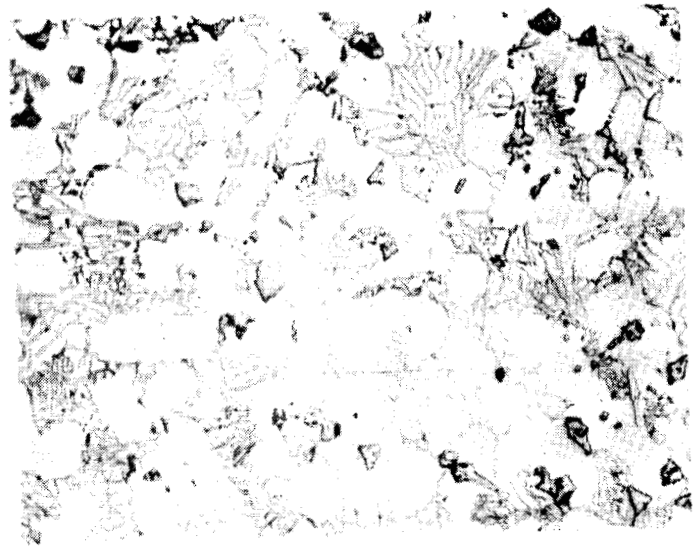

Alloy Ni-36 0.95 B, < 0.10 W, 3.89 Cb N10084

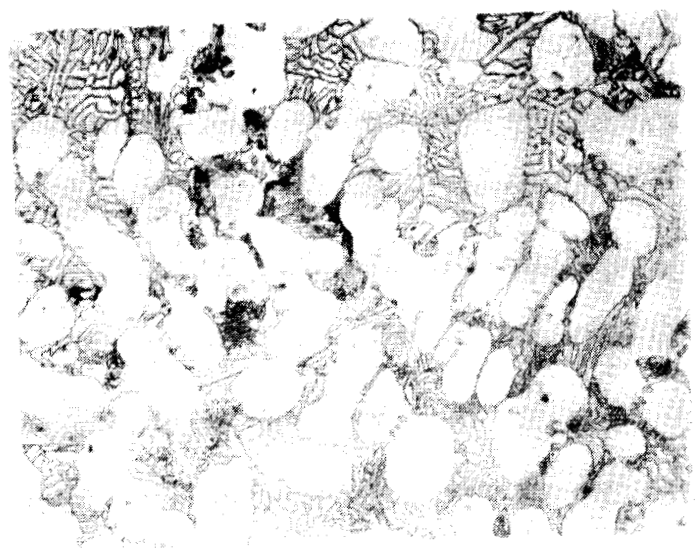

Alloy Ni-37 1.19 B, 3.58 W, 1.04 Cb N10085

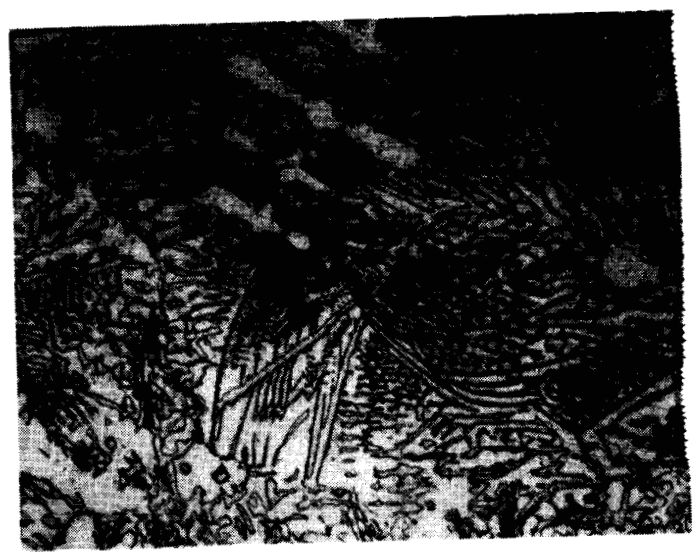

Alloy Ni-38 1.26 B, 3.59 W, 0.96 Cb N10075

F-35990-A

Figure 27.--Optical Micrographs of Sections Cut from Bottom Gating (1.5-cm by 2.54-cm Cross Section). Etchant: Fry's Reagent.

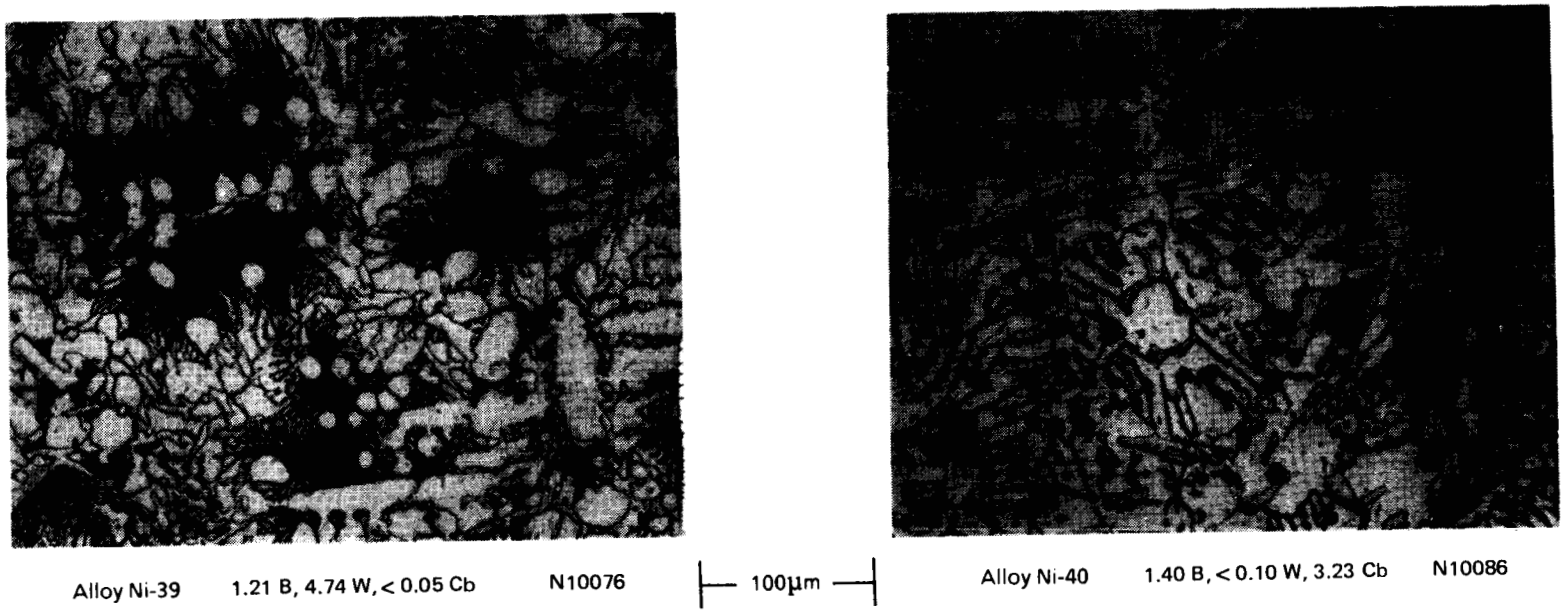

Figure 27.--Concluded.

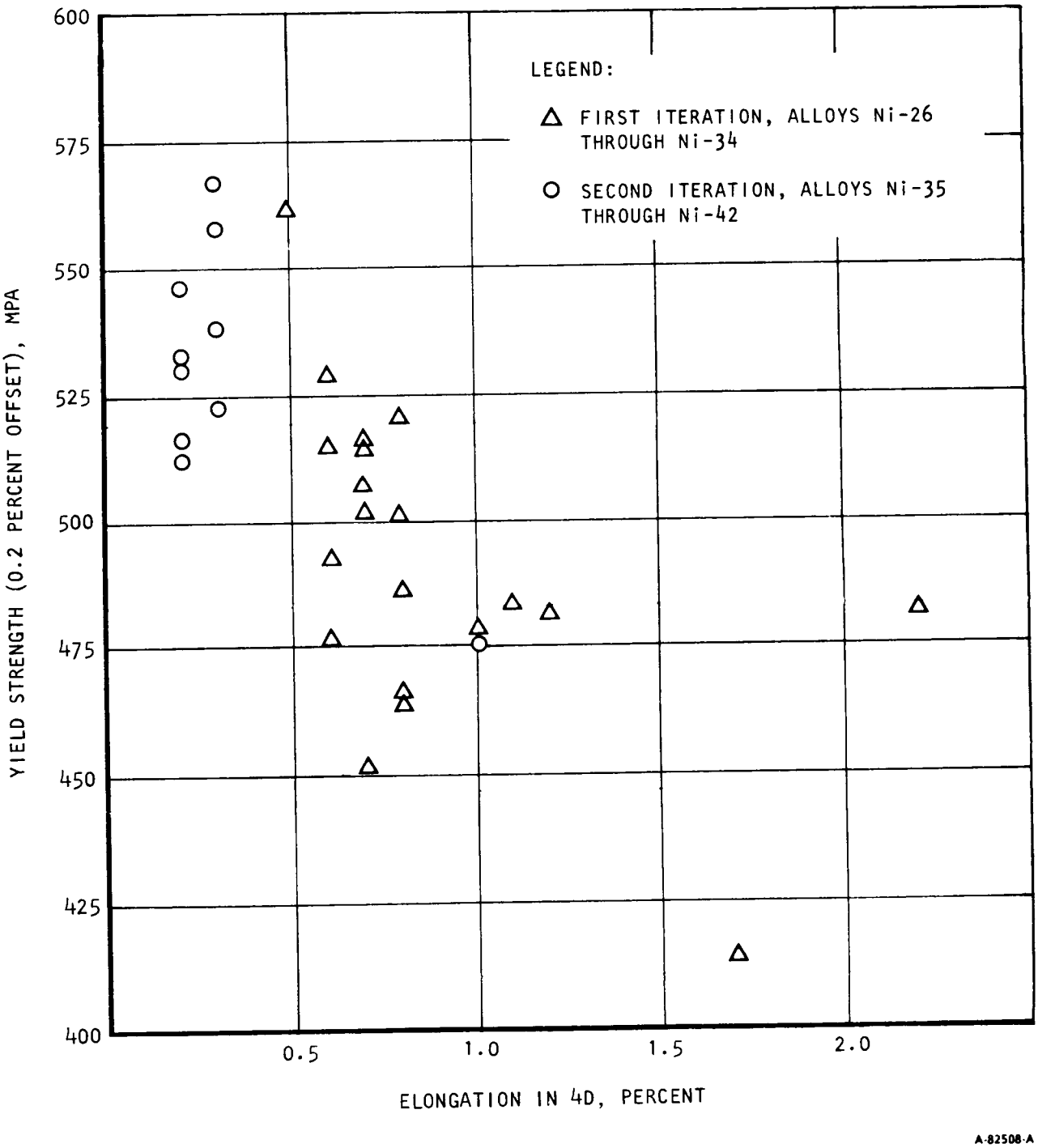

Figure 28.--Room-Temperature Yield Strength-Elongation Relationship for Alloys Ni-26 through Ni-42.

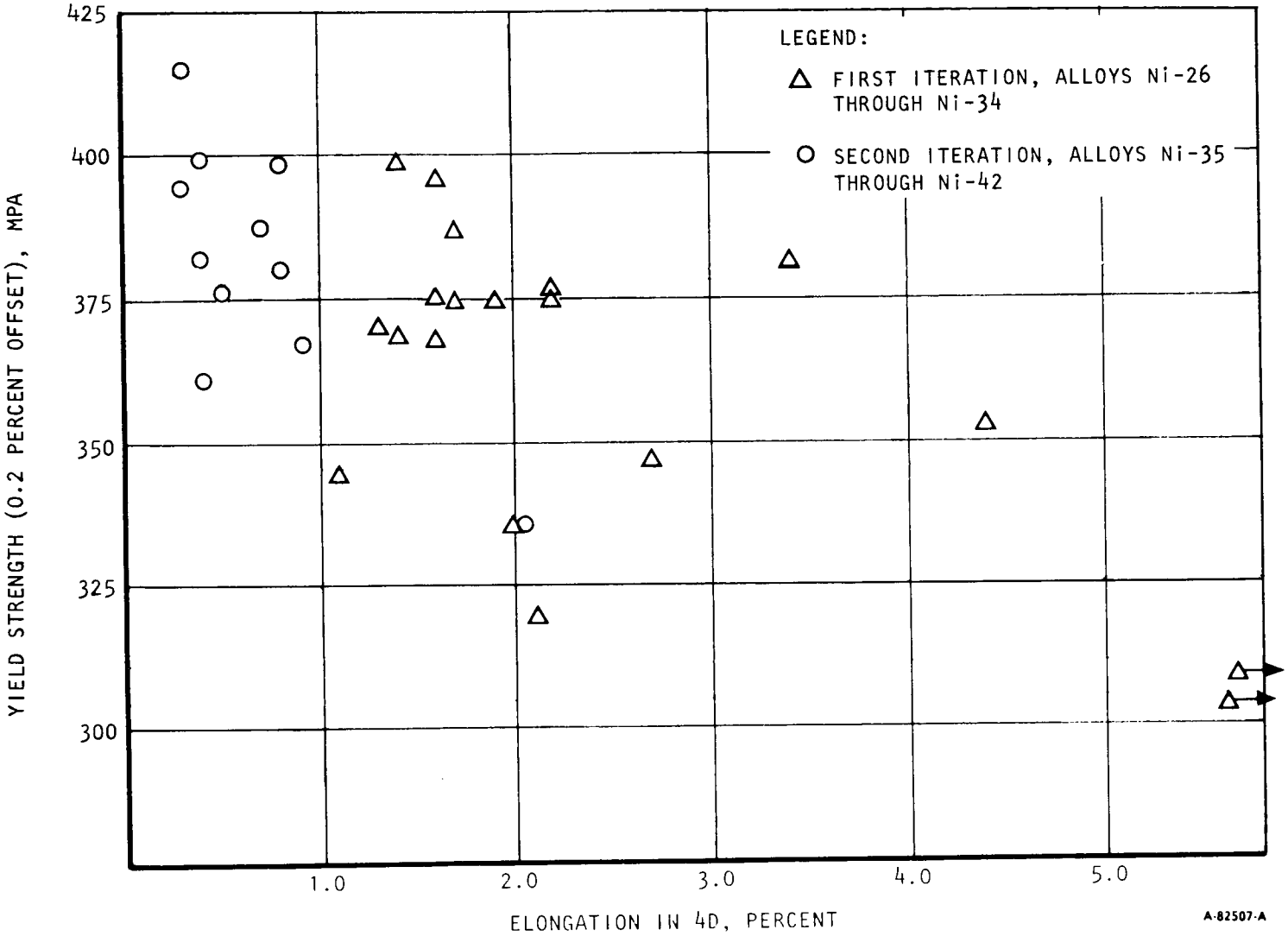

Figure 29.--775°C Yield Strength-elongation Relationship for Alloys Ni-26 through Ni-42.

TABLE 22

TENSILE TEST DATA AT 26°C

Alloy No.	Heat No.	As-cast specimens					Specimens exposed to H_2 for 100 hr at 236 MPa (gage) 775°C (except as noted)				
		Specimen No.	0.2% Offset YS, MPa	UTS, MPa	Elongation in 4D, %	Reduction of area, %	Specimen No.	0.2% offset YS, MPa	UTS, MPa	Elongation in 4D, %	Reduction of area, %
Ni-35	N10080	2	450	586	0.6	1.5	1	525	525	0.5	1.1
		20	475	657	1.0	0.8	9	541	541	0.4	1.4
							18(a)	507	508	0.3	1.2
Ni-36	N10084	13	426	694	1.3	2.4	(b)				
		20	412	637	0.9	1.7	(b)				
Ni-37	N10085	18	448	707	1.2	1.6	1	456	655	0.5	0.4
		19	415	664	0.4	1.5	4	475	682	0.6	1.5
Ni-38	N10075	14	521	572	0.3	0.9	4	474	519	0.8	0.5
		16	530	582	0.2	0.4	15	501	526	0.2	0.7
							3(a)	514	634	0.3	0.9
							17	518	606	0.7	1.1
Ni-39	N10076	17	529	586	0.2	0.4	3	492	581	0.5	0.9
		18	535	601	0.3	0.5	4	506	601	0.3	1.2
							15(a)	504	661	0.3	0.2
							20(a)	604	630	0.3	0.8
Ni-40	N10086	2	510	621	0.2	0.6	(b)				
		20	562	582	0.3	0.6	(b)				
	N10083						1	501	556	0.4	1.1
							4	477	746	0.8	1.4
							17(a)		415	-	-
Ni-41	N10087	18	543	581	0.2	0.9	1	528	610	0.4	0.9
		19	582				2	541	566	0.8	1.2
							10(a)	526	674	0.4	0.4
							11(a)	527	656	0.5	1.1
Ni-42	N10079	11	554	618	0.3	0.5	2	524	595	0.4	0.6
		12	514	606	0.2	0.4	15	541	656	0.8	1.4
							17(a)	506	668	0.3	1.1
							20(a)	528	650	1.1	1.1

(a) Argon exposure.
(b) Specimen not available for this test.
(c) Specimen failed in fillet before reaching yield.
(d) Specimen failed in threads.

TABLE 23

TENSILE TEST DATA AT 775°C

Alloy No.	Heat No.	As-cast specimens					Specimens exposed to H_2 for 100 hr at 236 MPa (gage) and 775°C (except as noted)				
		Specimen No.	0.2% Offset YS, MPa	UTS, MPa	Elongation in 4D, %	Reduction of area, %	Specimen No.	0.2% offset YS, MPa	UTS, MPa	Elongation in 4D, %	Reduction of area, %
Ni-35	N10080	16	357	554	0.9	1.1	11	358	541	1.2	1.6
		17	380	548	0.8	1.3	14	339	553	1.1	1.5
Ni-36	N10084	3	279	458	7.2	10.3	*				
		9	299	399	0.9	1.7	*				
Ni-37	N10085	13	320	523	1.9	2.2	17	309	548	1.8	2.5
		14	336	545	2.3	2.9	20	325	552	2.7	3.0
Ni-38	N10075	12	376	531	0.5	1.2	19	349	525	0.4	0.3
		13	414	539	0.3	1.3	20	332	539	0.4	0.3
Ni-39	N10076	14	394	579	0.3	0.8	9	349	574	0.8	0.3
		16	381	564	0.4	1.1	10	319	554	0.8	1.4
Ni-40	N10086	18	360	566	0.4	0.2	*				
		19	342	576	0.3	0.3	*				
	N10083	*					16	354	404	0.5	0.2
		*					20	348	518	0.8	1.4
Ni-41	N10087	16	399	582	0.8	0.9	3	285	514	1.1	0.9
		17	399	542	0.4	1.4	20	303	537	1.0	1.2
Ni-42	N10079	9	(53.2)	557	0.9	0.9	18	323	516	0.8	0.6
		10	387	541	0.7	1.1	19	301	541	1.2	1.6

*Specimens not available for this test

TABLE 24

CREEP-RUPTURE TEST DATA AT 775°C, 200 MPa

Alloy No.	Heat No.	Analysis, wt. %			Specimen No.	Strain on loading, %	Final creep reading		Durability at rupture*		Minimum creep rate, %/hr
		B	W	Cb			Time, hr	Deformation, %	Elongation in 4D, %	Reduction of area, %	
Ni-35	N10080	1.20	4.77	<0.10	3	0.170	301.1	1.001	2.6	2.8	0.00146
					4	0.166	176.9	1.001	1.8	1.9	0.00243
Ni-36	N10084	0.95	<0.10	3.89	2	0.178	26.5	1.054	3.6	4.8	0.0250
					4	0.181	32.4	1.002	4.9	4.3	0.0176
Ni-37	N10085	1.19	3.58	1.04	2	0.176	154.3	1.005	2.3	2.0	0.00312
					3	0.172	138.4	1.002	4.0	2.8	0.00347
Ni-38	N10075	1.26	3.59	0.96	9	0.173	496.4	1.003	1.8	1.8	0.00094
					10	0.178	500.0	0.961	1.5	1.8	0.00091
Ni-39	N10076	1.21	4.74	<0.05	12	0.185	384.5	1.005	1.5	1.7	0.00360
					13	0.180	408.6	1.007	1.4	1.8	0.00314
Ni-40	N10086	1.40	<0.10	3.23	15	0.170	94.0	1.017	2.0	2.0	0.00623
					16	0.175	104.2	1.005	1.5	1.6	0.00570
Ni-41	N10087	1.55	3.33	0.99	13	0.180	160.4	1.004	2.0	1.6	0.00284
					14	0.184	222.3	1.000	1.6	1.3	0.00222
Ni-42	N10079	1.21	2.49	1.97	3	0.171	136.5	1.005	1.5	1.7	0.00360
					4	0.178	164.0	1.007	1.4	1.8	0.00314

*Specimen up-loaded to failure after reaching either 1 percent creep or 500 hr.

TABLE 25

SECOND ITERATION: CYCLIC OXIDATION TEST DATA AFTER EXPOSURE IN AIR AT 870°C; 1-HR CYCLES

Alloy No.	Heat No.	Specimen No.	Specimen before exposure	Specimen plus crucible	Weight, g Specimen plus crucible at exposure times shown								Specimen only 100 hr	Specimen area, cm^2	Specific weight change in crucible (W/A), mg/cm^2	Specific weight change, specimen only (W/A), mg/cm^2
					1 hr	7 hr	14 hr	20 hr	40 hr	60 hr	80 hr	100 hr				
Ni-35	N10080	10	4.4881	8.9097	8.9099	8.9099	8.9091	8.9100	8.9100	8.9100	8.9104	8.9029[1]	4.4891	4.23	0.17[1]	0.24
		13	4.5267	8.9092	8.9093	8.9094	8.9086	8.9100	8.9096	8.9099	8.9100	8.9009	4.5271	4.23	0.17	0.09
Ni-36	N10084	10	4.4230	8.8689	8.8694	8.8697	8.8690	8.8711	8.8697	8.8707	8.8712	8.8712	4.4246	4.23	0.45	0.38
		11	4.3545	8.8087	8.8092	8.8095	8.8089	8.8100	8.8097	8.8101	8.8106	8.8104	4.3559	4.20	0.40	0.33
Ni-37	N10085	9	4.4716	8.7699	8.7701	8.7703	8.7697	8.7718	8.7708	8.7715	8.7717	9.1902[2]	4.4722	4.23	0.42[1]	0.14
		12	4.4413	8.6843	8.6847	8.6850	8.6838	8.6860	8.6855	8.6859	8.6860	8.6859	4.4423	4.23	0.38	0.24
Ni-38	N10075	1	4.4198	8.9124	8.9130	8.9135	8.9121	8.9138	8.9133	8.9135	8.9138	8.9136	4.4204	4.23	0.28	0.14
		2	4.4644	9.0475	9.0481	9.0481	9.0471	9.0490	9.0485	9.0488	9.0492	9.0490	4.4652	4.23	0.35	0.19
Ni-39	N10076	1	4.4726	8.8913	8.8915	9.8918	8.8900	8.8927	8.8917	8.8920	8.8926	8.8925	4.4732	4.23	0.28	0.14
		2	4.4554	8.8470	8.8470	8.4872	8.8466	8.8480	8.8471	8.8475	8.8480	8.8479	4.4561	4.23	0.21	0.17
Ni-40	N10086	14	4.3499	8.6251	8.6261	8.6266	8.6249	8.6276	8.6264	8.6275[3,4]	8.7719	8.7719	4.3518	4.23	0.61	0.45
		17	4.3352	8.7254	8.7264	8.7268	8.7259	8.7281	8.7270	8.7280[5]	8.8891	8.8890	4.3368	4.23	0.64	0.38
Ni-41	N10087	9	4.4130	9.0210	9.0215	9.0218	9.0199	9.0225	9.0217	9.0226	9.0227	9.0227	4.4142	4.23	0.40	0.28
		15	4.4027	8.9544	8.9549	8.9551	8.9535	8.9559	8.9560	8.9561	8.9564	8.9563	4.4039	4.23	0.45	0.28
Ni-42	N10079	13	4.3990	8.8141	8.8143	8.8144	8.8143	8.8154	8.8149	8.8148	8.8152	8.8151	4.399	4.23	0.24	0.21
		14	4.4024	9.1200	9.1210	9.1213	9.1200	9.1225	9.1216	9.1222	9.1225	9.1223	4.4035	4.23	0.54	0.26
N-155	N10066	7	4.3918	8.7787	8.7797	8.7800	8.7794	8.7819	8.7824	8.7824	8.7831	8.7841	4.3958	4.14	1.30	0.97
		8	3.7960	8.4177	8.4186	8.4190	8.4184	8.4199	8.4198	8.4198[6]	8.2399	7.4203	3.7974	3.81	0.66	0.37

NOTES:

1. Crucible chipped; total is for 80 hr.
2. New crucible weight = 4.7180. Old crucible disintegrated between 80 and 100 hr. Total is for 80 hr.
3. New crucible weight = 4.4199. At 60 hr, sample and spall weight = 4.3523 with additional spall = 0.0002.
4. Surface defect noted after test.
5. New crucible weight = 4.5521. At 60 hr, sample and spall weight = 4.3378 with additional spall = 0.0001.
6. New crucible weight = 4.4433. At 60 hr, sample and spall weight = 3.7981 with additional spall = 0.0004.

Discussion

The following discussion of test results and choices of alloy compositions draws upon data presented in this report. Because all alloys of the first iteration exhibited acceptable behavior in the braze wetting test and welding, the tests were not repeated for the second iteration. With regard to oxidation behavior, all alloys were shown to meet the behavior target comparable to that of N-155. In fact, all alloys investigated in the first and second iterations appear to have equivalent or better cyclic oxidation resistance than N-155.

Exposure to hydrogen and argon caused no significant deterioration of properties. Lowered yield and tensile strength were noted on some samples, but others showed no change. Elongation and reduction of area were unaffected.

When boron was in the 1-percent range, no substantial differences in tensile behavior occurred at room temperature or 775°C for alloys containing tungsten, columbium, or combinations of these. A boron level of 0.50 percent (with a carbon level of 0.50 percent) clearly provided sufficient strength. On the other hand, alloys with the highest boron content (1.40 percent and 1.55 percent for Heats N10086 and N10087, respectively) have low tensile ductility. Although this program includes no ductility requirement, these alloys also have low creep resistance.

The alloy property target initially identified as most important for this program was creep resistance. Although cost constraints prevented creep testing for the full 5000 hr of the stress-rupture target (5000 hr at 775°C and 200 MPa), experience with accelerated (830°C) stress-rupture testing during the screening study and with the 500-hr creep testing reported herein suggests that alloys exhibiting 1-percent creep in no less than about 300 to 500 hr will meet the creep resistance target.

Fig. 30 shows the creep behavior for all heats of the first and second iterations as averages of two specimens. The heats with the best combination of creep resistance and rupture ductility (N10060, N10069, and N10059) all have about 2.3 percent tungsten, with varying amounts of columbium. One alloy without tungsten, but with 1.6 percent columbium (N10058), has creep behavior of interest.

Selection of three alloys.--The choices of three alloys to be tested further was based on the best combination of strength and ductility. Fig. 30, as noted previously, points out those alloys meeting acceptable properties of 325 hr to reach 1-percent elongation under test conditions of 775°C and 200 MPa and having a minimum of 2-percent elongation at failure. Compositions corresponding to Heats N10058 (Ni-26), N10060 (Ni-28), and N10069 (Ni-32B) were specifically recommended as the three alloys to be used. The tentative ranges of the various elements are shown in table 26.

C-2

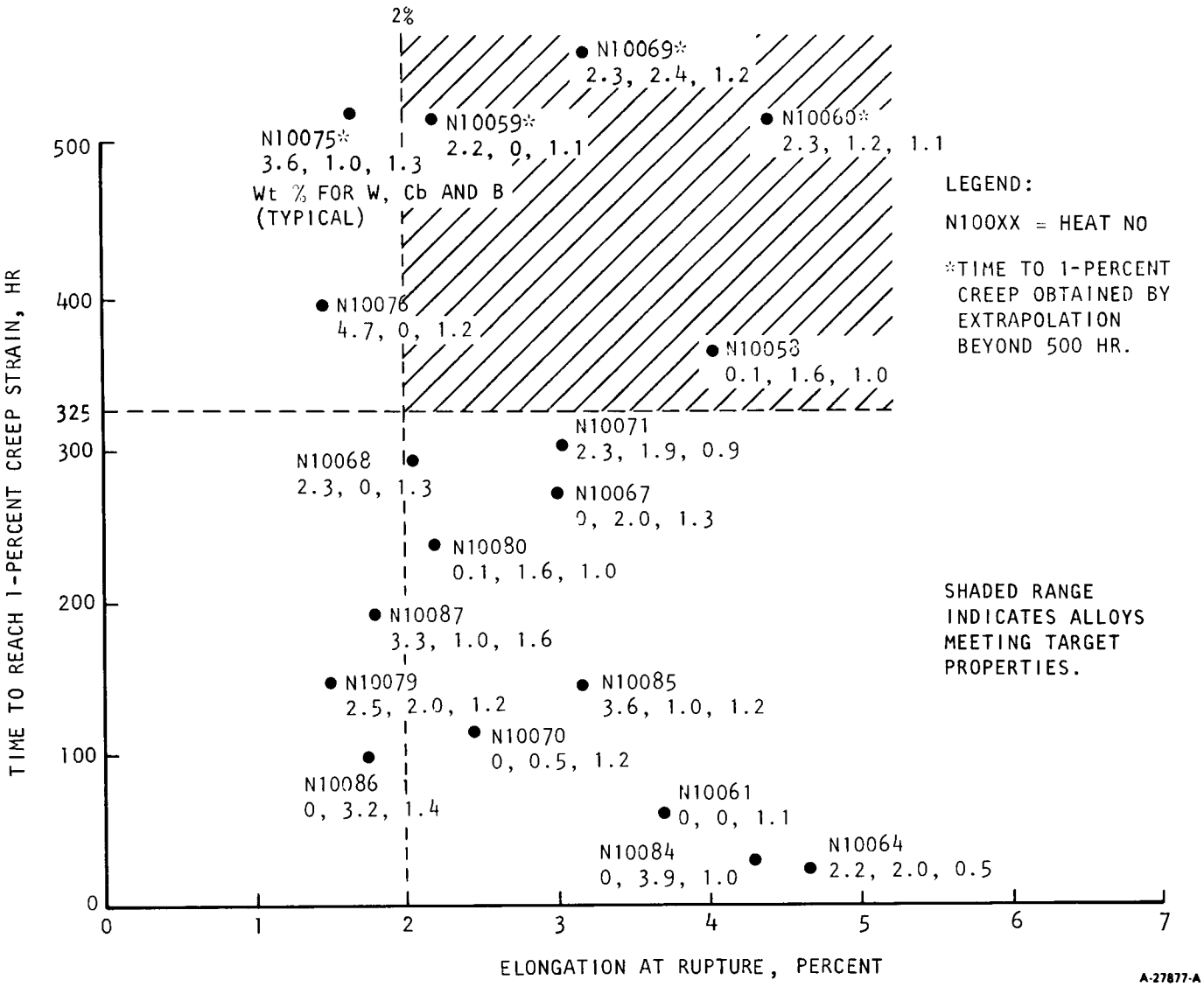

Figure 30.--Relationship Between Creep Behavior and Rupture Elongation (775°C/200 MPa).

TABLE 26

RECOMMENDED COMPOSITION
RANGES FOR FURTHER STUDY

	C	Mn	Si	Cr	Ni	Mo	W	Cb	W + 1.4 Cb	B	Fe
Minimum	0.45	0.15	0.25	16	17	4.5	-	-	2.75	1.0	Bal.
Maximum	0.55	0.35	0.45	19	19	5.5	2.75	2.5	-	1.3	

HEAT TREATMENT

On May 12, 1982, a program review was held at the NASA Lewis Research Center. The discussion introduced some new concerns and parameters regarding the program goals and requirements. As a result of these, the program was modified.

The main concern was fatigue resistance of candidate alloys. This parameter had not been considered in the initial program outline, so it was decided to hold up on continuing with the original program until some work had been done to improve fatigue characteristics. Also, it was agreed that the initial rupture life goal of 5000 hr at 200 MPa and 775°C could be reduced to 3000 hr without problem.

The outcome of this meeting was that two alloys having attractive properties (table 27) would be used as the basis for a limited heat treat program to improve ductility. Increasing the ductility of these alloys without significant decrease in strength was thought to improve the overall fatigue resistance.

TABLE 27

NASA STIRLING ENGINE Fe-BASE ALLOY
CHEMISTRIES OF TWO ALLOYS FOR HEAT TREATMENT

	Ni-38 (10075)	Ni-39 (10076)
Carbon	0.48	0.39
Manganese	0.26	0.24
Silicon	0.46	0.40
Chromium	18.81	18.64
Nickel	18.07	18.15
Molybdenum	5.18	5.08
Tungsten	3.59	4.74
Columbium	0.96	-
Boron	1.26	1.21
Nitrogen	420 ppm	390 ppm
Oxygen	73 ppm	49 ppm
Sulfur	0.004	0.004
Phosphorus	0.022	0.019
Iron	Bal.	Bal.

Procedure

Two alloys (Ni-38 and Ni-39) were selected and test bars were heat treated for 1, 2, and 4 hr at 1177°C. Microstructures were studied and, based upon these, a final heat treatment was selected. Bars were tested in tensile and stress rupture.

Alloy selection.--Investment cast test bars were selected from two alloys that had exhibited good mechanical properties. These alloys were Ni-38 (Heat N10065) and Ni-39 (Heat N10066), the chemistries of the alloys are given in table 27. The reason for selecting these two, apart from their mechanical properties, was that N10075 had approximately 1 percent Cb present, and N10076 had approximately 1 percent higher W content. A stable carbide, such as CbC, was thought to enhance the properties.

Heat treatment cycle selection.--The presence of eutectic carbides and borides in interdendritic areas could be the cause of the low ductilities of these alloys. (Elongation values around 0.1 to 0.3 percent were common.) If these eutectics could be heat treated to produce a more spheroid structure, improved ductility could result. Heat treating in the 1093°C to 1204°C range would be sufficient to dissolve some of the secondary carbides and spheroidize the primary carbides and borides. Previous work on this class of alloys by Sponseller (Ref. 11) indicated that 1177°C was necessary for this to occur. Therefore, test pieces were placed in an argon atmosphere furnace at 1177°C for 1, 2, and 4 hr.

Tensile tests were conducted at room temperature and 775°C. Stress-rupture tests were performed at 830°C and 200 MPa. The higher temperature was used to produce a rupture life in the 100- to 500-hr range, whereas the lower temperature of 775°C could result in a test running over 3000 hr.

Results

Micrographs of the solution-heat-treated specimens are shown in figs. 31 and 32. The results of the tensile tests and stress-rupture tests are shown in table 28.

Discussion

The as-cast structure is significantly modified by this heat treatment cycle of 1177°C for 1, 2, and 4 hr. The photomicrographs, figs. 31 and 32, reveal the effects of heat treatment. One hr at 1177°C shows minor change. However, the microstructure shows significant spheroidization of the carbides after 2 and 4 hr. Most of the effect is completed in the 2-hr cycle; therefore, the 2-hr cycle was selected for tensile and stress-rupture evaluation.

Table 28 shows that the strength properties are markedly increased (except at 775°C), but the tensile ductility was not dramatically effected by heat treating for 2 hr at 1177°C.

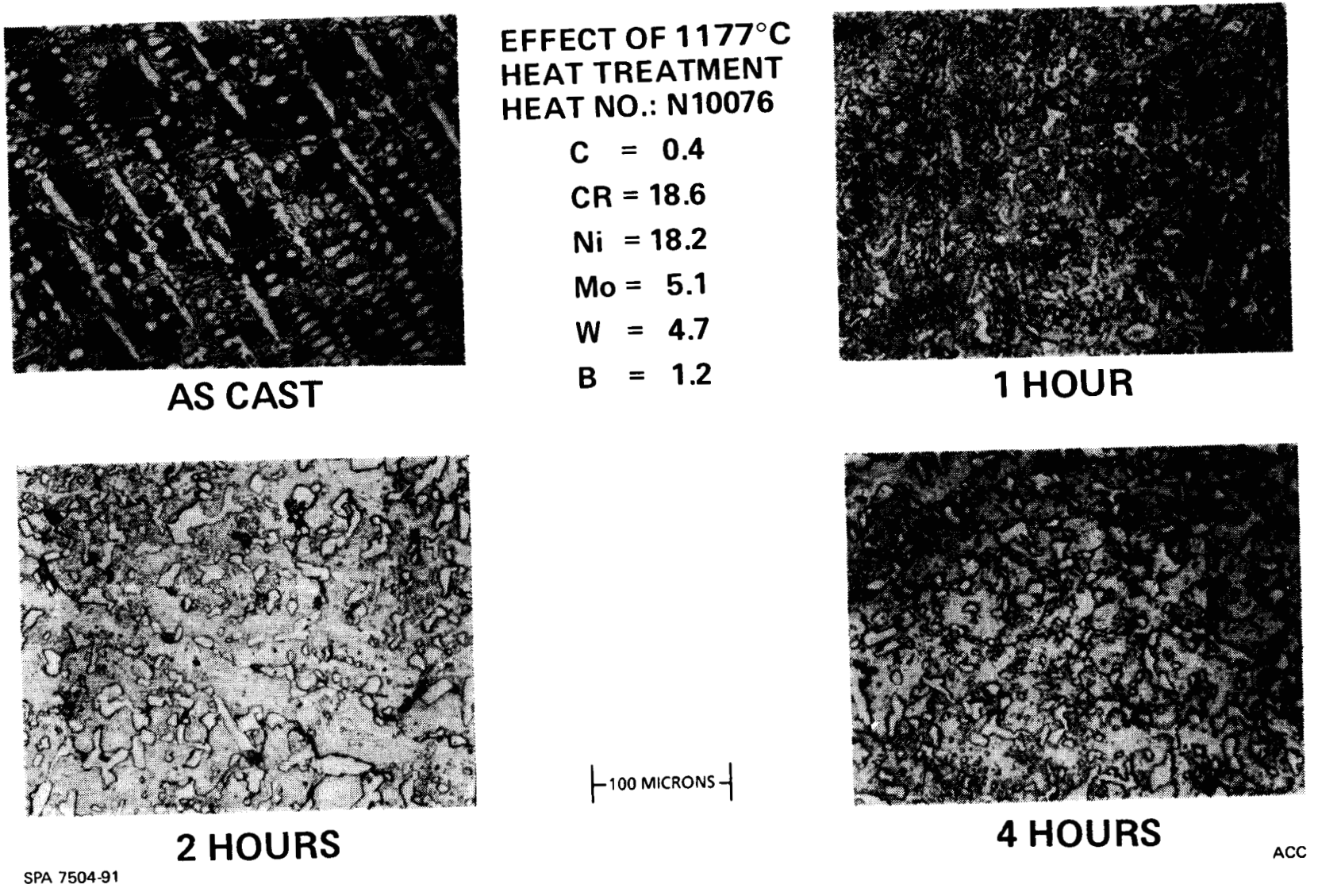

Figure 31.--Effect of 1177°C Heat Treatment (Heat No. N10076).

AS CAST

EFFECT OF 1177°C
HEAT TREATMENT
HEAT NO.: N10075

C = 0.48
CR = 18.8
Ni = 18.1
Mo = 5.2
W = 3.6
Cb = 1.0
B = 1.26

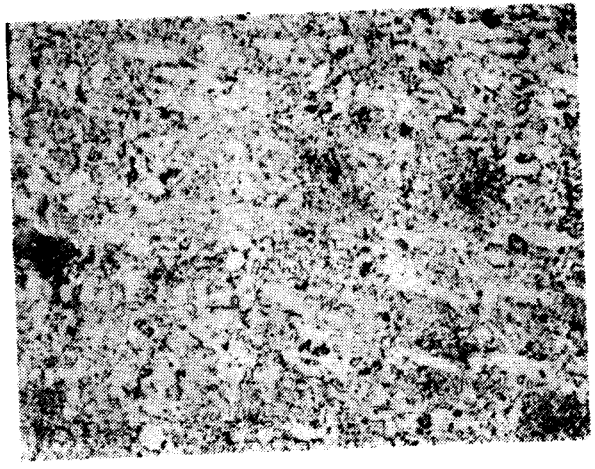

1 HOUR

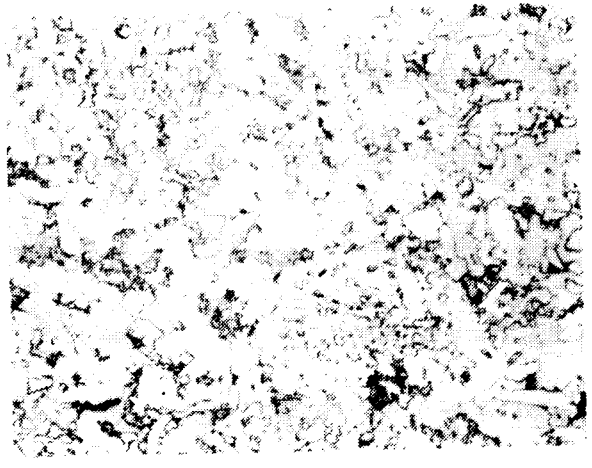

2 HOURS

100 MICRONS

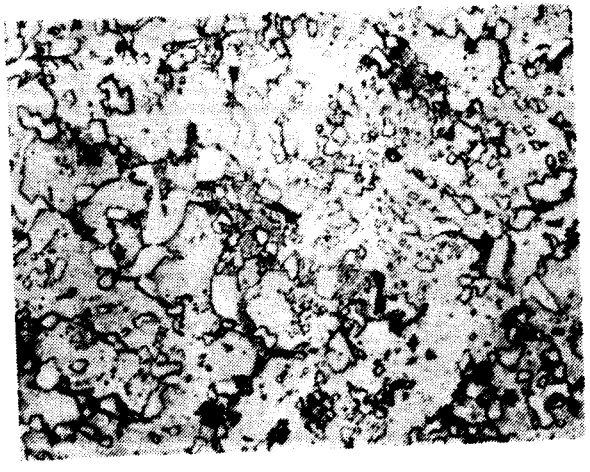

4 HOURS

SPA 7504-90

ACC

F-39405 -A

Figure 32.--Effect of 1177°C Heat Treatment (Heat No. N10075).

TABLE 28

NASA STIRLING ENGINE Fe-BASE ALLOY
EFFECT OF HEAT TREATMENT

	Ni-38		Ni-39	
Room temperature	Heat treated	As-cast	Heat treated	As-cast
Tensile				
UTS	95.2	84.4	95.0	84.9
YS	74.1	76.9	69.6	76.7
Elongation, %	1.0	0.2	1.0	0.2
Reduction of area, %	1.6	0.4	0.8	0.4
775°C tensile				
UTS	77.0	77.0	81.1	84.0
YS	55.4	54.5	59.1	57.1
Elongation, %	1.0	0.5	1.0	0.3
Reduction of area, %	0.8	1.2	0.8	0.8
Stress rupture (200 MPa)	Test temperature			
	(830°C)	(775°C)	(830°C)	(775°C)
Life (hr)	101.2	500	246.5	384.5
Elongation, %	5.0	1.6	8.0	1.5
Reduction of area, %	8.6	1.8	17.5	1.7
Larson-Miller*	24.3*	23.8	24.6**	23.6

*Theoretical life at 775°C = 1,500 hr
**Life at 775°C = 3,600 hr

Using the Larson-Miller parameter to extrapolate the values, alloy Ni-38 had a 500- to 1500-hr improvement, and Alloy Ni-39 a 384- to 3600-hr increase. Also, the rupture ductilities also were greatly increased 4 to 10 times the as-cast values. Alloy N10076, with a theoretical life of 3600 hr, certainly meets the revised material goal requirements of 3000 hr.

The data in table 28 are plotted on a Larson-Miller curve (fig. 33); the heat-treated samples appear to approach the NASA target and are superior to the cobalt base X-40.

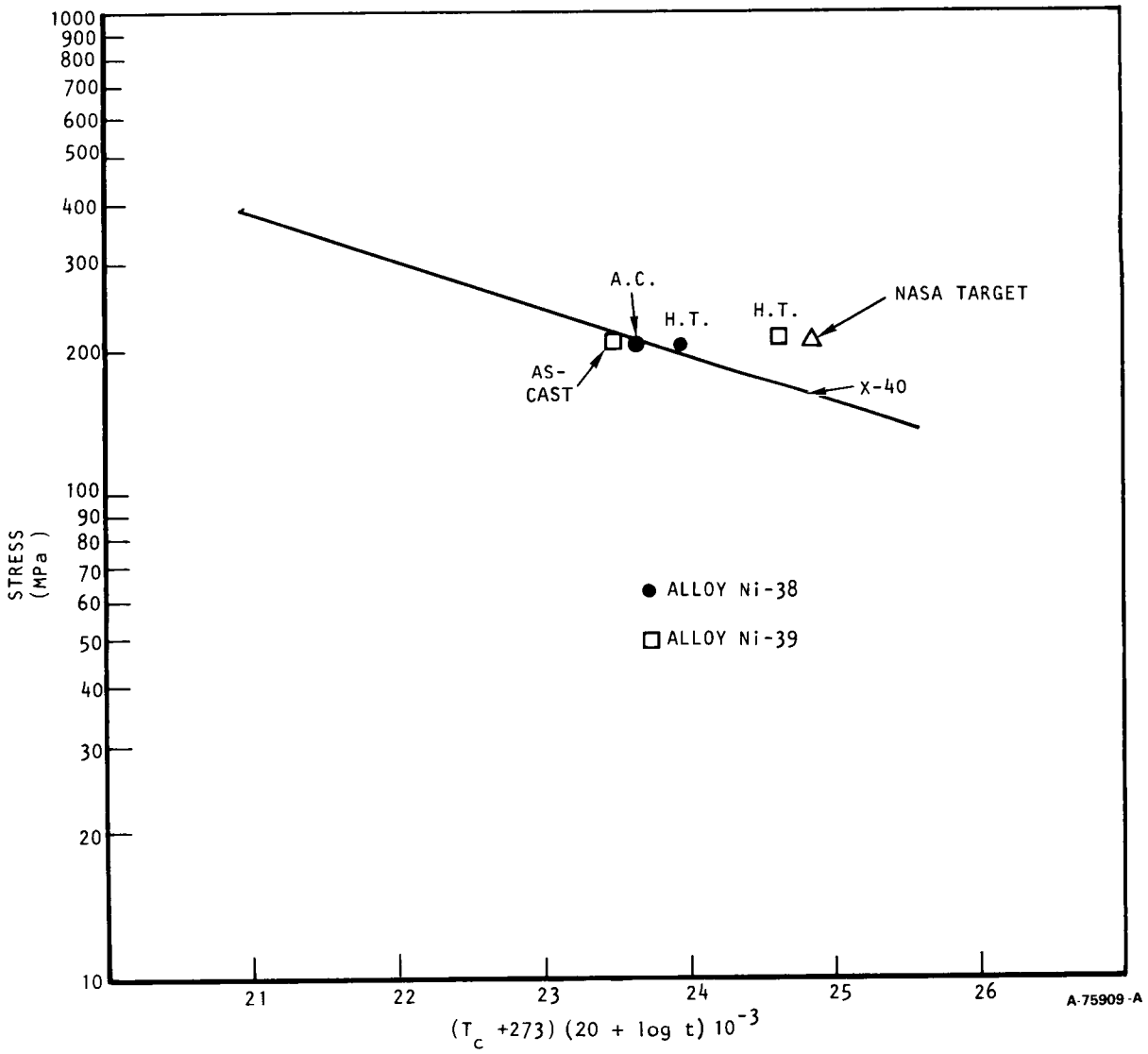

Figure 33.--Stress-Rupture Characteristics of Fe-Base Stirling Alloy in the Heat-Treated (1177°C, 2 hr) and As-Cast Condition.

SELECTION OF CASTING VARIABLES

Introduction

This portion of the program was aimed at producing the desired Fe-base housings at minimum cost while meeting property goals. To this point, investment casting had been the molding medium used. However, recognizing that sand casting offers real potential for savings and high volume production, testing was performed on bars machined directly from housings made in sand molds. A comparison of casting costs and properties between sand and investment casting could then be made.

Selection of Three Alloys

A reliable engineering material to meet program goals will require a minimum of 325 hr to reach 1-percent creep when tested at 775°C/200 MPa and exceed 2-percent elongation at rupture. Alloys Ni-26, Ni-28, and Ni-32B (table 14) were chosen as alloys most likely to meet these property goals. In earlier program efforts, these alloys met or surpassed the requirements for room and elevated temperature properties, oxidation resistance, hydrogen compatibility, weldability, and braze wetting. Reference to fig. 30 confirms that these alloys meet creep-rupture requirements and afford a good range of compositions for final evaluation.

Sand Cast Housings

Casting Procedure.--Molds for the regenerator castings made in this phase of the program were Airset bonded silica sand. The molds were heated above 100°C to evaporate residual moisture, then cooled to room temperature before pouring.

Because of the many alloy compositions used, a base alloy master heat (table 29) was produced, and the desired compositions of Ni-26, Ni-28, and Ni-32B achieved by elemental additions (table 30). There are advantages to this approach--the resultant heats are more consistent chemically, and homogeneity is much better than that of the virgin heats used earlier in the program. Further, a larger master heat can be more thoroughly deoxidized.

The initial master heat when analyzed for deleterious trace elements showed 19 ppm lead and 200 ppm tin, which is unacceptable when compared to industry standards of 5 ppm lead and 10 ppm tin. Subsequent master heats C-0795 and C-0796 (table 29) met target chemistries, including trace elements. The melting procedure (table 31) was the same for both sand and investment molds. A 159-kg airmelt furnace was used for melting. The average power input varied from 120 to 160 kw, depending on the element addition. Care was taken to dry all additions before adding to the melt. Weight of adds was calculated to the nearest 5 gms for each of the three alloys processed. Table 32 shows aim and actual pour temperatures. The liquidus temperature was determined using thermal arrest.

TABLE 29

MASTER MELT COMPOSITION, PERCENT

C-0795 Chemistry						
C 0.55	Mn 0.31	Si 0.57	P <0.02	S <0.01	Cr 18.6	Ni 18.6
Mo 4.8 Al <0.01	Cu 0 B 1.4	Co 0.01		Fe Bal	Cb + Ta <0.01	W <0.04
C-0796 Chemistry						
C 0.53	Mn 0.29	Si 0.57	P <0.02	S <0.01	Cr 18.4	Ni 18.5
Mo 5.3 B 1.4	Cu 0	Co <0.01	Fe Bal	Cb + Ta 0.04	W 0.04	Al <0.01

Trace element Content (Analyzed by Atomic Absorption)			
	Sn	Pb	Bi
C-0795	5.0	1.5 ppm	<1 ppm
C-0796	8.0 ppm	2.0 ppm	<2 ppm

TABLE 30

ELEMENTAL ADDITIONS

	Weight, lb		
	Ni-26	Ni-28	Ni-32B
C	0.03	0.10	0.08
Ni	0.84	2.63	1.95
FeMo	0.69	1.86	1.42
NiB	0.68	1.85	1.40
FeCb	4.67	7.29	4.37
Cr	1.58	4.28	3.25
Mn	0.03	0.07	0.05
W	-	5.0	5.0
Si	-	0.004	0.02
Master Alloy	191.5	177.0	182.45
Total Weight	200.02	200.08	199.99

TABLE 31

CHARGING PROCEDURE

Add Cr, Ni, W, FeMo
Add base alloy
Slow melt until bath is molten
Determine liquidus temperature (LT)
Slag at LT + 56°C
Add FeCb, if necessary for composition
Slag
Determine pour temperature
Heat to pour temperature + 27°C
Slag
Transfer to ladle
Cool to pour temperature
Pour molds
Pig ladle balance

TABLE 32

AIM TEMPERATURE VS ACTUAL POUR TEMPERATURES

Composition	LT	Aim Temp., °C	Actual Temp., °C
Ni-26	1260°C	1316 (LT+56)	1327 (LT+67)
N-10088		1361 (LT+111)	1377 (LT+117)
		1427 (LT+167)	1445 (LT+185)
Ni-28	1238°C	1294 (LT+56)	1305 (LT+73)
N10089		1349 (LT+111)	1349 (LT+111)
		1405 (LT+167)	1427 (LT+189)
Ni-32B	1250°C	1305 (LT+56)	1405 (LT+155)
N10090		1360 (LT+111)	1405 (LT+155)
		1416 (LT+167)	1405 (LT+155)

Testing.--Each of the heats was analyzed for chemistry. Table 33 lists aim vs actual results.

The castings were cut into 12 test bar blanks per casting (fig. 34). Blanks were X-rayed for internal defects. Those radiographically acceptable were machined into test bars, which were heat treated for 2 hr at 1177°C in an argon atmosphere. Mechanical testing included room and elevated temperature tensile testing and accelerated stress-rupture testing at 830°C and 200 MPa.

TABLE 33

AIM VS ACTUAL CHEMISTRIES

	Ni-26 N10088		Ni-28 N10089		Ni-32B N10090	
	Aim, %	Actual, %	Aim, %	Actual, %	Aim, %	Actual, %
C	0.5	0.53	0.5	0.52	0.5	0.51
Mn	0.20	0.26	0.20	0.22	0.20	0.21
Si	0.30	0.49	0.30	0.40	0.30	0.39
Cr	18.0	18.87	18.0	18.4	18.0	18.1
Ni	18.0	18.79	18.0	17.9	18.0	18.5
Mo	5.0	5.37	5.0	4.8	5.0	5.1
B	0.5	1.32	0.9	1.2	1.5	1.2
Cb	2.0	1.51	2.0	1.3	2.0	2.1
W	0	0.01	2.0	2.6	2.0	2.6
Fe	Bal.	Bal.	Bal.	Bal.	Bal.	Bal.

PRINT AND LAYOUT DIMENSIONS

Dimension, cm	A	B	C	D	E	F	G
Print	4.57	3.18	9.53	1.27	6.35	12.7	3.56
Layout	4.57	3.18	9.55-9.57	1.27-1.31	6.32	12.69-12.7	3.54

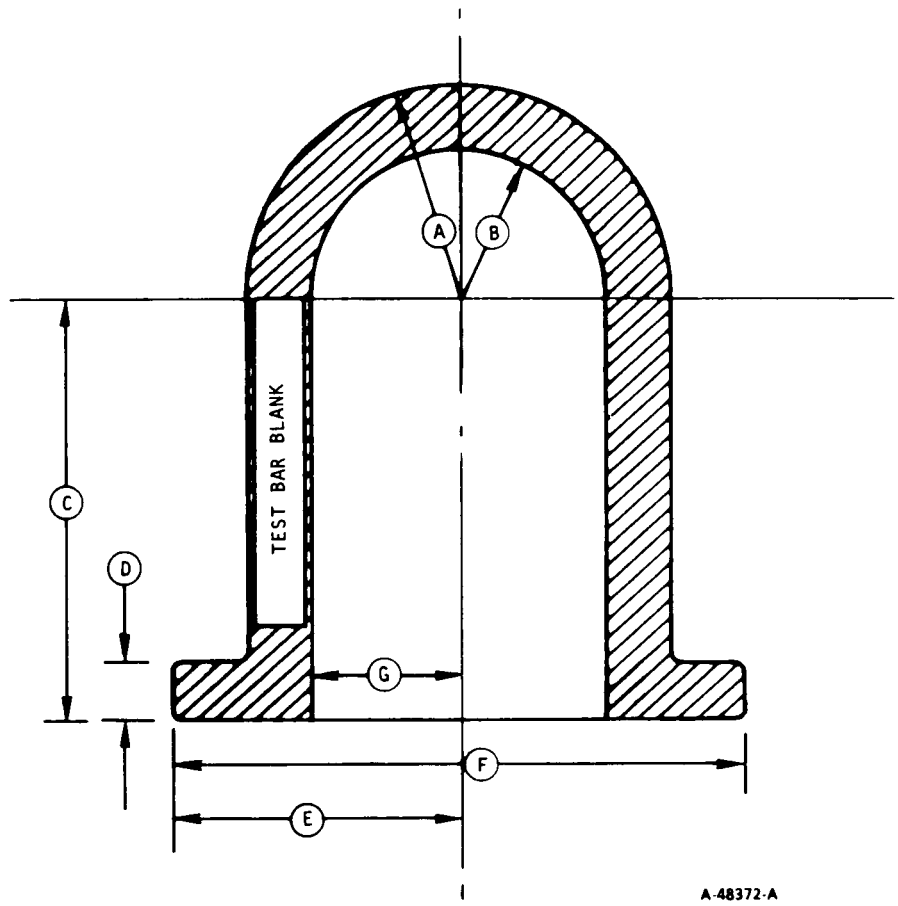

Figure 34.--Sample Casting Configuration.

Results

Visual.--Fig. 35 shows the excellent fluidity of the Fe-base alloys. At temperatures as low as 67°C above the liquidus temperature mold fill proved no problem whatever. By comparison, the same housing casting poured in Stellite 31 at 100°C above the liquidus temperature did not come close to filling.

The surface of the castings made from Airset sand molds was, as expected, rougher than that of the castings made from investment molds. There was also indication of inclusion-type defects in the castings.

X-ray.--Radiographic examination of the test blocks cut from castings reveals a varying degree of inclusion, gas, and shrinkage defects in many of the samples. Those with minimum indications were selected for heat treat, machining, and testing.

Testing.--Tables 34 through 39 summarize the mechanical property test results obtained at room and elevated temperatures for both the investment cast master heat qualification test bars and the bars initially cut as blanks from the Airset sand mold castings.

Table 34 shows mechanical properties of investment cast test bars from master heat C-0795, designed to duplicate Alloy No. Ni-28. Results compare favorably with earlier results for this alloy.

Table 35 shows elevated creep-rupture properties of investment cast test bars for each of the three alloys being studied. Again, results are generally comparable to earlier work. Alloy Ni-28 provides more consistent results than the other alloys do.

Table 36 shows room temperature tensile properties of bars cut from castings poured at different temperatures in Airset molds. Results are significantly lower than those from the investment cast test bars for alloy Ni-28 (table 32).

Table 37 shows elevated temperature test results for bars cut from Airset mold castings. Again, pour temperature was varied. These results also do not match those of the investment cast bars for alloy Ni-28 (table 32).

Table 38 shows stress-rupture test results for bars cut from Airset mold castings. Hours to fracture were very low.

Table 39 compares tensile properties of investment vs sand cast test bars at both room and elevated temperatures for alloy Ni-28.

Discussion

Despite the potential for cost savings, the use of Airset sand molds is likely to yield castings of lesser quality and thereby lower mechanical properties. It is essential that quality be maintained to meet the aims of this program.

Figure 35.--Model Regenerator Housings: Fe-Base Alloy and HS-31.

TABLE 34

MECHANICAL PROPERTIES*

MASTER HEAT QUALIFICATIONS

Master Heat C-0795
Alloy Ni-28

Room temperature tensile results						
Bar no.	Actual size, cm	Actual area, sq cm	Yield, Mpa	UTS, MPa	Elongation, %	R of A
1	0.645	0.327	433	594	2.0	-
2	0.630	0.311	489	630	2.0	-

775° tensile properties						
Bar no.	Actual size, cm	Actual area, sq cm	Yield, Mpa	UTS, MPa	Elongation, %	R of A
1	0.632	0.314	333	524	3.0	2.0
2	0.635	0.317	378	531	2.0	-

Accelerated stress rupture 830°C/200 MPa					
Bar no.	Actual size, cm	Actual area, sq cm	Stress, MPa	Time to fracture, hr	Elongation, %
1	0.637	0.319	200	118.0	4.0
2	0.637	0.319	200	134.7	3.0

*Investment cast test bars. Heat treated at 1177°C for 2 hr.

TABLE 35

CREEP-RUPTURE PROPERTIES AT 775°C/200 MPa (1427°F/29 ksi)
ON INVESTMENT CAST (I/C) BARS

	Rupture life, hr	Creep, %	Hr to 1% creep	Min. creep rate cm/cm/ hr x 10^{-6}	Larson-Miller parameter (C = 20)
Ni-26 N10088					
LT + 67°C	318.0	7.01	40	114.5	23.5
LT + 67°C	395.2	7.51	50	94.0	23.7
LT + 117°C	353.3	4.59	50	125.9	23.6
LT + 117°C	72.8	1.17	35	175.4	22.9
LT + 185°C	500.8 (D)	5.85	100	55.2	----
Ni-28 N10089					
LT + 73°C	501.8 (D)	3.01	100	44.0	----
LT + 111°C	413.0	4.17	60	70.9	23.8
LT + 189°C	512.8 (D)	2.84	120	46.0	----
LT + 189°C	502.0 (D)	2.63	130	40.4	----
Ni-32B N10090					
LT + 155°C	291.7	1.85	130	45.5	23.5
LT + 155°C	504.5 (D)	2.06	200	29.7	----
LT + 155°C	201.4	1.86	75	55.6	23.4
LT + 155°C	501.6 (D)	2.62	160	39.0	----
LT + 155°C	362.0	1.52	200	34.4	23.6
LT + 155°C	99.5	0.67	---	30.3	23.1

(D) = Test discontinued at 500 hr

TABLE 36

ROOM TEMPERATURE TENSILE TEST RESULTS
(from castings poured in Airset™ molds)

		Yield, MPa	UTS, MPa	Elongation, %	R of A, %	Comments
Alloy Ni-26	Heat N10088					
	LT + 67°C	393	495	1.0	0.81	----
	LT + 117°C	386	475	1.0	0.82	PM/OQ
	LT + 185°C	369	532	1.0	1.60	OQ
	Avg	383	499	1.0	1.1	
Alloy Ni-28	Heat N10089					
	LT + 73°C	383	513	1.0	0.81	OQ
	LT + 111°C	392	588	1.0	1.66	OQ
	LT + 189°C	308	368	1.0	0.82	OQ
	Avg	367	490	1.0	1.1	
Alloy Ni-32B	Heat N10090					
	LT + 155°C	383	477	2.0	0.81	OQ
	LT + 155°C	389	537	1.0	0.81	OQ
	LT + 155°C	397	499	0.0	0	----
	Avg	390	504	1.0	0.5	

All castings heat treated at 1177°C/2 hr

PM = Punch mark fracture
OQ = Outer quarter fracture

TABLE 37

ELEVATED TEMPERATURE TENSILE TEST RESULTS (775°C)
(from Airset™ Casting)

		Yield, MPa	UTS, MPa	Elongation, %	R of A, %	Comments
Alloy Ni-26	Heat N10088					
	LT + 67°C	328	401	2.0	0.80	----
	LT + 117°C	252	282	1.0	0.81	----
	LT + 185°C	273	429	2.0	0.80	
	Avg	284	371	1.7	0.8	
Alloy Ni-28	Heat N10089					
	LT + 73°C	288	495	3.0	2.4	----
	LT + 111°C	300	419	4.98	3.80	----
	LT + 189°C	305	413	1.0	0.79	PM/OQ
	Avg	293	443	3.0	2.3	
Alloy Ni-32B	Heat N10090					
	LT + 155°C	273	362	0	0	R/OQ
	LT + 155°C	286	437	1.0	0.80	----
	LT + 155°C	299	446	2.0	0.80	----
	Avg	286	414	1.0	0.53	

All castings heat treated at 1177°C/2 hr
No misruns were encountered in the experiment.

PM = Punch mark fracture
OQ = Outer quarter fracture
R = Radius fracture

TABLE 38

STRESS-RUPTURE TEST RESULTS 830°C/200 MPa

Ni-26 N10088			Ni-28 N10089			Ni-32B N10090		
	Hr	Elong., %		Hr	Elong., %		Hr	Elong., %
LT + 67°C	20.0	5.0	LT + 73°C	55.4	8.0	LT + 155°C	3.0*	3.0
	22.3	8.0		61.7	5.0		19.3	2.0
LT + 117°C	26.9	8.0	LT + 111°C	20.7	4.0	LT +155°C	15.5	3.0
	37.1	8.0		93.4	5.0		60.9	6.0
LT + 185°C	36.0	6.0	LT + 189°C	35.6	3.0	LT + 155°C	27.6	2.0
	*9.8	*2.0		59.7	7.0		56.0	4.0
Avg	28.5	7.0	Avg	54.4	5.3	Avg	35.9	3.4

*Not included in the average

All preceding values are from heat treated (1177°C/2 hr) sand cast housings.

TABLE 39

TENSILE TEST RESULTS ON INVESTMENT BARS
ALLOY Ni-28 HT. NO. N10089

Room temperature	UTS, MPa	YS, MPa	Elong., %	RA, %
	519	449	0	0
	521	453	0	0
	534	457	0	0
	600	406	0	0
	501	393	0	0
Average I/C bar	535	432	0	0
Average sand cast bar	490	357	1.0	1.1
755°C (1427°F)				
	476	312	2.0	8.5
	408	260	2.0	14.4
	507	339	3.0	0.83
	499	342	4.0	0.76
	502	337	2.0	4.8
Average I/C bar	479	318	2.6	5.9
Average sand cast bar	443	314	3.0	2.3

The excellent fluidity of the Fe-base alloys systems being studied allows castings to be poured at very low temperatures. This minimizes shrinkage; however, gas indications are more prevalent under such pour conditions, especially with sand molds, which tend to generate gas from the mold binders after pouring.

Conclusion

In discussions with NASA personnel, it was decided that investment casting would be the preferred manufacturing method. The Airset mold process is unacceptable for this alloy system.

Although property results are not as consistent as desired, lower pour temperatures have yielded acceptable properties. Because the alloys with 1.2-percent boron have such excellent fluidity, pouring at a low pour temperature and low mold preheat temperature is most practical.

Based on a detailed review of the test data obtained from these heats, an optimum chemical composition, which should offer the best combination of properties, was determined. This alloy (table 40) was designated NASACC-1. The composition is essentially that of alloys Ni-28 and Ni-32B, which were targeted to differ only in boron content (table 33), but in actual chemical analysis showed the same boron level and only a difference in columbium content. Both these alloys exhibited properties exceeding target goals throughout testing.

Baseline data for alloy NASAAC-1 were developed to conclude the program.

TABLE 40

NASACC-1 CHEMISTRY RANGE

	Target Composition	Actual Composition
C	0.45 - 0.55	0.51
Mn	0.20 - 0.40	0.27
Si	0.45 - 0.65	0.55
Cr	18.0 - 19.0	18.40
Ni	18.0 - 19.0	18.82
Mo	5.0 - 5.5	5.04
W	2.2 - 2.7	2.70
Cb	1.6 - 2.2	2.20
B	1.0 - 1.4	1.20
S	0.03x	0.01
P	0.03x	0.01
Cu	0.25x	0.05
Pb	20 ppmx	1 ppm
Sn	20 ppmx	7 ppm
Fe	Balance	Balance

DEVELOPMENT OF PRELIMINARY DATA BASE FOR NASAAC-1 ALLOY

Objectives

In the preceding section specific conclusions were reached. These included selection of investment molding as the method of casting, establishment of low mold preheat and metal pour temperatures as most effective in improving properties, and determination of an optimum chemical composition providing the best combination of properties.

The chemistry range established for candidate alloy NASAAC-1 is shown in Table 40. As a final step in this program, it is mandatory to define realistic baseline data for the alloy, including information relative to:.

(1) Stress rupture
(2) Creep rupture
(3) Room temperature tensile
(4) Elevated temperature tensile
(5) Low cycle fatigue
(6) Metallography
(7) Dilatometry
(8) Thermal conductivity
(9) Specific heat
(10) Thermal expansion

Cyclic oxidation, hydrogen compatibility, and braze and weld characteristics were performed on similar alloys in prior work, and all tests surpassed minimum requirements.

To establish this objective data base, the following casting and testing program was performed:

(1) Casting of 20 specimen casting blanks; nondestructive examination

(2) Tensile testing (two each temperature); room temperature, 300°, 400°, 500°, 600°, 600°, 775°, 800°, and 850°C.

(3) Creep-rupture testing (500 hr maximum, two each condition) to determine the effect of temperature on time to reach 0.5, 1.0, and 1.5 percent creep. Test temperatures: 600°, 775°, and 800°C.

(4) Thermal expansion; room temperature to 850°C.

(5) Specific heat; room temperature to 850°C.

(6) Thermal conductivity; room temperature to 850°C.

(7) Metallographic support

(8) Shipment of 30 tensile/creep-rupture specimens to NASA

Procedure

Casting.--A 352-kg master heat of NASACC-1 alloy was purchased from Certified Alloy Products, Inc. Two lots of castings were poured in a 159-kg induction furnace using identical melting procedures. Four molds (two housing blanks per mold) (fig. 36) were poured in the first lot and eight molds in the second lot. The gates on two molds had alumina (Kaowool™)insulation around them; however, no difference was noticed between the wrapped and unwrapped molds. Therefore, the molds in the second lot were not wrapped.

The masterheat liquidus was determined to be 1549°C using an immersion thermocouple. Next, superheating the alloy to 1642°C (LT + 93°C) and pouring metal into the preheated (1038°C) ladle caused the ladle temperature to increase to a temperature closer to the liquid metal. The metal was poured back into the furnace and stabilized at LT + 49°C. Finally, the melt was poured into the ladle, where the metal was held until the temperature reached LT + 43°C, and the metal poured into an investment mold preheated to 1038°C.

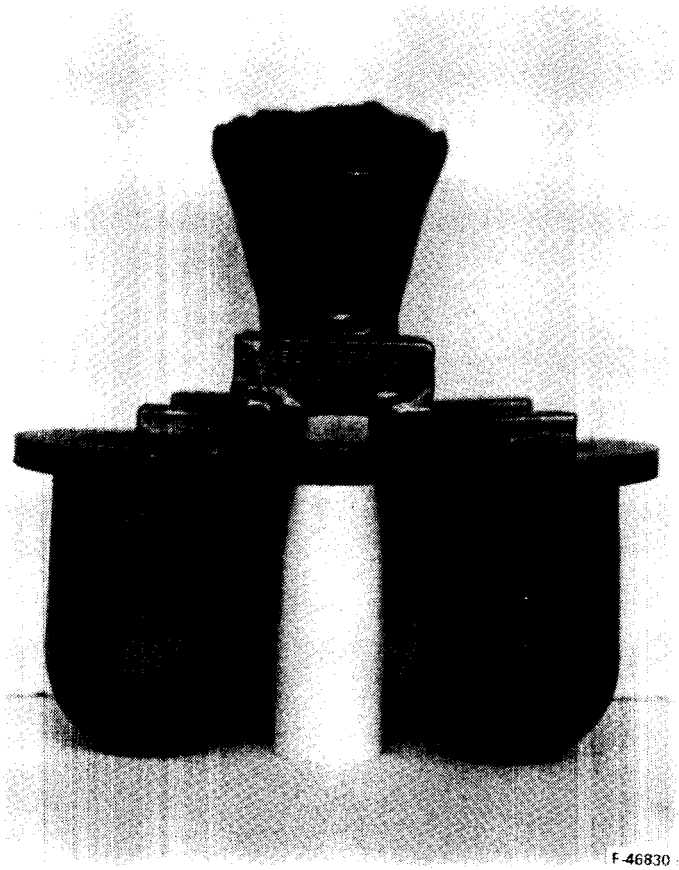

Figure 36.--Sandblasted Housing Castings with Risers and Gating Attached. Casting Poured into an Investment Shell Mold.

The castings were made by using the investment wax process. The wax patterns were dipped in a refractory slurry of zircon flour in a colloidal silica suspension. Seven coats were applied using alumina stucco with a minimum of 2 hr between coats. Once the outer shell was dry and hard, the wax patterns were melted out, leaving the mold cavity. The shell was preheated to 1038°C and removed from the preheat oven just before pouring.

Chemical analysis.--Samples for analysis were taken from castings. Actual composition is shown in table 40.

Heat treatment.--All castings that were used for testing received a 2-hr, 1177°C cycle in a protective argon atmosphere. Also, the castings were wrapped in protective foil for further safeguarding.

Testing. Specimens were identified by the casting from which they were taken. Castings poured in the first lot were numbered at random (9 through 16); therefore, test specimen 9-1 was the number one specimen for Casting 9.

The second lot of castings was numbered in pouring order and, because there were two castings per mold, Castings 2A and 2B came from the second mold poured. Test specimens from Casting 2A were identified as 2A-1, 2A-2, 2A-3, etc.

All mechanical tests were performed on 0.635-cm test bars with a 5.08-cm gage length. The bars were machined from annealed (1177°C for 2 hr) regenerator housing blanks.

All mechanical testing, except for fatigue testing, was performed by Accurate Metallurgical Services, Santa Fe Springs, California. Tensile tests were conducted at 26°, 300°, 400°, 500°, 600°, 700°, 775°, 800°, and 850°C. The loading rate was 0.005 cm/cm/min. Data were recorded for 0.2-percent offset yield, ultimate tensile stress, and percent of elongation.

Creep- and stress-rupture tests were performed at 700°, 775°, and 800°C, with stress values ranging from 100 to 345 MPa. Tests were usually discontinued after 500 hr, and percent creep versus time was recorded on a printout.

LCF strain-controlled fatigue tests were performed on NASACC-1 and X-40 at Martest, Inc. in Cincinnati, Ohio. Percent strain ranged from 0.6 to 0.3 percent, with a stress ratio (R) of minus one. A triangle wave form was used with a frequency of 25 cpm.

Three specimens were sent to AMAX Materials Research Center in Ann Arbor, Michigan, for phase analysis. The thermal history of the specimens is as follows: 8A-11 as-cast, 6A-7 heat treated (1177°C for 2 hr) in argon, and 5A-9 heat treated and stress-rupture tested at 775°C at 200 MPa for 381 hr.

The phases were identified by X-ray diffraction of extracted residues and by EDAX analysis in the scanning electron microscope (SEM). Extracts had been obtained electrolytically with a solution of 20 percent HCl and 1-percent tartaric acid in methanol. This technique was used because in-situ X-ray analysis

of thin platelets or small particles carries with it the possibility of excitation of the surrounding austenite, thereby shifting the apparent composition of the subject phase toward that of the austenitic matrix.

The coefficient of thermal expansion was determined at the Signal UOP Research Center using a Mettler TA 3000 thermal mechanical analyzer (TMA). The expansion was measured along the length of the annealed (1177°C for 2 hr) test bar.

Thermophysical Properties Research Laboratory at Purdue University uses a Perkin-Elmer Model DSC-2 differential scanning colorimeter to measure specific heat from room temperature to 676°C and extrapolated the results from 676° to 850°C. The experiments were performed under computer control, and the results are automatically calculated at equal temperature intervals.

Thermal conductivity (λ) is calculated indirectly by measuring bulk density (d), thermal diffusivity (D), and specific heat (Cp), and multiplying the three measured values (λ=DCpd).

The flash method subjects the front face of a small disc-shaped sample to a short laser burst, and the resulting rear-face temperature rise is recorded to calculate the thermal diffusivity.

Results

Tensile.--The NASACC-1 alloy has superior yield (0.2 percent offset) strength to X-40 (table 41) and other similar alloys, and the ultimate tensile strength (UTS) is comparable. The elongation is lower in NASACC-1, but many commercial nickel-base superalloys have similar ductilities.

Fig. 37 conveys the effect of temperature on tensile properties. No drastic decreases in yield strength or UTS occur until temperatures exceed 800°C. The UTS increases, as expected with this alloy system, between 500° to 800°C. Furthermore, the elongation is tripled from room temperature to 800°C.

Creep-rupture.--Stress versus time to percent creep at 0.5, 1.0, and 1.5 percent is shown in figs. 38, 39, and 40, respectively. The effect of temperature on time to reach a particular percent creep is shown using these three graphs.

Fig. 41 shows stress versus the Larson-Miller parameter. The Larson-Miller parameter enables the prediction of stress to failure as a function of various combinations of temperature and rupture time.

Low-cycle fatigue (LCF).--LCF results (fig. 42) give information on safe working strain limits and allows better understanding of material behavior due to fatigue strains.

TABLE 41

TENSILE PROPERTIES AT 800°C

	UTS, MPa	Yield strength, MPa	Elongation, %
NASACC-1	414	317	2
XF 818	331	193	21
19-9 DL	483	207	50
X-40	449	241	15
D5 NiRESIST	89.7	55.2	50

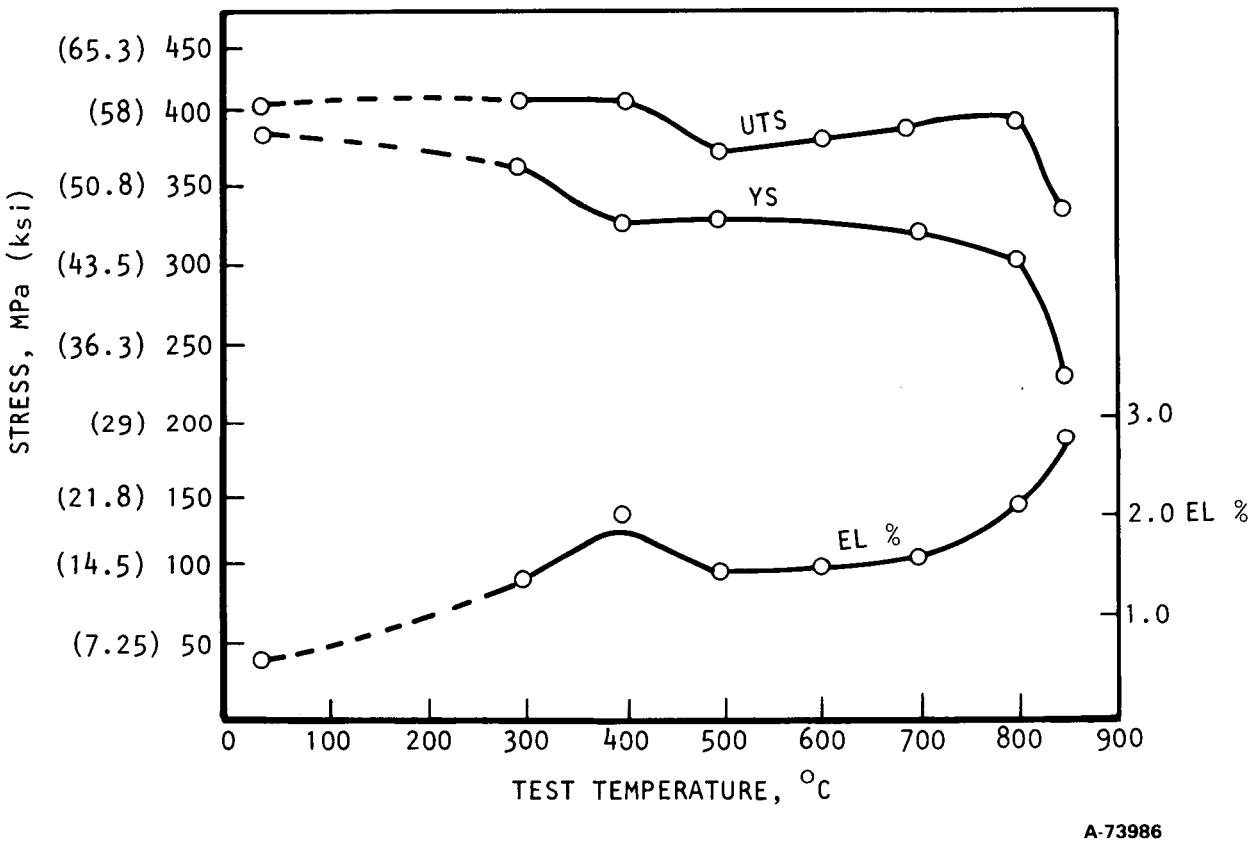

Figure 37.--NASACC-1 Elevated Temperature Tensile Properties.

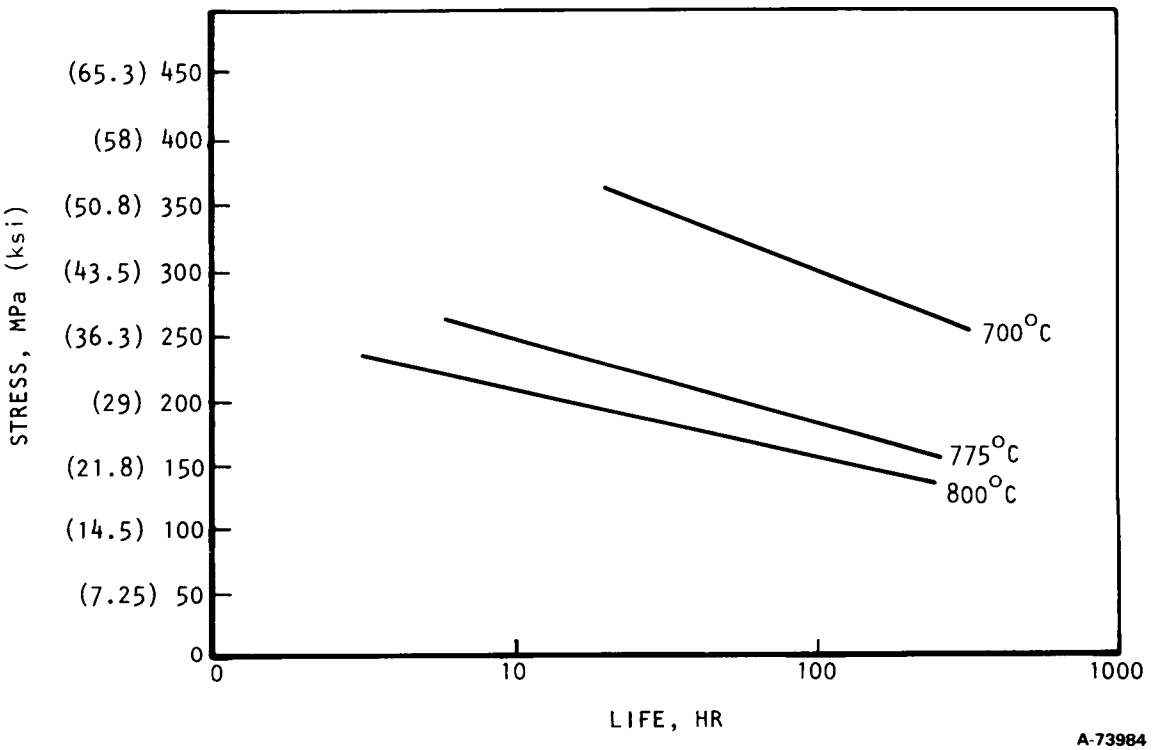

Figure 38.--NASACC-1 Time to 0.5-Percent Creep.

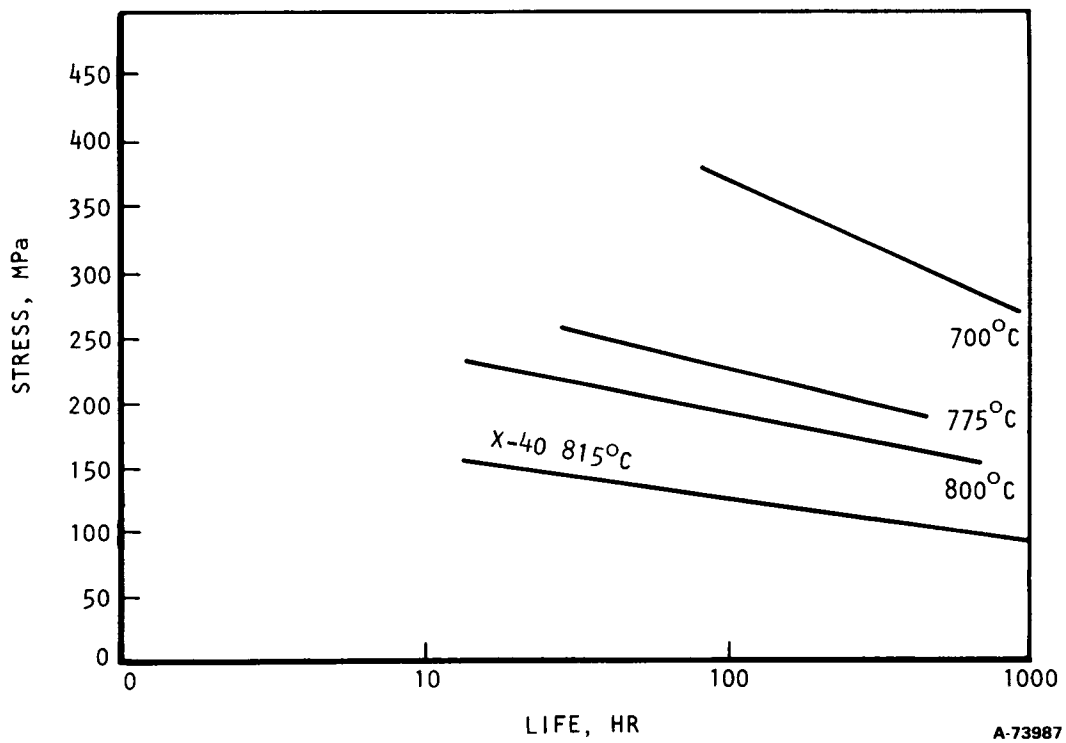

Figure 39.--NASACC-1 Time to 1-Percent Creep.

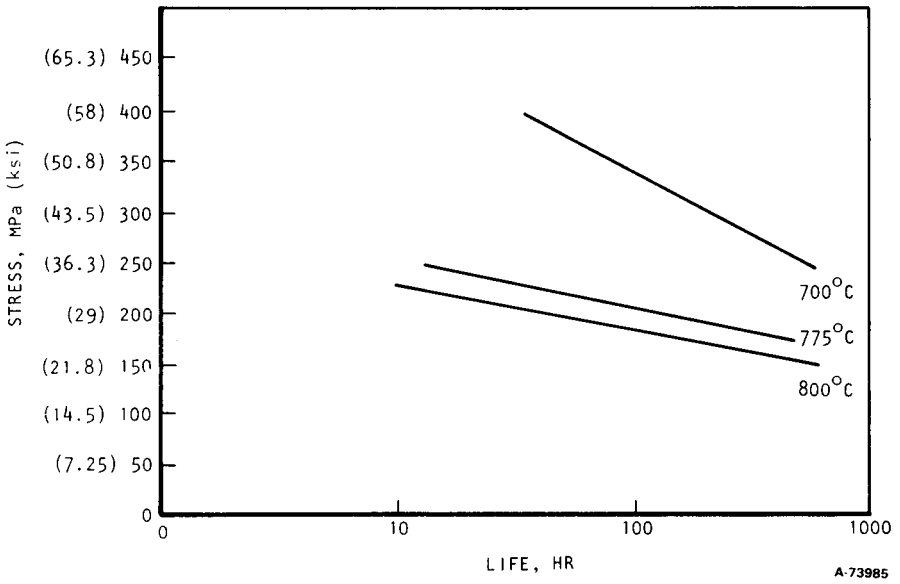

Figure 40.--NASACC-1 Time to 1.5-Percent Creep.

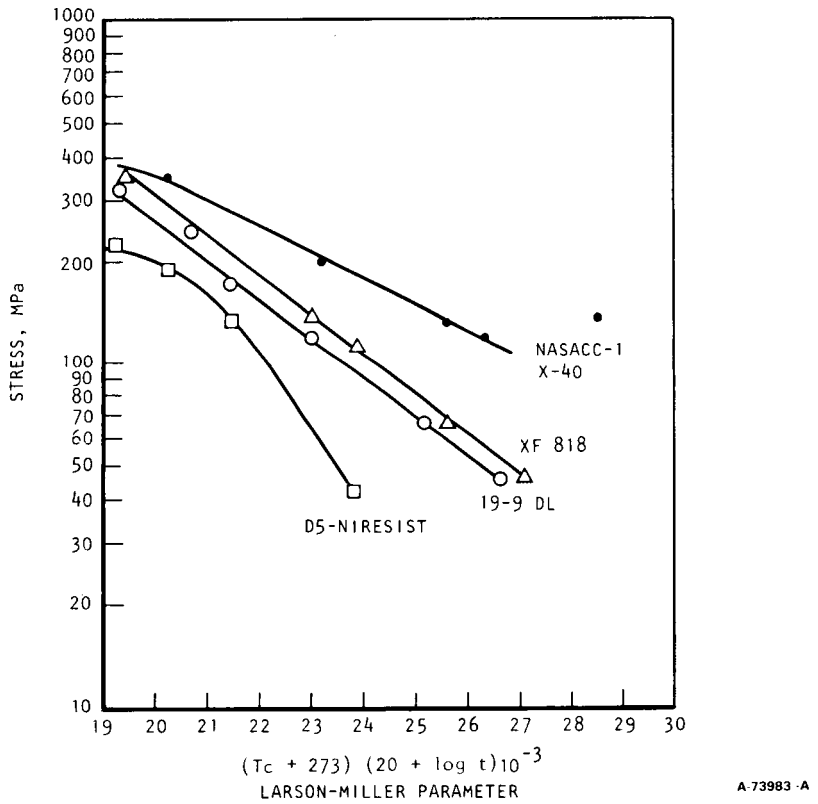

Figure 41.--Comparative Stress-Rupture Properties.

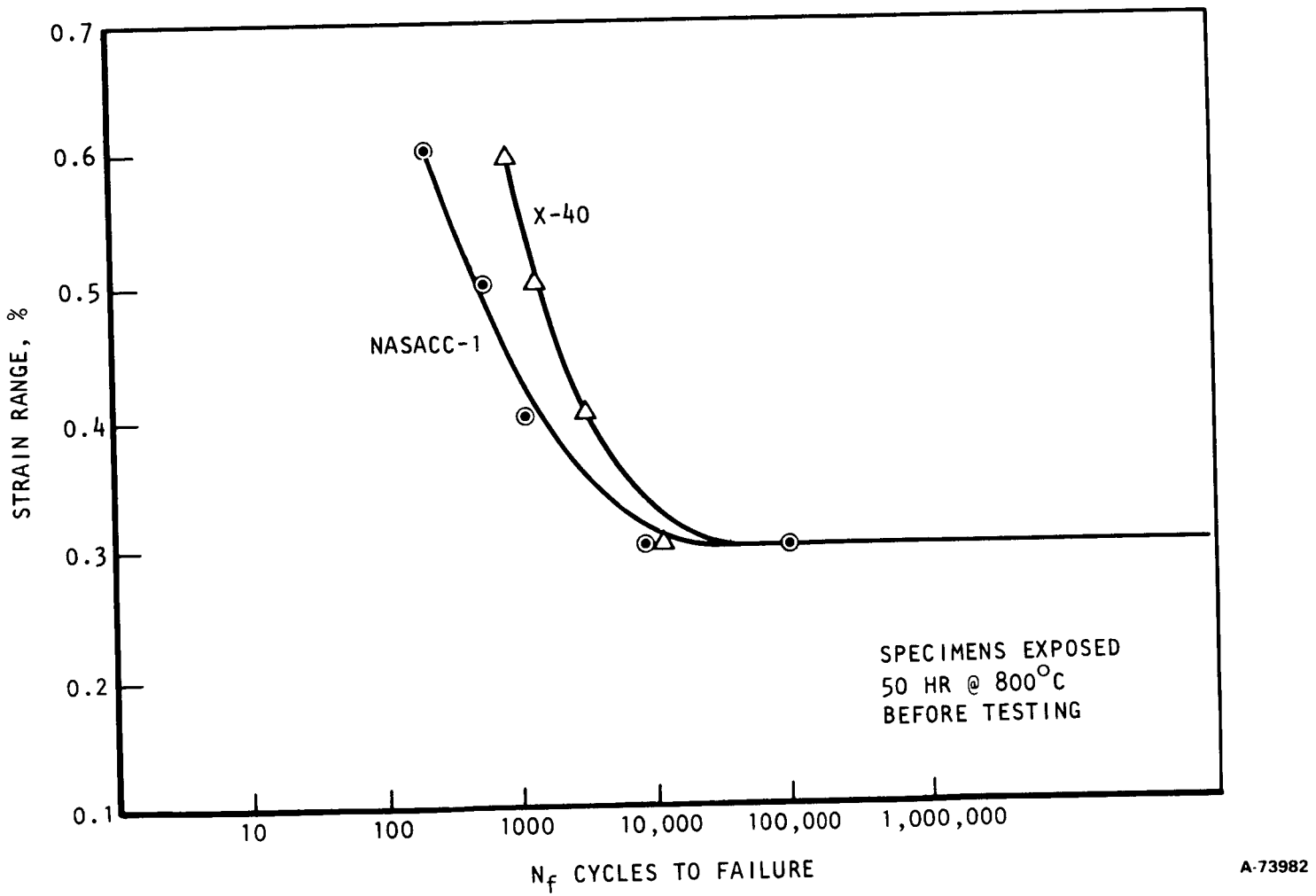

Figure 42.--Low-Cycle Fatigue at 800°C.

Physical properties.--The physical properties of the NASACC-1 alloy are summarized as follows:

(1) The coefficient of thermal expansion for X-40, NASACC-1, and similar Fe-base alloys is shown in fig. 43. NASACC-1 essentially has a consistent linear expansion coefficient over the temperature range.

(2) NASACC-1 shows a greater specific heat value (fig. 44) as compared to the other two alloys.

(3) The effect of temperature on thermal conductivity is seen in fig. 45. NASACC-1 has equivalent values to that of X-40 and 19-9DL.

Discussion

Metallography.--NASACC-1 alloy has an Fe-base austenitic matrix strengthened by M_3B_2, MC, and $M_{23}C_6$ precipitates, and solid solution strengthened by molybdenum (Mo), chromium (Cr), nickel (Ni), and tungsten (W) (table 42).

When heat treated (1177°C for 2 hr), small amounts of $M_{23}C_6$ and M_3B_2 dissolve, and partial spheroidizing of the M_3B_2 occurs (fig. 46). $M_{23}C_6$ precipitates within the matrix at 649° to 816°C. These precipitates form fine, evenly dispersed particles. During long exposures to temperatures (649° to 816°C) (fig. 47), such as creep-rupture testing, the MC carbide (fig. 46) also precipitates within the matrix.

Tensile.--Fig. 37 shows the effect of temperature on tensile properties. The peak in the ultimate tensile strength (UTS) is due to the precipitation of secondary $M_{23}C_6$ carbides. At the same time, the ductility trough between 400° and 800°C was caused by the carbide precipitation. The ductility values between 500° and 800°C are typical for carbide-strengthened alloys, particularly those with an austenitic matrix.

Creep-rupture.--The creep-rupture resistance of NASACC-1 is derived from the combination of solid solution and precipitation strengthening (fig. 38). Molybdenum, chromium, and tungsten combine with boron to form a necessary stable precipitate (M_3B_2 type boride). Task 1 shows that increasing the boron content up to 1.3 percent increases the creep-rupture life. Molybdenum, chromium, and tungsten are also solid-solution strengtheners. The creep resistance is improved by the austenitic matrix and further enhanced by the solution of molybdenum, chromium, and tungsten in the matrix.

MC precipitates tend to be the most stable precipitate. The MC carbides add stability, and their resistance to solutioning enhances the long time strengthening characteristics.

Fig. 41 shows the overall effect of these strengthening mechanisms. The Fe-base NASACC-1 alloy had rupture lives equal to X-40 and better than XF-818 and 19-9DL.

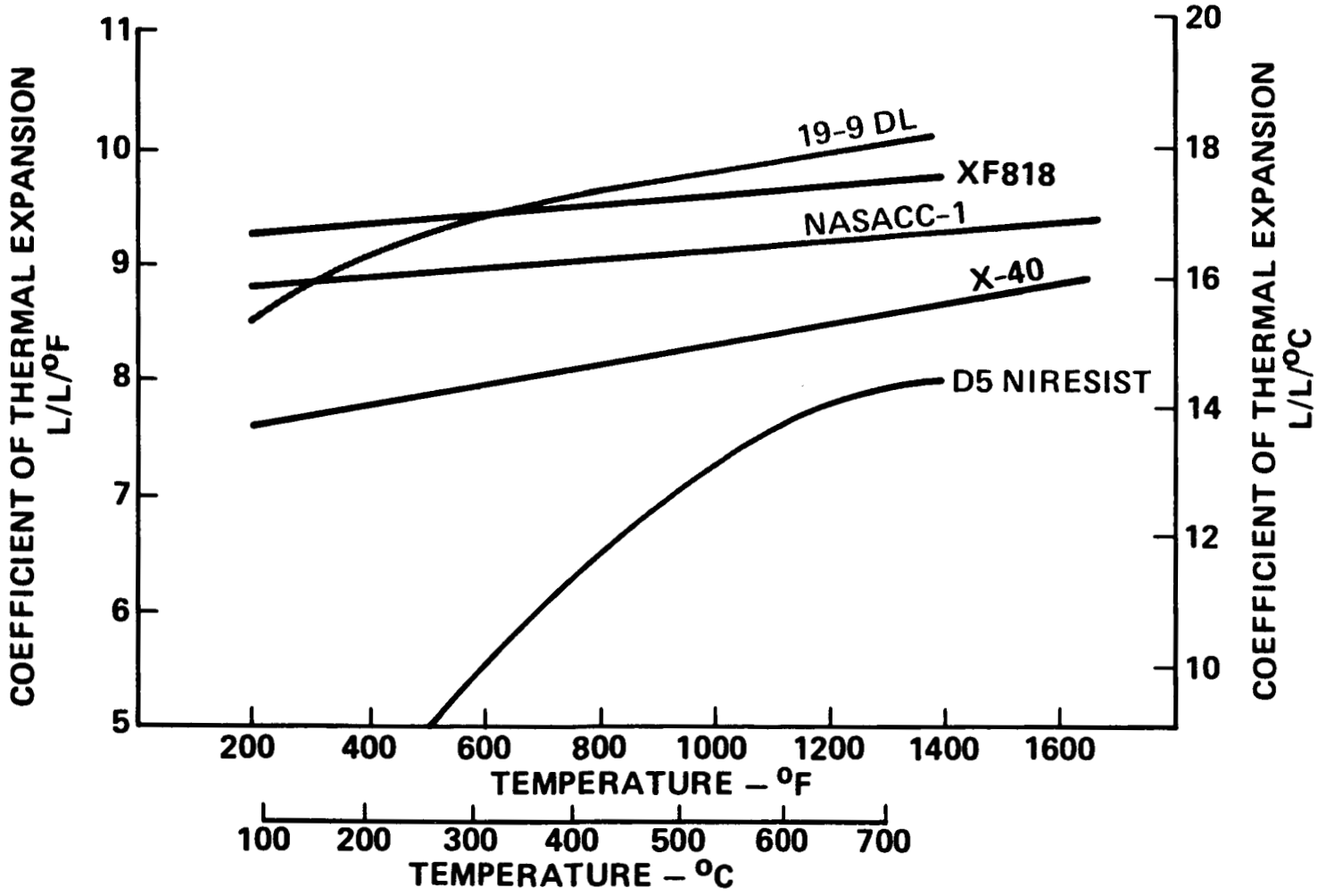

Figure 43.--Comparative Thermal Expansion.

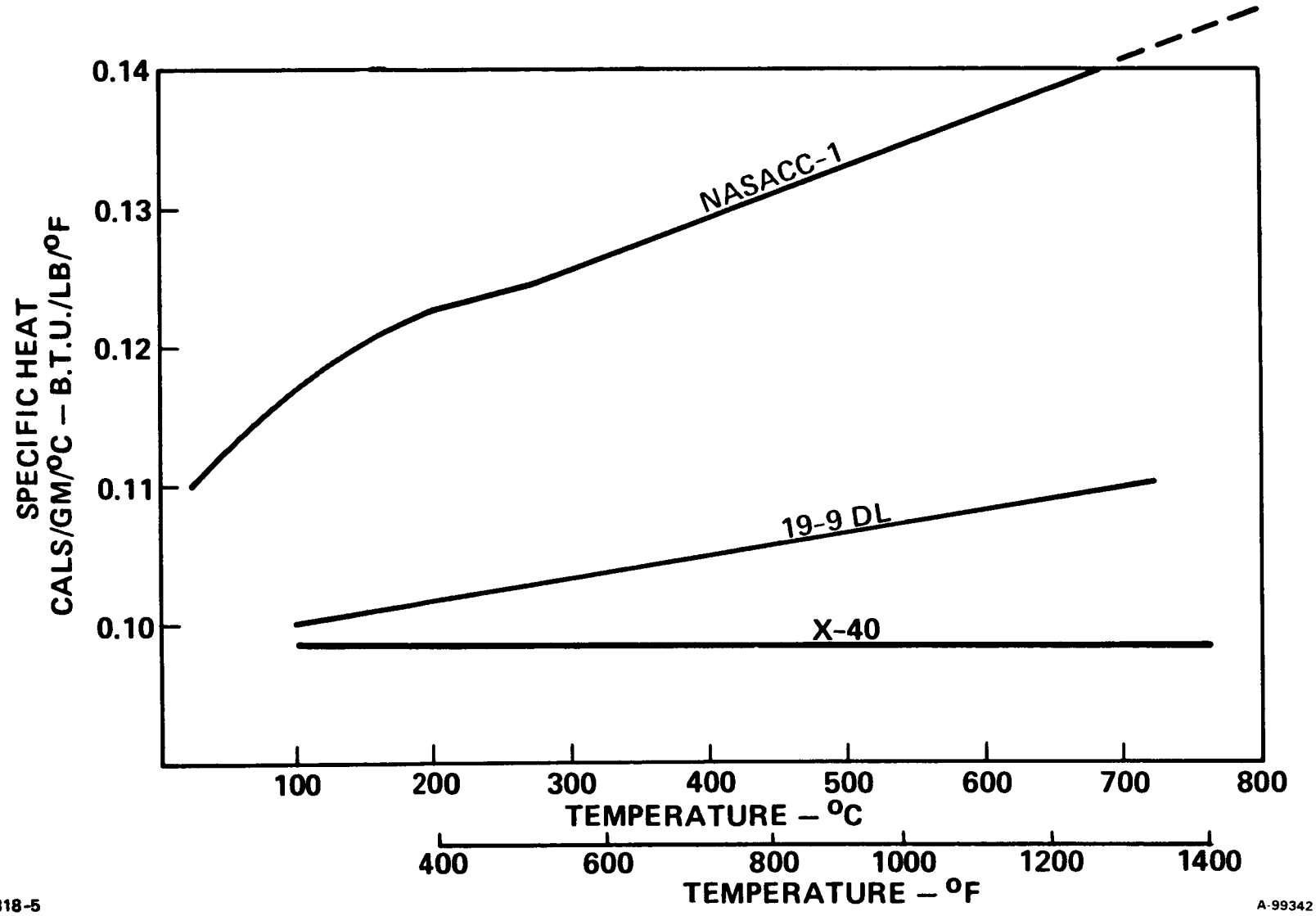

Figure 44.--Comparative Specific Heat.

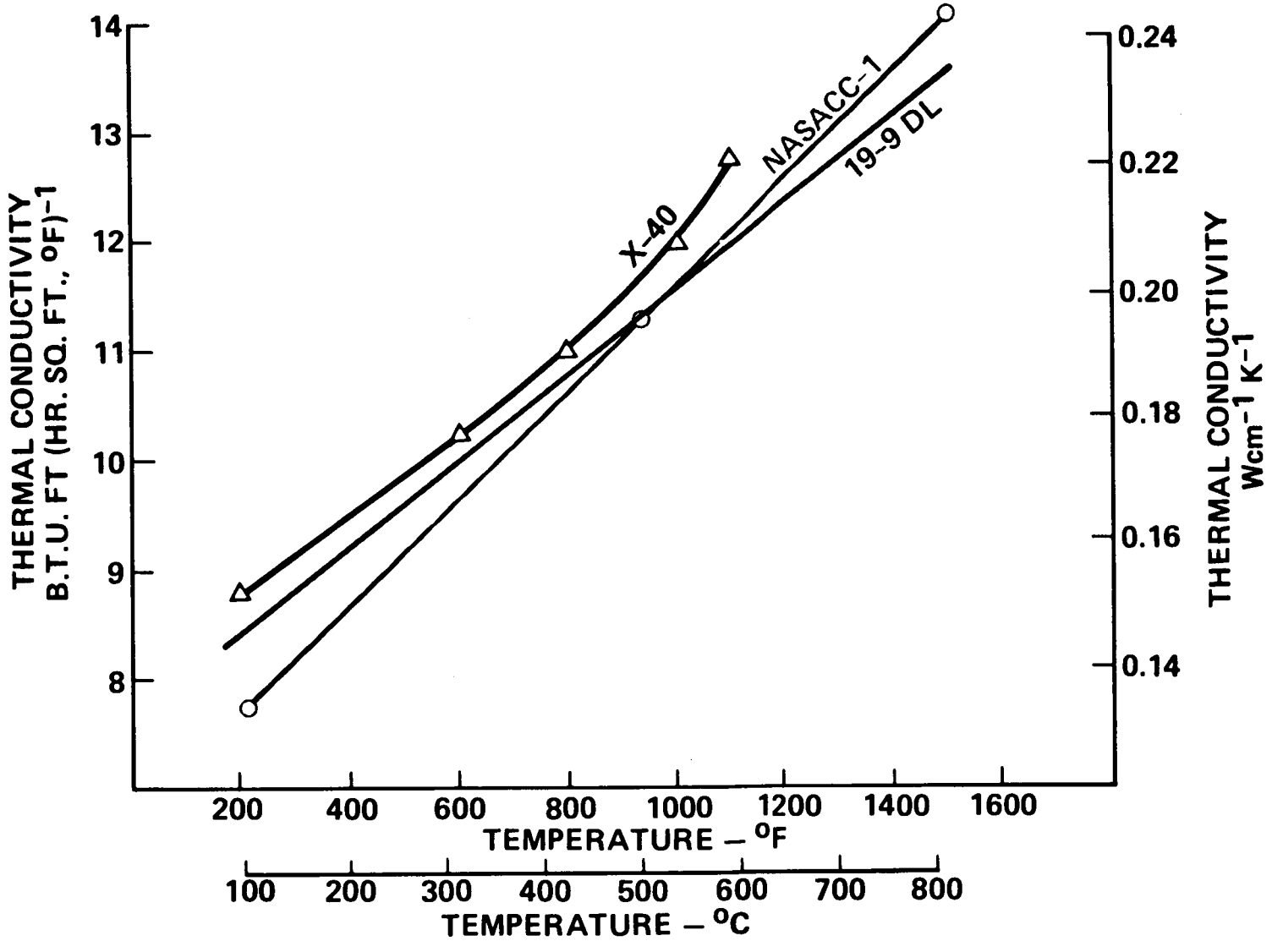

Figure 45.--Comparative Thermal Conductivity.

TABLE 42

CONCENTRATIONS OF TRANSITION METALS IN VARIOUS PHASES OF NASACC-1 SPECIMENS

Phase	Element, %						
	Fe	Cr	Ni	Mo	W	Nb	Mn
NASACC-1 (nominal)*	50.8	18.5	18.2	5.0	2.7	2.3	0.26
Spec. 8A-11 (as-cast)							
Austenite matrix	57.8	15.9	20.0	1.8	(3.8)**	0.5	0.2
M_3B_2	14.9	23.5	1.9	28.6	21.7	9.3	0.1
MC	1.4	1.2	0.4	5.3	2.9	88.8	0.1
Fine $M_{23}C_6$ + austenite	42.2	41.4	5.5	6.1	(3.9)**	0.7	0.2
Spec. 6A-7 (1177°C for 2 hr)							
Austenite matrix	57.8	16.1	20.0	1.6	(3.9)**	0.3	0.2
M_3B_2	14.5	30.1	1.4	28.5	18.6	6.8	0.1
MC	1.4	1.3	0.4	5.2	2.3	89.5	0.1
Fine $M_{23}C_6$ + austenite	40.1	45.4	3.7	6.1	(3.7)**	0.9	0.3
Spec. 5A-9 (Stress-rupture 775°C for 381 hr)							
Austenite matrix	60.5	15.5	18.5	1.2	(3.6)**	0.2	0.4
M_3B_2	13.4	30.1	1.1	28.9	18.8	7.5	0.2
MC	4.7	3.9	1.1	5.4	4.7	80.1	0.03
$M_{23}C_6$	29.5	63.6	0.9	3.1	2.4	0.3	0.3
M_3B_2	13.9	25.0	1.2	35.7	16.5	7.5	0.1
$M_{23}C_6$ ppt.	50.4	29.2	12.5	3.3	3.8	0.3	0.5

*Also contains 0.5 percent C, 0.55 percent Si, and 1.2 percent B.

**The apparent tungsten concentration is augmented disproportionately by interference from any silicon present. This mainly affects the austenite matrix results. The nominal silicon content in NASACC-1 is 0.55 percent.

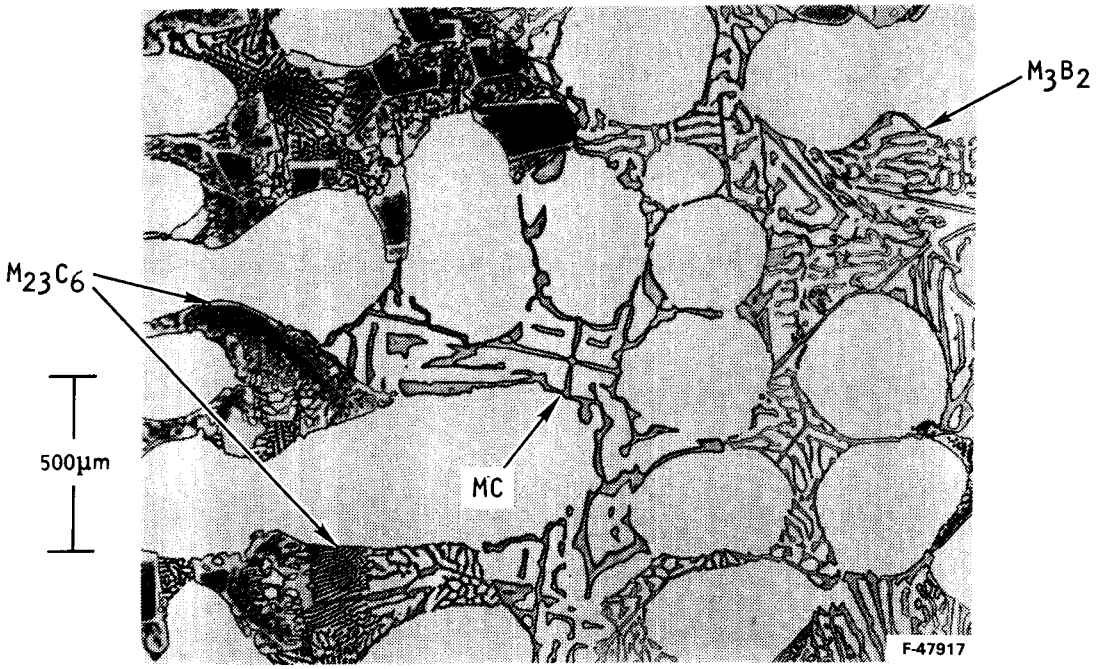

Figure 46.--As-Cast NASACC-1.

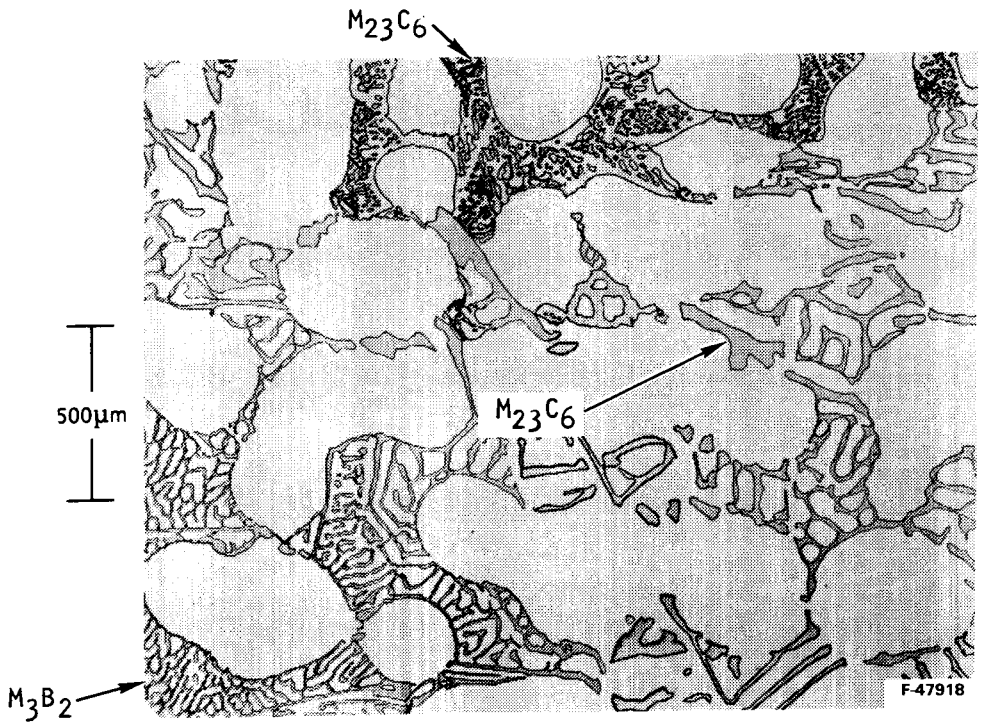

F-48001 -A

Figure 47.--NASACC-1, Heat Heated at 1177°C for 2 Hr.

Low-cycle fatigue.--Low-cycle-fatigue testing was added midway into the program because of an uncertainty over fatigue properties. The lower limits (fig. 42) are identical, and the fatigue lives (between 0.3 and 0.6 percent strain) of NASACC-1 and X-40 are essentially equal, at 800°C.

Physical properties.--Physical properties of NASACC-1 compare favorably with the reference alloys. The NASACC-1 alloy has a linear coefficient of expansion (fig. 43), whereas 19-9DL and D-5 ni-resist show considerable range over the range of testing temperatures. Also, NASACC-1 will have less volume change during working temperatures than that of 19-9DL and X-40. Specific heat of NASACC-1 is considerably higher than that of either X-40 or 19-9DL, increasing over the range of testing temperatures. Thermal conductivity of the alloy is closely comparable to both X-40 and 19-9DL.

Alloy cost.--NASACC-1 alloy cost is slightly greater than 19-9DL, but significantly less than X-40 (table 43). The NASACC-1 alloy price is based on virgin material. When enough of the alloy is generated, revert and scrap material can be used and the cost would decrease.

TABLE 43

COMPARATIVE RAW MATERIAL COSTS

19-9DL	1.0
D5 NiResist	1.3
XF 818	1.7
NASACC-1	2.1
X-40	11.0

NOTE: Above data compared to 19-9DL as unity, August 1984; subject to periodic raw material variations and scrap availability.

CONCLUSIONS

The goal of this programs as discussed in the Introduction was to develop a Stirling engine cylinder/regenerator housing iron-base alloy. This alloy had to meet or exceed the specific characteristics outlined.

The cast iron-base alloy NASACC-1, using nonstrategic metals, meets or exceeds mechanical and fatigue properties when tested at the prescribed conditions of 200 MPa at 775°C. Table 44 is a tabulation of data for the alloy.

The data tabulation of table 44 shows the physical properties of the alloy, including thermal expansion, specific heat, and thermal conductivity characteristics.

TABLE 44

TABULATION OF PROPERTY DATA FOR NASAAC-1 ALLOY

Tensile Properties (table 41 and fig. 37)

	Room Temp.	700°C	800°C
Ultimate Tensile Strength, MPa	415	390	414
Yield Strength, MPa	380	330	317
Elongation, %	0.6	1.5	2.0

Creep-Rupture (figs. 38, 39, and 40)

At 775°C and 200 MPa, 95 hr to reach 0.5 percent creep.
At 775°C and 200 MPa, 350 hr to reach 1.0 percent creep.
At 775°C and 200 MPa, 400 hr to reach 1.5 percent creep.

Low-cycle fatigue (fig. 42)

At a strain rate of 0.3 percent cycles to failure under test conditions of 775°C/200 MPa should exceed 10,000.

Coefficient of thermal expansion (fig. 43)

In the temperature range of 100° to 800°C thermal expansion is linear from 15.8 L/L/°C at 100°C to 17.0 L/L/°C at 800°C.

Specific heat (fig. 44)

In the temperature range of 100° to 800°C, thermal expansion is nonlinear, especially at lower temperatures. The increase from referenced fig. 44 is from 0.117 cals/gm/°C at 100°C to 0.145 cals/gm/°C at 800°C as determined by linear extrapolation.

Thermal conductivity (fig. 45)

Heat conductivity increases linearly from 0.136 $Wcm^{-1}\ K^{-1}$ at 100°C to 0.242 $Wcm^{-1}\ K^{-1}$ at 800°C.

Fatigue properties of the alloy, based on the data obtained, equal those of X-40 and exceed those of XF-818.

The alloy possesses excellent oxidation/corrosion resistance, is compatible with hydrogen, and has highly satisfactory welding and brazing characteristics.

The cost does exceed that of 19-9DL, but is significantly lower than the cobalt-base X-40.

NASAAC-1 alloy is a strong candidate material for Stirling engine cylinder/regenerator housing application.

REFERENCES

1. The Superalloys, Sims, C. T., and Hagel, W. C., eds., John Wiley and Sons, New York, 1972.

2. Structural Alloys Handbook, Thomas D. Moore, ed., Mechanical Properties Data Center, Traverse, Michigan, 1978.

3. Allegheny Ludlum Steel Corp., Blue Sheets for 200-Type Stainless Steels, Pittsburgh, Pennsylvania.

4. ARMCO Steel Corp., ARMCO Advanced Materials Technical Data Manual, Baltimore, Maryland, 1974.

5. Novak, C. J., "Structure and Constitution of Wrought Austenitic Stainless Steels," Handbook of Stainless Steels, Peckner and Bernstein, eds., McGraw-Hill, New York, 1977.

6. MacFarlane, R. R.; DeFries, R. S.; Reynolds, E. E.; and Dyrkacz, W. W.: "Development of Wrought and Cast Alloys for High Temperature Applications," WADC TR 55-23, April, 1955.

7. Eberle, F.; Leyda, W. E.; Feduslea, W.; and Snyder, F. B.: "Development of Cast Iron-Base Alloys of Austenitic Type for High Heat Resistance and Scale Resistance," Second Quarterly Progress Report prepared by Babcock and Wilcox Research Center, Alliance, Ohio, under WADC Contract No. AF 33 (616)-2413, November 15, 1954.

8. Eberle, F.; Holse, I. H.; and Leyda, W. E.: "Development of Cast Iron-Base Alloys of Austenitic Type for High Heat Resistance and Scale-Resistance," WADC TN 55-290, Part II, January, 1957.

9. Salvaggi, J.; and Guarnieri, G. I.: "Summary Report on Development of Lean-Alloy Chromium-Nickel Stainless Steels for High Temperature Use." Report No. KA-797-M-7, prepared by Cornell Aeronautical Laboratory, Inc., Buffalo, New York, for Bureau of Aeronautics under Contract NOa(s)-52-368-C, June 30, 1953.

10. Sponseller, D. L., Climax Molybdenum Co. of Michigan, Ann Arbor, Michigan, personal communication.

11. Sponseller, D. L.; Kraft, R. W.; and Flinn, R. A.: "Additive Effects of Alloying Elements on the Mechanical Properties of Cast Austenitic Alloys at 1500°F," Trans. ASM, Vol. 54, 1961, p. 526.

12. Sponseller, D. L., "The Development of Improved Iron-Base Cast Alloys for Gas Turbine Blades," Report RP-31-73-01, Climax Molybdenum Company of Michigan, Ann Arbor, Michigan, July 25, 1975.

13. Bauerle, P. C., and Sponseller, D. L.: "An Evaluation of Iron-Base Cast Alloys for Exhaust Valves of Automotive Internal Combustion Engines," Report J-4074, Climax Molybdenum Co. of Michigan, Ann Arbor, Michigan, December 26, 1964.

14. Sponseller, D. L., "Effects of Compositional Variation and Solidification Rate on the Properties of an Iron-Base Cast Superalloy Prepared for Symposium of High Temperature Alloys Committee of AIME," St. Louis, Missouri, October 16 and 17, 1978.

15. Sponseller, D. L., and Hagel, W. C.: "Cobalt-Free, Iron-Base Cast Superalloys" prepared for Fourth International Symposium on Superalloys, Seven Springs, Pennsylvania, September, 1980.

16. Hagen, F. A., Chrysler Corporation Research Officer, Detroit, Michigan, personal communication.

17. Fujioka, T.; Kinugasa, M.; and Lizumi, S.: "Effects on Rare Earth Elements and Calcium Upon High Temperature Oxidation of Austenitic Heat-Resisting Alloy Containing High Silicon," Proceedings of the Third International Symposium on Superalloys: Metallurgy and Manufacture, Seven Springs, Pennsylvania, September 12-15, 1976, Claitor's Publishing, Baton Rouge, 1976, pp. 159-169.

18. American Society for Testing and Materials, Hot Corrosion Problems Associated with Gas Turbines, ASTM STP421, 1967.

19. Pickering, H. W.; Beck, F. H.; and Fontana, M. G.: "Rapid Integranular Oxidation of 18-8 Stainless Steels by Oxygen and Dry Sodium Chloride at Elevated Temperatures," Transactions ASM, Vol. 53, 1961, pp.793-804.

20. Fontana, M. G.; and Greene, N. D.: Corrosion Engineering, McGraw-Hill, New York, 1967, pp. 223-241.

21. Morris, L. A., "Resistance to Corrosion in Gaseous Atmospheres," Handbook of Stainless Steels, Peckner and Bernstein, eds., McGraw-Hill, New York, 1977.

22. Thompson, A. W., "Stainless Steels in High-Pressure Hydrogen," Handbook of Stainless Steels, Peckner and Bernstein, eds., McGraw-Hill, New York, 1977.

23. Smugeresky, J. E., "Effect of Hydrogen on the Mechanical Properties of Iron-Base Superalloys," Met. Trans. A. 8A, August 1977, p. 1283.

24. Thompson, A. W.; and Brooks, J. A.: "Hydrogen Performance of Precipitation-Strengthened Stainless Steels Based on a-286," Met. Trans. A., 6A, July, 1975, p. 1431.

25. Simmons, W. F., "Compilation of Chemical Compositions and Rupture Strength of Superalloys," ASTM Data Series Publication No. DS9E, Philadelphia, Pennsylvania.

26. Aggen, G., Allegheny Ludlum Steel Corporation, Brackenridge, Pennsylvania, personal communication.

27. Haynes Stellite Company, H. S. Alloy No. 31, Data Book, April, 1958.

28. Titran, R. H., "Creep-Rupture Behavior of Candidate Stirling Engine Alloys After Long-Term Aging at 760°C in Low-Pressure Hydrogen," NASA Lewis Research Center, Cleveland, Ohio, 44135, May, 1984.

NASA
National Aeronautics and Space Administration

Report Documentation Page

1. Report No.	2. Government Accession No.	3. Recipient's Catalog No.
NASA CR-182116		

4. Title and Subtitle
Cast Iron-Base Alloy for Cylinder/Regenerator Housing

5. Report Date
August 1985

6. Performing Organization Code

7. Author(s)
Stewart L. Witter, Harold E. Simmons, and Michael J. Woulds

8. Performing Organization Report No.

10. Work Unit No.

9. Performing Organization Name and Address
Garrett Processing Company
Garrett Metals Casting Division
19800 Van Ness Ave.
Torrance, California 90509

11. Contract or Grant No.
DEN 3-234

13. Type of Report and Period Covered
Contractor Report

12. Sponsoring Agency Name and Address
U.S. Department of Energy
Office of Vehicle and Engine R&D
Washington, D.C. 20545

14. Sponsoring Agency Report No.
DOE/NASA/0234-1

15. Supplementary Notes
Final Report. Prepared under Interagency Agreement DE-AI01-85CE50112. Project Manager, C. Scheuermann, Materials Division, NASA Lewis Research Center, Cleveland, Ohio 44135.

16. Abstract
NASACC-1 is a castable iron-base alloy designed to replace the costly and strategic cobalt-base X-40 alloy used in the automotive Stirling engine cylinder/generator housing. Over 40 alloy compositions were evaluated using investment cast test bars for stress-rupture testing. Also, hydrogen compatibility and oxygen corrosion resistance tests were used to determine the optimal alloy. NASACC-1 alloy was characterized using elevated and room temperature tensile, creep-rupture, low cycle fatigue, heat capacity, specific heat, and thermal expansion testing. Furthermore, phase analysis was performed on samples with several heat treated conditions. The properties are very encouraging. NASACC-1 alloy shows stress-rupture and low cycle fatigue properties equivalent to X-40. The oxidation resistance surpassed the program goal while maintaining acceptable resistance to hydrogen exposure. The welding, brazing, and casting characteristics are excellent. Finally, the cost of NASACC-1 is significantly lower than X-40.

17. Key Words (Suggested by Author(s))	18. Distribution Statement
Iron Iron alloy Stirling engine	Unclassified - Unlimited Subject Category 26 DOE Category UC-96

19. Security Classif. (of this report)	20. Security Classif. (of this page)	21. No of pages	22. Price*
Unclassified	Unclassified	142	A07

NASA FORM 1626 OCT 86

*For sale by the National Technical Information Service, Springfield, Virginia 22161